CORRELATIONS BETWEEN ULTRASONIC PULSE VELOCITIES AND MECHANICAL PROPERTIES OF ROCKS

Suwaphit Chamwon

A Thesis Submitted in Partial Fulfillment of the Requirements for the Degree of Master of Engineering in Civil, Transportation and Geo-Resources Engineering

Suranaree University of Technology

Academic Year 2020

ความสัมพันธ์ระหว่างความเร็วคลื่นดลอัลตร้าโซนิคและสมบัติเชิงกลของหิน

นางสาวสุวพิชญ์ ช้าวอน

วิทยานิพนธ์นี้เป็นส่วนหนึ่งของการศึกษาตามหลักสูตรปริญญาวิศวกรรมศาสตรมหาบัณฑิต
สาขาวิชาวิศวกรรมโยธา ขนส่ง และทรัพยากรธรณี
มหาวิทยาลัยเทคโนโลยีสุรนารี
ปีการศึกษา 2563

CORRELATIONS BETWEEN ULTRASONIC PULSE VELOCITIES AND MECHANICAL PROPERTIES OF ROCKS

Suranaree University of Technology has approved this thesis submitted in partial fulfillment of the requirements for a Master's Degree.

Thesis Examining Committee

(Assoc. Prof. Dr. Pornkasem Jongpradist)
Chairperson

(Dr. Thanittha Thongprapha)
Member (Thesis Advisor)

(Asst. Prof. Dr. Akkhapun Wannakomol)
Member

(Prof. Dr. Kittitep Fuenkajorn)
Member

(Assoc. Prof. Flt. Lt. Dr. Kontorn Chamniprasart)
Vice Rector for Academic Affairs and Internationalization

(Assoc. Prof. Dr. Pornsiri Jongkol)
Dean of Institute of Engineering

สุวพิชญ์ ช้ำวอน : ความสัมพันธ์ระหว่างความเร็วคลื่นดลอัลตร้าโซนิคและสมบัติเชิงกลของหิน (CORRELATIONS BETWEEN ULTRASONIC PULSE VELOCITIES AND MECHANICAL PROPERTIES OF ROCKS) อาจารย์ที่ปรึกษา : อาจารย์ ดร. ธนิษฐา ทองประภา, 106 หน้า.

วัตถุประสงค์ของการศึกษานี้เพื่อหาความสัมพันธ์ระหว่างความเร็วคลื่นดลอัลตร้าโซนิค สมบัติเชิงกายภาพ เชิงกล และเชิงแร่วิทยาของหินจำนวน 22 ชนิด ในประเทศไทย ตัวอย่างหินแบ่งออกเป็นหกกลุ่มคือ กลุ่มหินอัคนีบาดาล กลุ่มหินภูเขาไฟ กลุ่มหินคาร์บอเนต กลุ่มหินตะกอนอนุภาค กลุ่มหินซัลเฟต และกลุ่มหินซิลิเกต การทดสอบประกอบด้วย 1) การวัดความเร็วคลื่นดลอัลตร้าโซนิคเพื่อหาสมบัติแบบไดนามิก 2) การทดสอบการกดในแกนเดียวเพื่อหาสมบัติเชิงกลแบบสถิต 3) การวัดความพรุนเพื่อหาสมบัติเชิงกายภาพ และ 4) การวิเคราะห์การเลี้ยวเบนของรังสีเอกซ์เพื่อระบุแร่องค์ประกอบของหิน พบความสัมพันธ์เชิงเส้นตรงระหว่างคุณสมบัติเชิงกลกับความหนาแน่น กำลังรับแรงกดในแกนเดียวและค่าสัมประสิทธิ์ความหยืดหยุ่นเพิ่มขึ้นตามความหนาแน่นที่เพิ่มขึ้น พบความสัมพันธ์ที่ดีระหว่างค่าสัมประสิทธิ์ความหยืดหยุ่นแบบเชิงกลและแบบสถิต ความพรุนของหินที่หาจากผลการวิเคราะห์การเลี้ยวเบนของรังสีเอ็กซ์มีความสัมพันธ์เชิงเส้นตรงกับความเร็วของคลื่นได้ดีกว่าความพรุนที่ทดสอบแบบดั้งเดิม

สาขาวิชา เทคโนโลยีธรณี ลายมือชื่อนักศึกษา _____

ปีการศึกษา 2563 ลายมือชื่ออาจารย์ที่ปรึกษา _____

SUWAPHIT CHAMWON : CORRELATIONS BETWEEN ULTRASONIC PULSE VELOCITIES AND MECHANICAL PROPERTIES OF ROCKS. THESIS ADVISOR : THANITTHA THONGPRAPHA, Ph.D., 106 PP.

WAVE VELOCITY/ULTRASONIC TEST/STATIC PROPERTY/DYNAMIC PROPERTY/COMPRESSION TEST

The objective of this study is to determine the correlations between ultrasonic pulse velocities (UPV), physical, mechanical and mineralogical properties of twenty-two rock types in Thailand. Rock samples are divided into six groups: volcanic, plutonic, carbonate, clastic, sulfate and silicate groups. The testing includes: 1) ultrasonic pulse velocity measurements to determine dynamic properties, 2) uniaxial compression tests to determine static mechanical properties, 3) porosity measurements to determine physical properties, and 4) X-ray diffraction analysis to identify mineral compositions of the rocks. Linear relationship between mechanical properties and density is obtained. The uniaxial compressive strength and elastic modulus increase with increasing density. Good relationship is found between the dynamic and the static young's moduli of rocks. Calculated porosity determined from results of X-ray diffraction analysis can be more linearly correlated with the wave velocities than traditional porosity test.

School of Geotechnology

Academic Year 2020

Student's Signature

Advisor's Signature

ACKNOWLEDGEMENT

I wish to acknowledge the funding support from Suranaree University of Technology (SUT).

I would like to express thanks to Dr. Thanittha Thongprapha, thesis advisor, who gave a critical review. I appreciate her encouragement, suggestions, and comments during the research period. I would like to express thanks to Prof. Dr. Kittitep Fuenkajorn, Assoc. Prof. Dr. Pornkasem Jongpradist and Asst. Prof. Dr. Akkhapun Wannakomol for their valuable suggestions and comments on my research works as thesis committee members. Grate thanks are given to all staffs of Geomechanics Research Unit, Institute of Engineering who supported my work.

Finally, I most gratefully acknowledge my parents, Mr. Olav Bergfjord and my friends for all their supported throughout the period of this study.

Suwaphit Chamwon

TABLE OF CONTENTS

Page

TABLE OF CONTENTS (Continued)

Page

TABLE OF CONTENTS (Continued)

Page

LIST OF TABLES

Table **Page**

LIST OF TABLES (Continued)

Table **Page**

LIST OF FIGURES

Figure **Page**

LIST OF FIGURES (Continued)

Figure **Page**

LIST OF FIGURES (Continued)

Figure **Page**

SYMBOLS AND ABBREVIATIONS

A	=	Empirical constant for equation (5.1)
B	=	Empirical constant for equation (5.1)
C	=	Empirical constant for equation (5.2)
D	=	Empirical constant for equation (5.2)
E	=	Empirical constant for equation (5.3)
E_d	=	Dynamic Young's modulus
E_s	=	Static Young's modulus
F	=	Empirical constant for equation (5.3)
G	=	Empirical constant for equation (5.4)
H	=	Empirical constant for equation (5.4)
S.G.	=	Specific gravity of each mineral
n	=	Calculated porosity
n_e	=	Effective porosity
E	=	Static elastic modulus
V_v	=	Volume of voids in specimen
V_p	=	P-wave velocity
V	=	Sample bulk volume
V_s	=	S-wave velocity
W_i	=	Wight of each mineral in specimen
W_{rock}	=	Mass of oven-dry test specimen in air
W_{sat}	=	Saturated-surface-dry mass

SYMBOLS AND ABBREVIATIONS (Continued)

W_{sub}	=	Buoyant mass of submerged test specimen in water
ν_d	=	Dynamic Poisson's ratio
ν_s	=	Static Poisson's ratio
ρ	=	Density of specimen
ρ_{water}	=	Density of water
σ_c	=	Uniaxial compressive strength

CHAPTER I

INTRODUCTION

1.1 Background and rationale

Pulse velocity measurements have long been used both in laboratory and site to determine the dynamic properties of rocks. The measurement is a non-destructive tool involving indirect testing method with relatively high precision and low cost. This technique has been used to study the properties of various rock types (e.g., Kurtulus et al., 2012; Khandelwal, 2013; Rahmouni et al., 2013; Azimian et al., 2014; Azimian and Ajalloeian, 2015; Kassad and Weller, 2015; Najibi et al., 2015; Kurtulus et al., 2016a; Chawre, 2018). Determination of the required geotechnical parameters in the design of structures located on bedrock (including rock foundations, tunnels, intact rock and rock mass classification and etc.) is benefit to civil and mining engineering.

Even extensive measurements have been made on various rock types, the relationship between the pulse velocities and the mineral compositions of the rocks have rarely been made. This research is aimed to obtain wave velocity data of the particular rocks using the pulse velocity measurement, to understand relationships between the rock properties and mineral compositions. The knowledge gained from this study can be further applied to predict the mechanical property of the rock mass in the field.

1.2 Research objectives

The objective of this study is to determine the relationship between the ultrasonic pulse velocity (UPV), physical, mineralogical and mechanical properties of various rocks in Thailand. The uniaxial compression test is conducted after performing the UPV test. The X-ray diffraction technique (XRD) is performed to correlate mineral compositions with the UPV values. The comparison between the dynamic and static mechanical properties is made.

1.3 Research methodology

The research methodology comprises of 6 steps including 1) literature review, 2) sample collection and preparation, 3) laboratory testing, chemical composition analysis and petrographic analysis, 4) data analysis, 5) discussions and conclusions and 6) thesis writing and presentation (Figure 1.1).

1.3.1 Literature review

Literature reviews are carried out to improve an understanding of ultrasonic pulse velocity test on various rock types. The effect of physical, mechanical and mineral properties on ultrasonic pulse velocity is studied. The sources of information are from textbooks, journals, and conference papers. A summary of the literature review is given in Chapter II.

1.3.2 Samples preparation

Twenty-two rock types encountered in Thailand are used in this study. The rock samples are divided into 6 group including volcanic, plutonic, carbonate, clastic, sulfate and silicate groups. Sample preparation is carried out in the laboratory at the Suranaree University of Technology. The specimens are prepared to obtain

cylinders with nominal length-to-diameter ratios (L/D) of 2.0 to 2.5, with diameter not less than 47 mm (ASTM D7012-14).

1.3.3 Ultrasonic pulse velocity measurement

Primary and Secondary waves velocities is measured using OYO Sonic Viewer 170 (Model 5338) before subjected to the mechanical testing. The test method and calculation follow the ASTM D2845-08 standard practice. The wave velocity can be used to calculate dynamic young's modulus and Poisson's ratio with the static mechanical properties.

1.3.4 Physical measurement

Density measurement is carried out following the ASTM D6473- 15 standard practice. Determination of effective porosity follows the ASTM C97-02 standard practice. The measurement results are used to explain the rock properties obtaining form UPV measurements and mechanical tests.

1.3.5 Uniaxial compression test

The uniaxial compression test is conducted following the ASTM D7012-14 standard practice. The axial and lateral deformations are monitored and recorded. The results are used to the determine static young's modulus, Poisson's ratio and uniaxial compressive strength.

1.3.6 X-ray diffraction (XRD) analysis

The XRD analysis (ASTM E1426-14e1) is performed on finely ground rock powder with particle sizes less than 0.25 mm pressed into coherent pellets. The analysis is performed after uniaxial compression test. The X-ray diffraction (Bruker, D2 Phaser) is used. The results can be used to identify the mineral compositions of the test specimens.

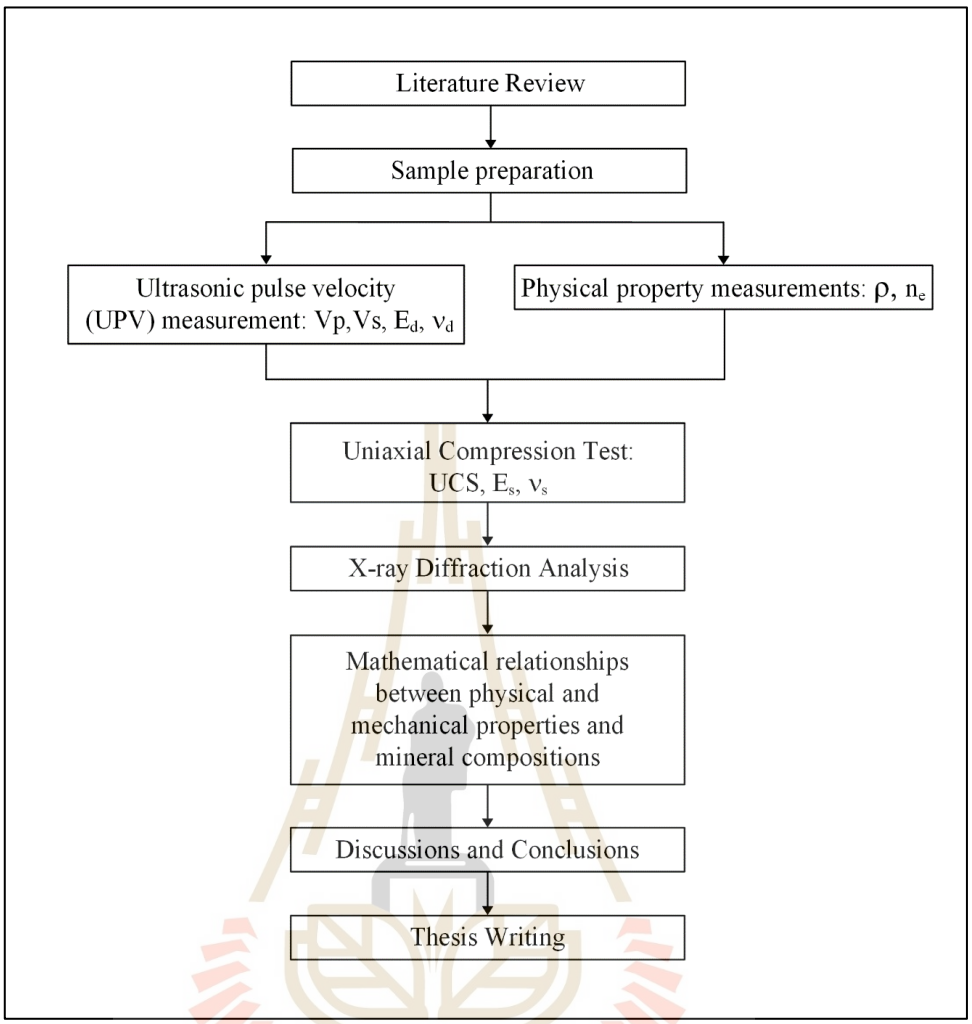

Figure 1.1 Research methodology.

1.3.7 Mathematical relations

The results obtained from the pulse velocity test, uniaxial compression test and XRD analyses of rock are used to determine the relationship between physical, mechanical and mineral compositions with the pulse velocity to predict the mechanical properties of rocks from physical properties and XRD.

1.3.8 Discussions, conclusions and thesis writing

Discussions are made to describe the reliability and adequacy of the test data. Comparison of the results obtained here with those obtained elsewhere is made in terms of similarity and discrepancy. Explanations on these issues are offered. Conclusions from the research study is drawn. The research or findings are published in the conference proceedings or international journals. All research activities and results are documented and complied in the thesis. This study can be applied to determination relationship pulse velocity and uniaxial compression tests and mineral compositions. The findings are published in the conference proceedings or journals.

1.4 Scope and limitations

Efforts and variables used in this study include as follows:

1) Laboratory tests are 22 rock types exposed in Thailand including: volcanic, plutonic, carbonate, clastic, sulfate and silicate groups.

2) The rock specimens are prepared to obtain cylindrical specimens with nominal diameters of 62 mm. The length-to-diameter ratios (L/D) are 2.0-2.5.

3) Ultrasonic pulse velocity test method and calculation follow the ASTM D2845-08 standard practice. OYO sonic viewer (model 5338) with transmitter and receiver transducers is used with frequencies of 63 kHz for P-wave velocity and 33 kHz for S-wave velocity measurements.

4) Uniaxial compression test procedures are performed in accordance with the ASTM D7012-14 standard practice.

5) Mineral compositions are analyzed using X-ray diffraction method (XRD) following the ASTM E1426-14e1 standard practice.

6) Density is measured in accordance with the ASTM D6473-15 standard practice.

7) Effective porosity is measured in accordance with the ASTM C97 standard practice.

8) Calculated porosity is determined using XRD results.

1.5 Thesis contents

The first Chapter introduces the thesis by briefly describing the background of significance of the study, and identifying the research objectives, methodology, scope and limitations. The second Chapter summarizes results of the literature review. Chapter three describes the rock sample preparations, Chapter four presents the pulse velocity, Chapter five presents the relationships between pulse velocity and mechanical properties. Chapter six presents the apparent porosity from mineral compositions of rock. Chapter seven provides the discussion, conclusions, and recommendations for future studies. Details of the laboratory experimental results are given in Appendix A.

CHAPTER II

LITERATURE REVIEW

2.1 Introduction

This chapter summarize the results of literature review carried out to improve an understanding of the relationship between wave velocity (P-wave and S-wave velocity) with physical and mechanical properties and mineral compositions of rock. The topics reviewed here include wave velocity of rocks in the laboratory and in the field, and factors controlling the wave velocities of rocks.

2.2 Ultrasonic pulse velocity of rock

Pulse velocity is one of the tools used in geophysical exploration, in order to explore the physical characteristics of the materials and study of the subsurface geological structures and natural phenomena, such as earthquake and liquefaction etc. Pulse velocity is used for preliminary mineral exploration, structure work on foundations and petroleum exploration. In general, the device consists of a transmitter and receiver by relying on two types of waves (P-wave and S-wave). The speed of the two waves traveling through material is different depending on the mechanical and physical properties of the materials. This method is easy, fast, economical and does not destroy the rock samples. Therefore, pulse velocity is often used in geotechnical engineering to determine the rock properties (Yasar and Erdogan, 2004; Fener, 2011).

Diamantis et al. (2011) study the P- and S-waves velocity of rocks. These two parameters demonstrate that the S-wave velocity shows the linear correlation with the

P-wave velocity (Figure 2.1). The test results agree well with Soroush and Qutob (2011) and Cheng et al. (2019). Juneja and Endait (2017) measure P-wave and S-wave of basalt rock. The S-wave velocity is nearly equal to one-half of the compressional wave velocity. Ultrasonic techniques are used to testing various types of rocks. The results show the range of pulse velocity (P-wave, V_p and S-wave, V_s), Table 2.1. shows P-wave and S-wave measured under different rock types that are compiled from various investigators.

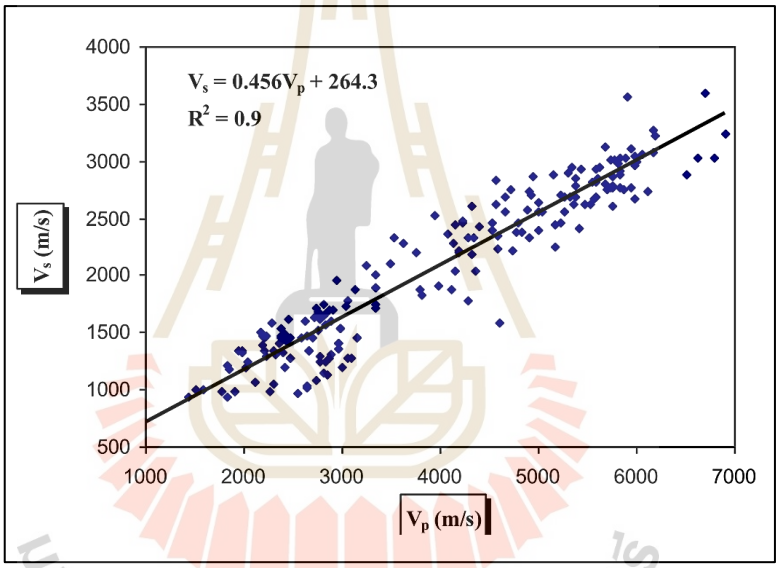

Figure 2.1 Relation between shear and compressional waves (Soroush and Qutob, 2011).

Table 2.1 Pulse velocity data from various researchers.

Rock Type	ρ (g/cm^3)	P-wave (km/s)	S-wave (km/s)	References
Limestone	2.15-2.54	3.29-5.37	2.16-2.93	Assefa et al. (2003)
Quartz-mica schist	2.62-2.78	2.30-4.98	1.66-3.86	Chawre (2018)
Amphibolite	2.73-2.95	4.44-5.44	2.60-3.18	Esamaldeen (2015)
Travertine	2.34-2.72	3.78-5.13	-	Jamshidi et al. (2016)

Table 2.1 Pulse velocity data from various researchers (Cont.).

Rock Type	ρ (g/cm^3)	P-wave (km/s)	S-wave (km/s)	References
Basalt	2.44-2.74	2.32-5.73	1.15-3.26	Juneja et al. (2017)
Dolomite	2.92	6.30	-	Kahraman (2001)
Diabase	2.96	5.20	-	
Serpentine	2.88	5.00	-	
Dacite	-	4.55-4.39	-	Karaman et al. (2015)
Vesicular basalt	-	3.39-3.33	-	
Sandstone	2.62-2.80	2.33-3.39	1.03-2.40	Kassab et al. (2015)
Marlstone	2.22-2.44	1.84-2.67	1.10-1.53	Moradian et al. (2009)
Sandstone	2.09-2.32	2.45-3.89	1.31-2.04	
Limestone	2.10-2.92	1.84-6.54	0.90-3.42	
Calcarenite rocks	1.60-1.75	3.56-3.80	-	Rahmouni et al. (2013)
Shale	2.34±0.04	2.49±0.10	-	Sarkar et al. (2012)
Coal	1.93±0.05	1.52±0.04	-	
Granite	2.83±0.11	4.42±0.35	-	
Gypsum	2.3	3.08-3.40	-	Selçuk and Nar (2016)
Andesite	2.4	3.05-3.11	-	
Siltstone	2.5	3.67-3.71	-	
Dolomite	2.71-2.93	2.07-7.85	1.64-4.77	Tandon et al. (2013)
Gneiss	2.60-2.89	2.11-5.62	1.18-4.04	
Metabasics (Amphibolite, meta dolerite)	2.92-3.19	1.71-6.45	1.10-3.55	
Quartzite	2.57-2.76	2.11-5.53	0.99-3.96	

2.3 Effect of physical properties on ultrasonic pulse velocity

Assefa et al. (2003) study the relationship between the porosity and pulse velocity of limestones. The results indicate that the P-wave and S-wave decrease with increasing porosity. Aşcı et al. (2017) determine the physical properties such as density, void ratio, porosity, water absorption with ultrasonic pulse velocities that are used to develop relationship equation for UPV.

Gupta and Sharma (2012) study the correlation between textures and wave velocity for quartzite. It is found that textural parameters like grain size, aspect ratio and shape preferred orientation are related to the P-wave and S-wave velocities. All parameters increase with an increase in velocity.

Many researchers (Khandelwal and Singh, 2009; Azimian and Ajalloeian, 2015; Boulanouar et al., 2013; Kassab and Weller, 2015; Kurtulus et al., 2016b; Chawre, 2018; Aleeky and Hattamleh, 2018) have studied the relationship between pulse velocity and physical characteristics of rocks. It is concluded that physical properties are closely related to pulse velocity. Pulse velocity increases with an increase in the rock density. The pulse velocity decreases when increasing porosity. The results agree well with those of Rahmouni et al. (2013) who study relationship between wave velocities and density in saturated-dry condition of calcarenite rocks. The results indicate that the P-wave velocity is higher in the fully saturated state (Table 2.2).

Esamaldeen (2015) measure the P- and S- wave velocities of anisotropic rocks as a function of orientation of foliation plane ($\beta = 0^{\circ}$, 30°, 60° and 90°). Both waves display high wave velocities parallel to foliation always faster than those perpendicular to the foliation planes. The foliation of rock is the basis parameter causing anisotropy between two orthogonal directions. The results agree well with Kurtulus et al. (2012).

Song et al. (2004) determines the P- and S- wave velocities under hydrostatic confining pressures. The compressional and shear wave velocities increase with pressure which is mainly caused by progressive closure of microcracks which agree with obtained by Kern et al. (2009).

Table 2.2 Physical properties of calcarenite rocks (Rahmouni et al., 2013).

Sample	P-wave velocity, V_p (km/s)		Density, ρ (g/cm^3)	
	Dry	Saturated	Dry	Saturated
1	3.80	3.83	1.75	2.00
2	3.70	3.74	1.68	1.97
3	3.62	3.69	1.64	1.95
4	3.64	3.62	1.59	1.92
5	3.61	3.65	1.60	1.95
6	3.56	3.59	1.60	1.94

2.4 Effect of mechanical properties on ultrasonic pulse velocity

The relationship between P-wave velocity and mechanical properties of rocks have been studied more than decades by many researchers. Mostly, they found a positive linear relationship that the P-wave velocity increase of the mechanical properties. These include uniaxial compressive strength (Kahraman, 2001; Kurtulus et al., 2010 and Azimian et al., 2014), Young's modulus (Vasconcelos et al., 2008), point load strength (Rabat et al., 2020) and schmidt hardness (Aşcı et al., 2017). However, some mechanical properties found a negative linear with P-wave velocity that is Poisson's ratio (Khandelwal, 2013), as shown in Figure 2.2. Selçuk and Nar (2016) propose empirical relationships relating the P-wave with the uniaxial compressive strength of intact rocks. Good prediction is obtained.

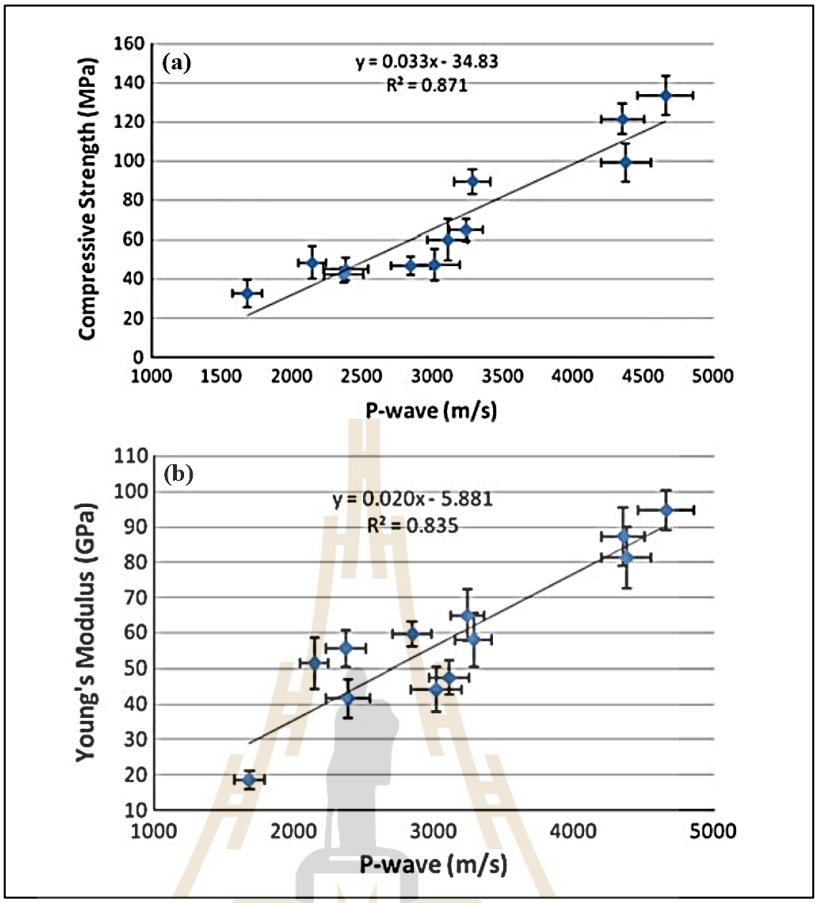

Figure 2.2 Relations of rock strength (a) and Young's modulus (b) with P-wave velocity (Khandelwal, 2013).

Kurtulus et al. (2016b) study the correlation between physico-mechanical properties; dry unit weight, P-wave velocity, compressive strength, point load strength index, effective porosity, tensile strength and Schmidt hardness of intact rocks by regression analysis. Statistical equations have been proposed for estimating rock the physico-mechanical properties. Kahraman (2001) correlated the UCS of different rock types with P-wave in according to the equation.

Majstorovic et al. (2019) establish the connection between the rock compressive strength with dynamic elastic modulus and P-wave. Dynamic elastic modulus is

calculated on the basis of the pulse velocities and density. The results indicate that compressive strength increases with increasing dynamic elastic modulus. Dynamic elastic modulus, P-wave and compressive strength have a good correlation. This agrees with the results obtained by Rabat et al. (2020), as shown in Figure 2.3.

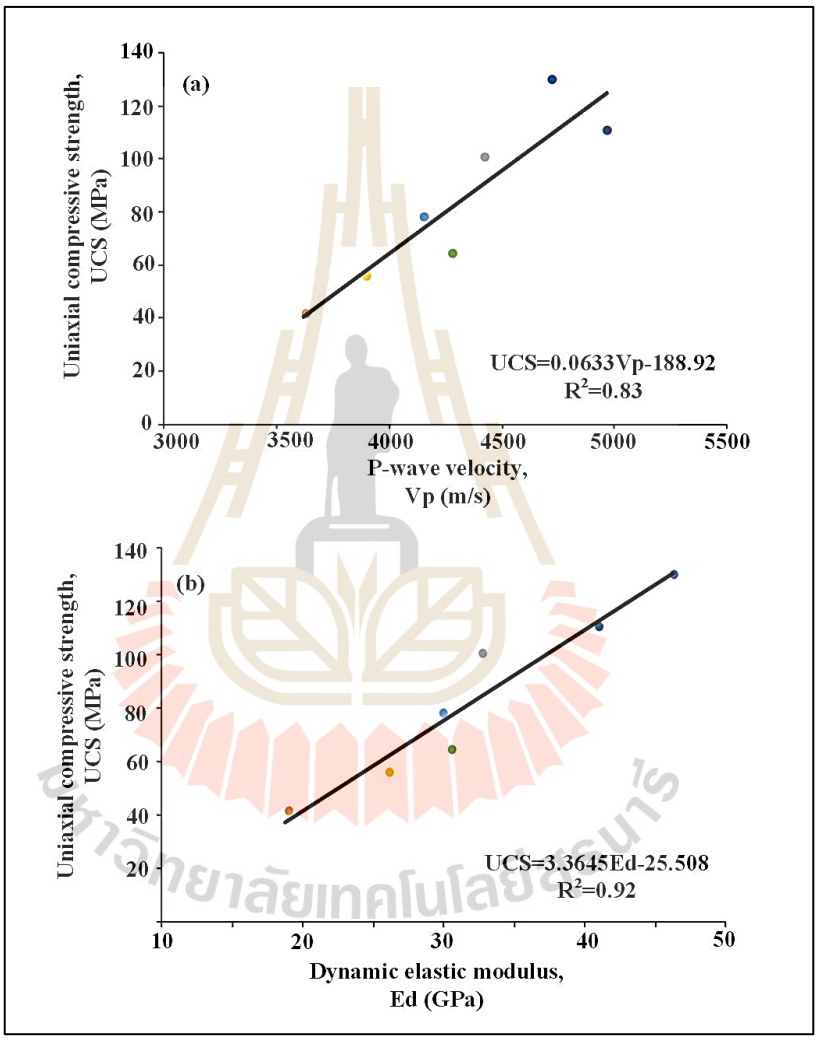

Figure 2.3 Rock strength as a function of P-wave velocity (a) and of dynamic elastic modulus (b) (Majstorovic et al., 2019).

Good correlations are also found between the static and dynamic properties of rocks (Starzec, 1999; Mockovciakova and Pandula, 2003; Moradian and Behnia, 2009;

Najibi et al., 2015; Onalo et al., 2018). Static elasticity modulus can be determined by using dynamic elasticity modulus (Soroush and Qutob, 2011). Static Young's modulus and Poisson's ratio are always less than those of the dynamic Young's modulus and Poisson's ratio (Yin et al., 2016; Blake et al., 2019), as shown in Figure 2.4.

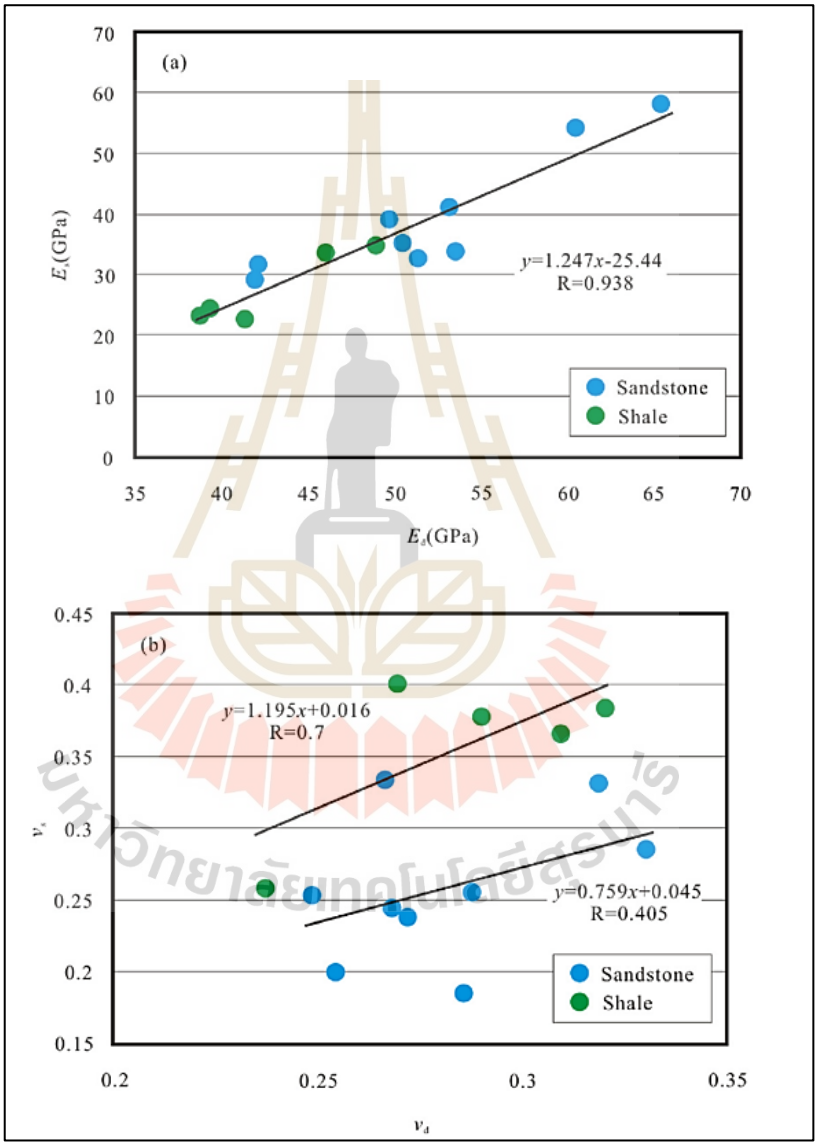

Figure 2.4 Static and dynamic Young's modulus (a), static and dynamic Poisson's ratio (b) (Yin et al, 2016).

2.5 Effect of mineral composition on ultrasonic pulse velocity

Carlson and Miller (2004) study the influence of pressure and mineralogy on pulse velocity in oceanic gabbro. P-wave and S-wave velocities measured at 200 MPa. The gabbro data line on the same trend as the minerals that comprise them (The primary minerals in oceanic gabbro are plagioclase, pyroxene, and olivine; some mineral compositions on pulse velocity as shown in Table 2.3.), suggesting that the properties of these rocks are controlled largely by their mineralogy as shown in Figure 2.5. Saxena et al. (2016) study the impact of mineralogy on P-wave and S-wave trends in nature. P-wave and S-wave trends are dominated by mineralogy, and the impact of the microstructure is less significant. This does not mean, that the microstructure has no effect on P-wave and S-wave, but only that it impacts P-wave and S-wave in a similar way. Fawad et al. (2011) uniaxial compression experiments on different types of sand show that porosity and pulse velocities (Vp and Vs) at any given effective stress level are dependent on grain size, sorting, shape and mineralogy.

Tandon and Gupta (2013) state that the petrophysical and mechanical properties are primarily controlled by its mineral constituents and various textural parameters. The role of plagioclase/quartz on the seismic wave velocity. The increase of plagioclase/quartz in rock results in an increase of wave velocity (Vp and Vs), as shown in Figure 2.6. This is because the Vp and Vs of quartz are 6050 m/s and 4090 m/s, and of feldspar are 6240 m/s and 3390 m/s. This perceptible because plagioclase has a higher density and velocity than quartz. This result agrees with other researchers on various rock types (Tugrul and Zarif, 1999; Rao et al., 2006).

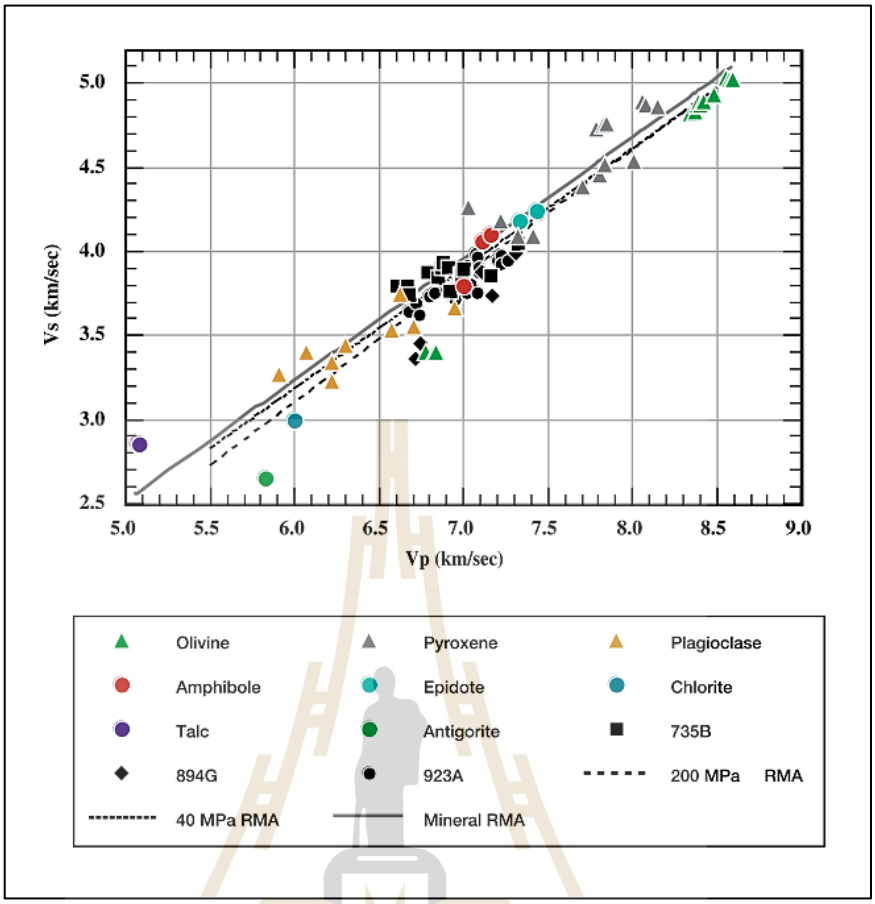

Figure 2.5 S-wave as a function of P-wave in selected minerals and gabbro (Carlson and Miller, 2004).

Table 2.3 Pulse velocity data from various researchers.

Mineral	P-wave (km/s)	S-wave (km/s)	Density (g/cm^3)	References
Dolomite	7.50	-	2.85	Palmstrøm (1995)
Magnetite	7.40	-	5.18	
Orthoclase	5.80	-	2.57	
Pyrite	8.00	-	5.02	
Albite	5.90	3.27	2.62	Carlson and Miller (2004)
Anorthite	6.95	3.66	2.76	
Antigorite	5.82	2.65	2.59	

Table 2.3 Pulse velocity data from various researchers (Cont.).

Mineral	P-wave (km/s)	S-wave (km/s)	Density (g/cm^3)	References
Augite	7.20	4.20	3.32	
Chlorite	5.42	3.32	3.06	
Epidote	7.33	4.18	3.5	
Forsterite	8.56	5.03	3.22	
Hornblende	7.16	4.10	3.25	
Talc	5.07	2.82	2.79	
Tremolite	7.10	4.06	2.98	
Amphibole	7.20	3.77	3.07	Kern et al. (2009)
Biotite	6.01	3.00	3.05	
Calcite	6.54	3.43	2.71	
Chlorite	6.01	3.00	3.00	
Diopside	7.80	4.45	3.27	
Garnet	8.50	4.80	4.32	
Graphite	11.64	6.95	2.25	
K-feldspar	5.93	3.26	2.56	
Muscovite	5.81	3.37	2.83	
Olivine	8.59	5.03	3.22	
Plagioclase	6.30	3.45	2.66	
Quartz	6.05	4.09	2.65	
Serpentine	5.85	3.00	2.59	
Tremolite	6.92	3.77	2.98	
Anhydrite	6.50	-	2.90	Jones et al. (2014)

Effect of petrographic variables on the uniaxial compressive strength has also been studied. Yilmaz et al. (2011) find negative correlations between K-feldspar content, grain size of K-feldspar, grain size of rock-forming minerals, quartz grain size

and uniaxial compressive strength. Yusof and Zabidi (2016) determined such relations by simple regression analysis. Abundance of quartz and feldspar can affect the rock strength. High content of mica minerals can decrease the strength of rocks.

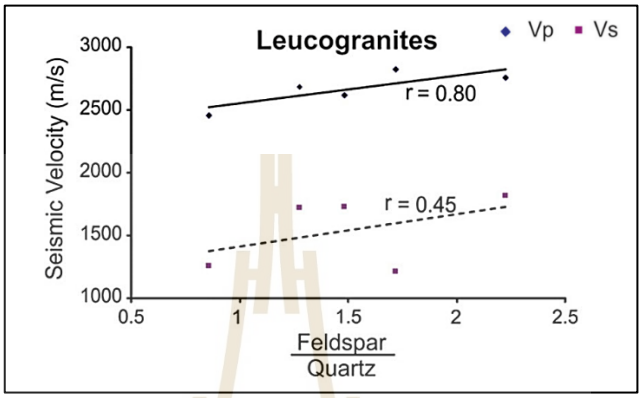

Figure 2.6 Seismic velocity as a function of feldspar/quartz (Tandon and Gupta, 2013).

2.6 Effect of porosity on ultrasonic pulse velocity

Pappalardo (2015) compare the relationship P-wave velocity with two methods for porosity (total porosity and effective porosity). The results show that total porosity show good correlation with P-wave than effective porosity. The effective porosity has volume, lower than total porosity, as shown in Figures 2.7 and 2.8. The total porosity (n) and effective porosity (n′) are calculated by the following formula:

$$n = (1 - \rho_{bulk} / \rho_r) \times 100 \quad (2.1)$$

where ρ_{bulk} (bulk density) is a measure of the mass of the rock per unit volume (solids + pore space), ρ_r is the volumetric mass density (mass per unit volume).

$$\rho_{bulk} = m_s / m_h \times \rho_{rh} \quad (2.2)$$

where m_d is the dry mass of the specimen, m_s is the wet mass of the specimen, m_h is the hydrostatic weight of the specimen, and ρ_{rh} is the density of water.

$$n' = \left(m_s - m_d / m_s - m_b\right) \times 100 \tag{2.3}$$

Esteban et al. (2015) experiments the water porosity by measuring the weight of the sample before and after saturation to compare the helium gas or mercury porosity form helium expansion is monition and the pore volume of rock sample, as a result both volume of porosity method are similar results.

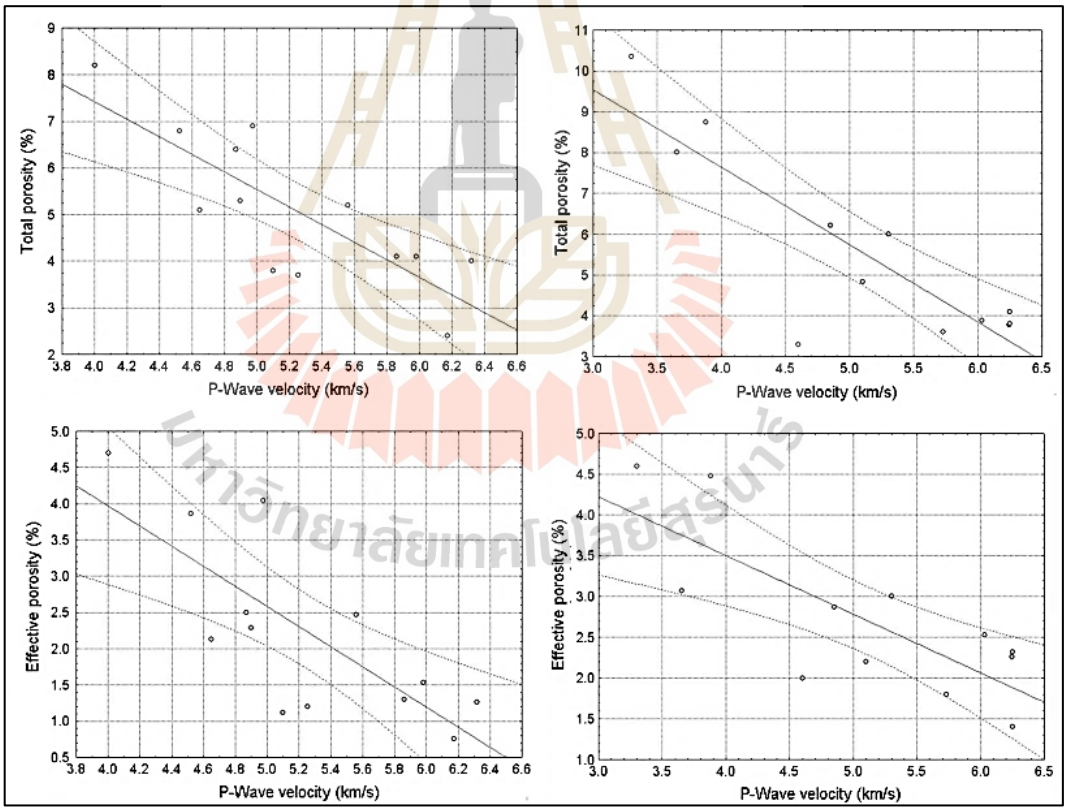

Figure 2.7 Total porosity and effective porosity as a function of P-wave velocity (Pappalardo, 2015).

Baechle et al. (2004) correlation the P-wave velocity with both macroporosity (helium porosity) and microporosity (image porosity) from thin section analysis in carbonate rocks. The results show that correlation between microporosity to P-wave velocity is much higher and better than the correlation of total porosity to P-wave velocity, the helium porosity shows estimate porosity higher than image porosity.

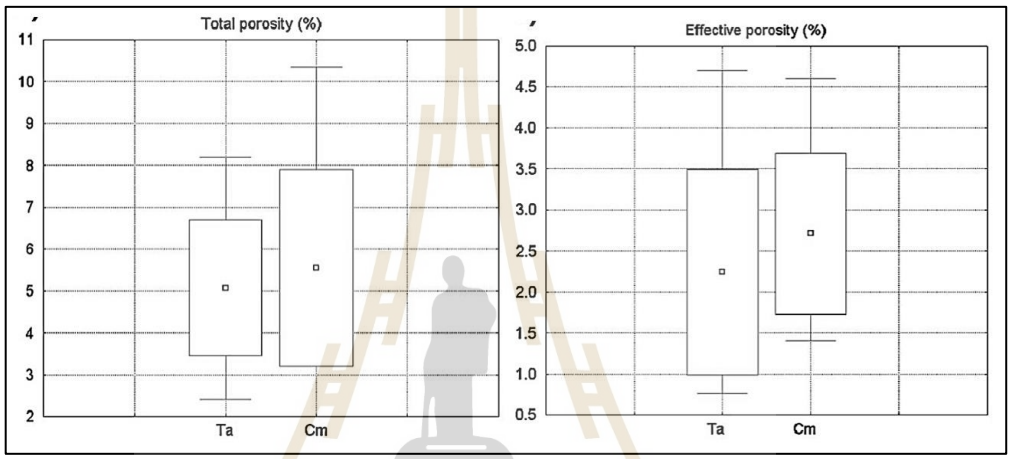

Figure 2.8 Box plots total porosity and effective porosity (Ta taomina, Cm Castelmola) (Pappalardo, 2015).

CHAPTER III

SAMPLE PREPARATION

3.1 Introduction

This chapter describes information of each rock types, sample preparation for the compression test and ultrasonic pulse velocity test. Mineral compositions of some specimens are determined by x-ray diffraction analysis.

3.2 Rock sample

Twenty-two rock types have been selected for this study. They are divided into six main groups: plutonic, volcanic, carbonate clastic, sulfate and silicate groups. These rocks represent the exposed outcrops that are commonly found in Thailand. The classification of each rock group is performed by texture, mineral compositions and origin. Table 3.1 gives rock types, locations from which they have been collected in Thailand and Laos and formations to which they belong. A map shown in Figure 3.1 gives the locations where the rock samples have been obtained in Thailand. The key criterion of sample selection is that the rock matrix should be as homogeneous as possible. This is to minimize the intrinsic variability of the test results.

Table 3.1 Rock samples used in this study.

Group	Rock Type	Code	Rock Unit	Location	Period
Plutonic	Diorite	Trgr	Khao Phra Ngam Unit	Lopburi	Triassic
	Granite	Cgr	Tak Batholith	Tak	Carboniferous-Cretaceous
	Granite	Kgr	Unknow	Ranong	Cretaceous
	Granite	Mz1	Unknow	Laos	Cretaceous-Permian
Volcanic	Basalt	Qbs	Buriram Basalt Unit	Buriram	Quaternary
	Vesicular Basalt	Qbs	Buriram Basalt Unit	Nakhon Ratchasima	
	Andedsite	PTrv	Undifferentiated Volcanic Rock	Saraburi	Permian-Triassic
	Ryorite	PTrv			
	Tuff	PTrv			
Carbonate	Marble	Pkd	Khao Khad Formation	Lopburi	Permain
	Travertine	Pkd	Khao Khad Formation	Saraburi	
	Limestone	Pkd			
	Limestone	Trls	Limestone Unit	Tak	Triassic
	Limestone	Mz1	Unknow	Laos	Julassic-Cretaceous
Clastic	Calcareous Lithic Sandstone	Jpk	Phu Kradung Formation	Nakhon Ratchasima	Jurassic
	Quartz Sandstone	Kpp	Phu Phan Formation		Cretaceous-Jurassic
	White Quartz Sandstone	JKpw	Phra Wihan Formation		Cretaceous
	Sandstone	Mz1	Unknow	Laos	
Sulfate	Anhydrite	Tkb	Krabi Group	Suratthani	Tertiary
	Gypsum	Tkb			
Silicate	Pyrophyllite	PTrv	Undifferentiated Volcanic Rock	Saraburi	Permian-Triassic
	Dickite	PTrv			

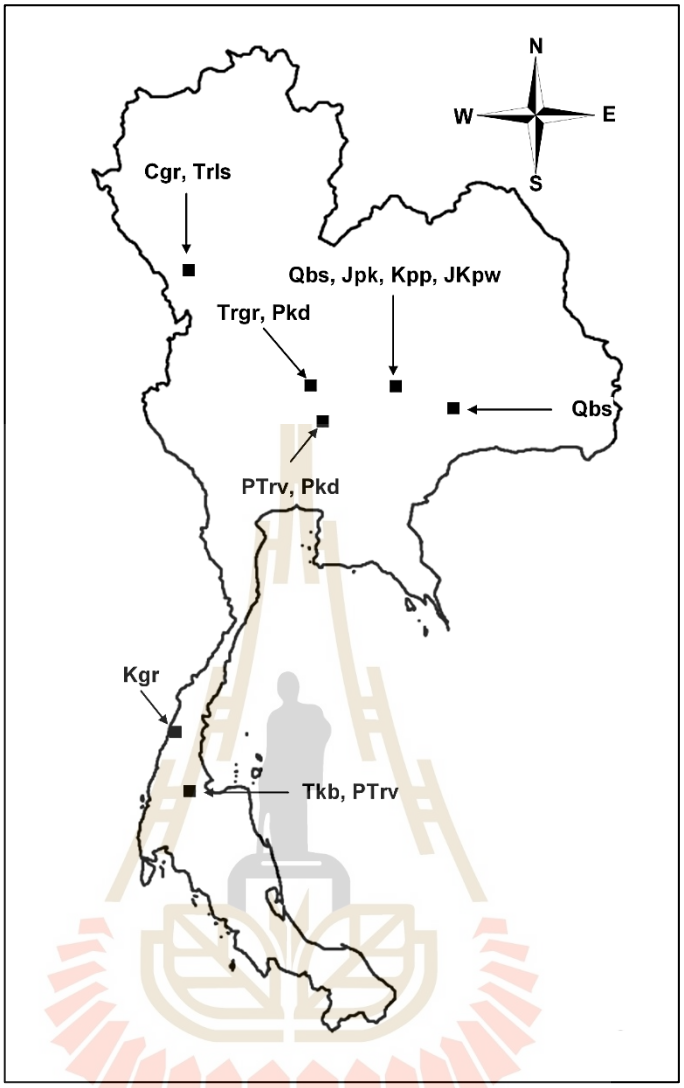

Figure 3.1 Locations where the rock samples are obtained.

3.3 Sample preparation

The cylindrical specimens used in this study having nominal length-to- diameter ratios (L/D) of 2.0 and 2.5, with diameter of not less than 47 mm (ASTM D4543-07) are prepared with bedding planes normal to the core axis plane (Figure 3.2). The ends of specimens are cut and grind to obtain the flat and smooth ends. A total of 206 samples have been prepared. Tables 3.2 through 3.7 summarize physical properties of specimens including rock types, weights, lengths, dimensions.

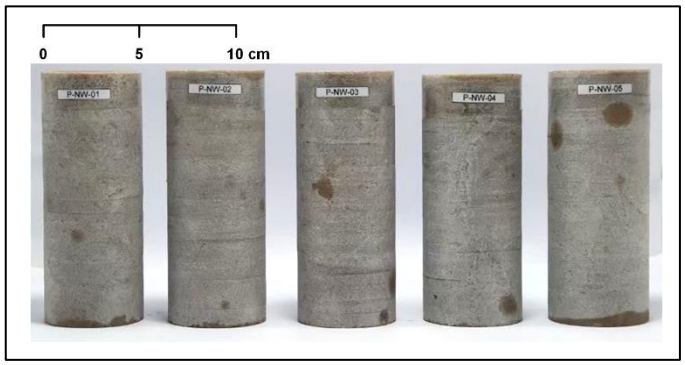

Figure 3.2 Examples of cylindrical specimens used in this study.

The cylindrical specimens were tested, and after the failure, Representatives of each rock type performed on crushed into fine power (Figure 3.4) (with less than 2 μm in size) for the X-ray diffraction analysis (XRD) which powder is then spread uniformly over the surface of a glass slid, using a small amount of adhesive binder. The instrument is so constricted that this slide, when clamped in place, rotates in the path of collimated X-ray beam while a counting tube, mounted on an arm, rotates about is to pick up the reflected X-ray beam. The samples were analyzed at The Center of Scientific and Technological Equipment, Suranaree University of Technology. The mineral compositions determined are used as data basis to correlate with the mechanical properties and the wave velocities.

Figure 3.3 Rock power prepared for XRD analysis.

Table 3.2 Plutonic group specimens.

Plutonic Group	Weight (g)	Length (mm)	Diameter (mm)
Diorite (Trgr)	648.30	110.40	54.00
	646.83	120.46	54.00
	646.83	109.00	54.00
	793.51	133.32	54.00
	799.97	134.32	54.00
	654.24	109.72	54.00
	641.33	107.00	54.00
Granite (Kgr)	556.71	94.30	54.50
	804.19	135.00	54.50
	823.20	136.20	54.72
	831.99	137.00	54.50
	829.00	136.38	54.50
Granite (Cgr)	765.47	131.00	54.00
	800.28	135.58	54.00
	643.77	109.00	54.00
	641.53	108.62	54.00
	641.77	108.62	54.00
	813.66	136.60	54.12
	789.25	131.48	54.32
	751.18	119.00	55.70
	801.46	137.74	53.40
	803.00	134.00	54.18
	760.80	126.48	54.00
Granite (Mz1)	1019.83	133.00	61.20
	1150.27	149.80	61.20
	1148.82	148.80	61.20
	1106.77	143.80	61.00

Table 3.2 Plutonic group specimens (Cont.).

Plutonic Group	Weight (g)	Length (mm)	Diameter (mm)
Granite (Mz1)	645.62	107.00	54.00
	1162.57	150.00	61.20
	647.02	107.00	54.00
	648.36	107.70	53.80
	1185.25	153.50	60.80
	656.67	109.00	53.70

Table 3.3 Volcanic group specimens.

Plutonic Group	Weight (g)	Length (mm)	Diameter (mm)
Basalt (Qbs)	878.87	110.30	54.10
	887.96	137.60	54.00
	863.87	133.80	54.00
	882.65	136.68	54.00
	875.52	136.58	54.00
	875.52	135.50	54.00
	724.43	111.70	54.10
	878.87	135.40	54.00
	712.70	135.90	54.00
Andesite (PTrv)	824.03	134.70	824.03
	806.91	131.90	806.91
	830.75	135.70	830.75
	813.51	132.60	813.51
	839.88	131.80	839.88
	937.88	136.00	937.88
	1435.98	156.60	1435.98
	938.13	136.00	938.13
	899.50	136.48	899.50

Table 3.3 Volcanic group specimens (Cont.).

Plutonic Group	Weight (g)	Length (mm)	Diameter (mm)
Andesite (PTrv)	874.44	126.82	874.44
	1451.12	156.60	1451.12
	868.80	131.84	868.80
	939.68	135.80	939.68
	910.95	131.00	910.95
Rhyorite (PTrv)	842.79	137.20	55.34
	649.43	107.60	54.70
	787.12	132.70	54.00
	817.65	135.86	54.38
	818.40	135.00	54.52
	616.35	100.90	54.70
	834.18	135.54	54.54
	816.37	135.00	54.42
	812.23	134.22	54.42
	801.25	134.72	53.92
	807.57	135.32	54.00
	668.39	109.00	54.70
	811.93	137.20	54.48
	811.93	135.72	54.00
	833.14	136.68	54.46
	767.22	128.12	53.90
	668.14	108.50	54.60
	675.65	109.60	54.60
	821.77	136.28	54.00
	812.23	137.46	54.40

Table 3.3 Volcanic group specimens (Cont.).

Plutonic Group	Weight (g)	Length (mm)	Diameter (mm)
Vesicular Basalt (Qbs)	745.65	134.00	54.86
	636.04	111.20	54.80
	745.04	132.30	54.08
	768.79	136.78	54.00
	694.31	123.16	54.08
	659.08	115.92	53.90
	768.01	134.82	53.90
Tuff (PTrv)	739.84	115.20	54.32
	709.90	110.40	54.32
	849.78	134.64	53.62
	763.79	118.68	54.00
	687.46	108.40	53.58

Table 3.4 Carbonate group specimens.

Plutonic Group	Weight (g)	Length (mm)	Diameter (mm)
Marble Pkd	741.56	110.24	54.00
	741.56	113.00	55.70
	839.72	135.50	54.00
	712.91	131.00	53.26
	716.63	108.00	55.50
	794.45	129.00	53.32
	672.62	108.50	55.00
	839.40	128.80	54.50
	887.74	135.20	54.68
	887.74	118.52	53.00

Table 3.4 Carbonate group specimens (Cont.).

Plutonic Group	Weight (g)	Length (mm)	Diameter (mm)
Travertine Pkd	751.18	118.00	55.50
	729.87	118.50	55.32
	751.18	118.00	55.00
	846.79	134.42	54.42
	663.33	107.40	53.82
	669.29	107.38	54.00
	842.19	134.86	53.76
	841.10	133.38	54.00
	809.30	129.10	53.80
	845.20	134.12	53.90
	853.49	134.92	54.00
Limestone (Mz1)	907.43	134.98	54.16
	885.25	135.90	55.34
	862.57	134.70	54.70
	883.68	131.90	54.00
	876.78	135.70	54.38
	891.50	132.60	54.52
	895.57	131.80	54.70
	810.35	136.00	54.54
	835.05	132.70	54.00
	806.70	135.86	54.62
	819.83	135.00	62.90
	865.95	134.86	54.00
Limestone (Trls)	818.87	136.52	54.12
	795.01	132.36	53.66
	678.33	112.56	53.44
	808.04	135.00	53.12
	832.85	138.64	53.00

Table 3.4 Carbonate group specimens (Cont.).

Plutonic Group	Weight (g)	Length (mm)	Diameter (mm)
Limestone (Pkd)	886.30	156.70	62.90
	1315.89	158.30	62.80
	1299.35	156.20	62.80
	832.40	135.50	53.52
	836.10	136.00	53.52
	829.52	134.82	53.52
	828.91	134.50	53.52

Table 3.5 Clastic group specimens.

Plutonic Group	Weight (g)	Length (mm)	Diameter (mm)
Sandstone (Mz1)	686.55	127.39	51.39
	687.83	127.35	51.36
	692.90	127.24	51.32
	686.20	125.77	51.58
	700.50	90.50	51.39
	692.90	126.75	51.44
	694.10	119.47	51.11
	614.45	110.82	51.54
	700.50	127.85	51.19
	687.75	127.28	51.01
Sandstone (Jpk)	773.87	136.60	54.00
	767.60	135.00	54.00
	616.61	108.00	54.00
	633.42	110.00	54.00
	741.00	128.66	54.00
	895.37	145.18	55.64
	895.37	105.50	54.00

Table 3.5 Clastic group specimens (Cont.).

Plutonic Group	Weight (g)	Length (mm)	Diameter (mm)
Sandstone (Kpp)	671.40	120.08	55.64
	725.75	136.00	54.00
	761.63	137.22	55.00
	762.00	137.18	54.92
	581.38	108.00	54.00
	566.80	98.54	55.66
	764.90	137.00	54.80
	599.05	110.00	54.00
	716.90	131.60	54.00
	591.13	108.34	54.00
Sandstone (JKpw)	564.00	108.00	54.00
	702.17	137.16	54.00
	677.90	132.00	54.00
	693.28	134.30	54.00
	560.33	108.44	54.00
	552.46	109.00	54.00

Table 3.6 Sulfate group specimens.

Plutonic Group	Weight (g)	Length (mm)	Diameter (mm)
Anhydrite (Tkb)	809.03	136.00	54.00
	809.03	124.00	54.00
	876.52	122.00	54.00
	800.73	122.20	54.00
	813.18	124.00	54.00
	800.73	119.30	54.00
	904.73	136.88	54.00
	796.52	134.42	54.00

Table 3.6 Sulfate group specimens (Cont.).

Plutonic Group	Weight (g)	Length (mm)	Diameter (mm)
Gypsum (Tkb)	603.86	110.60	54.00
	603.86	118.50	54.00
	555.77	108.00	54.00
	555.77	109.00	54.00
	553.95	108.16	54.00
	563.52	132.82	54.00
	559.16	108.40	54.00
	550.39	108.44	54.00

Table 3.7 Silicate group specimens.

Plutonic Group	Weight (g)	Length (mm)	Diameter (mm)
Pyrophyllite (PTrv)	810.03	134.32	55.00
	784.92	132.60	54.22
	810.03	136.60	54.26
	794.98	132.00	54.52
	669.38	111.30	54.48
	756.61	127.00	54.22
	786.60	132.30	54.14
	713.44	119.80	54.16
	791.90	133.46	54.00
	793.81	133.42	54.06
	768.16	130.00	53.82
	789.43	133.20	53.90
	706.10	118.62	54.00
	802.71	135.20	53.90
	784.92	134.40	53.80
	803.47	135.30	53.90

Table 3.7 Silicate group specimens (Cont.).

Plutonic Group	Weight (g)	Length (mm)	Diameter (mm)
Pyrophyllite (PTrv)	764.37	128.06	53.88
	760.69	128.00	53.74
	802.06	135.00	53.72
	811.83	124.76	53.72
Dickite (PTrv)	800.49	138.18	53.34
	743.06	128.74	53.00
	802.96	138.00	53.00

CHAPTER IV

LABORATORY TESTING AND RESULTS

4.1 Introduction

This chapter describes the method and results of the laboratory experiments, including physical properties (density and effective porosity) test, ultrasonic pulse velocity measurement, uniaxial compression test, and X-ray diffraction analysis. A new technique is proposed here to obtain true porosity of the samples by calculating from mineral compositions of rocks.

4.2 Physical property

4.2.1 Density

The density of the specimens is determined based on the ASTM D6473 (2015) standard practice which can be calculated as:

$$\rho = (W_{rock} \times \rho_{water}) / (W_{rock} - W_{sub}) \quad (4.1)$$

where ρ is density of specimen (g/cc), W_{rock} is mass of oven-dry test specimen in air (g), W_{sub} is buoyant mass of submerged test specimen in water (g) and ρ_{water} is density of water (g/cc).

The density test results are shown in Figure 4.1 (details in Appendix A, Tables A.1 through A.6). The density (ρ) of all rock groups ranges from 2.01 to 2.77 g/cc. The volcanic group show the largest fluctuation of the density which range from

2.50 to 2.76 g/cc. The andesite (PTrv) indicates the highest fluctuation density in the group as compared to all rock types of this study.

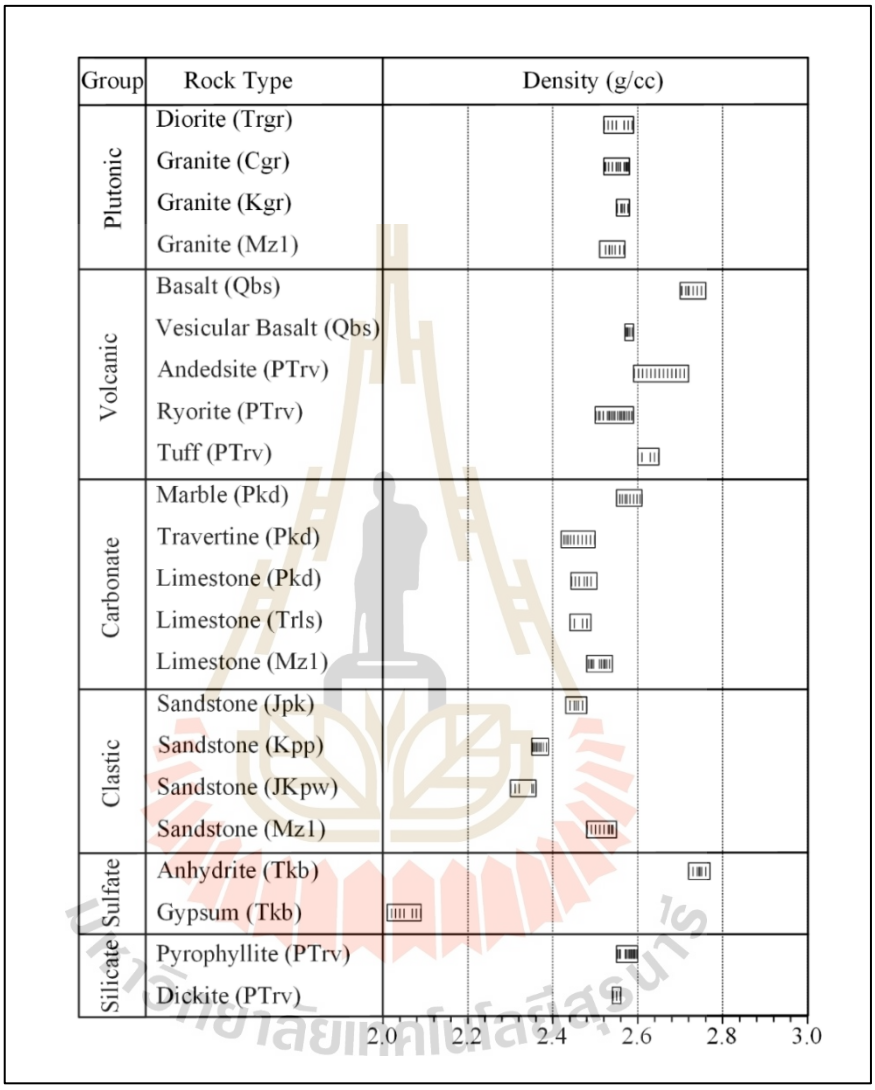

Figure 4.1 Ranges of specimens' densities for this study.

4.2.2 Effective porosity

All rock specimens are submerged under water in pressure vacuum chamber until its weight becomes unchanged. The negative pressure of -1 atm is used.

These specimens are referred to as saturated specimens (Figure 4.2). Effective porosity is calculated from (ASTM C97 (2002)):

$$n_e = (V_v / V) \times 100 \quad (4.2)$$

where n_e is effective porosity of specimen (%), V_v is pore volume of specimen (cm^3) and V is sample bulk volume (cm^3).

The pore and volumes are calculated by:

$$V_v = (W_{sat} - W_{rock}) / \rho_{water} \quad (4.3)$$

$$V = (W_{sat} - W_{sub}) / \rho_{water} \quad (4.4)$$

where W_{sat} is saturated-surface-dry mass (g).

The effective porosity test results are shown in Figure 4.3 (details in Appendix A, Tables A.1 through A.6). The effective porosity of all rock groups ranges from 0.03 to 12.15 %. The clastic and sulfate groups show high fluctuation of the porosities. Sandstone (JKpw) have the highest effective porosity and limestone (Mz1) have the lowest effective porosity.

The density and porosity are an important factor affecting wave velocity moving through the specimen (Kassab and Weller, 2015).

Figure 4.2 Rock specimens submersed under water in vacuum chamber.

4.3 Ultrasonic pulse velocity measurement

Wave velocity measurement was performed on the cylindrical shaped specimens with L/D = 2.0 - 2.5 by using Sonic viewer 170 (Model 5338) as shown in Figure 4.4. The direct transmission method was conducted for measuring of P- and S-waves velocities of the specimen. The end faces of the specimens were flattened and smooth to provide tight contacts of transducers. The test procedures and calculation follow the ASTM D2845 (2008) standard practice. Wave velocity through the specimen is calculated from the travel time from the generator to the receiver at the opposite ends. Using the measured wave velocity and density, the dynamic mechanical properties can be calculated as follows:

$$E_d = [\rho V_s^2 (3V_p^2 - 4V_s^2) / (V_p^2 - V_s^2)] \quad (4.5)$$

$$\nu_d = (V_p^2 - 2V_s^2) / [2(V_p^2 - V_s^2)] \quad (4.6)$$

where V_p is P-wave velocity (km/s), V_s is S-wave velocity (km/s), E_d is dynamic young's modulus (GPa) and ν_d is dynamic Poisson's ratio.

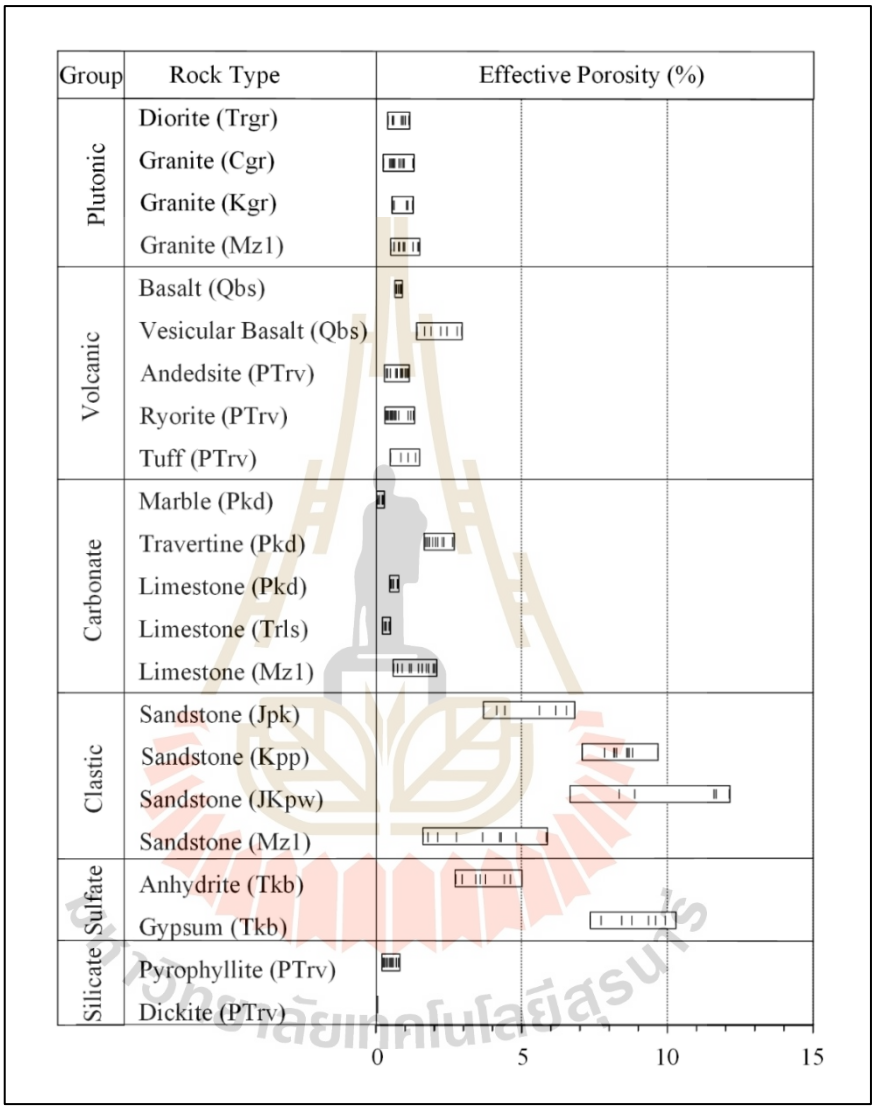

Figure 4.3 Ranges of effective porosity for this study.

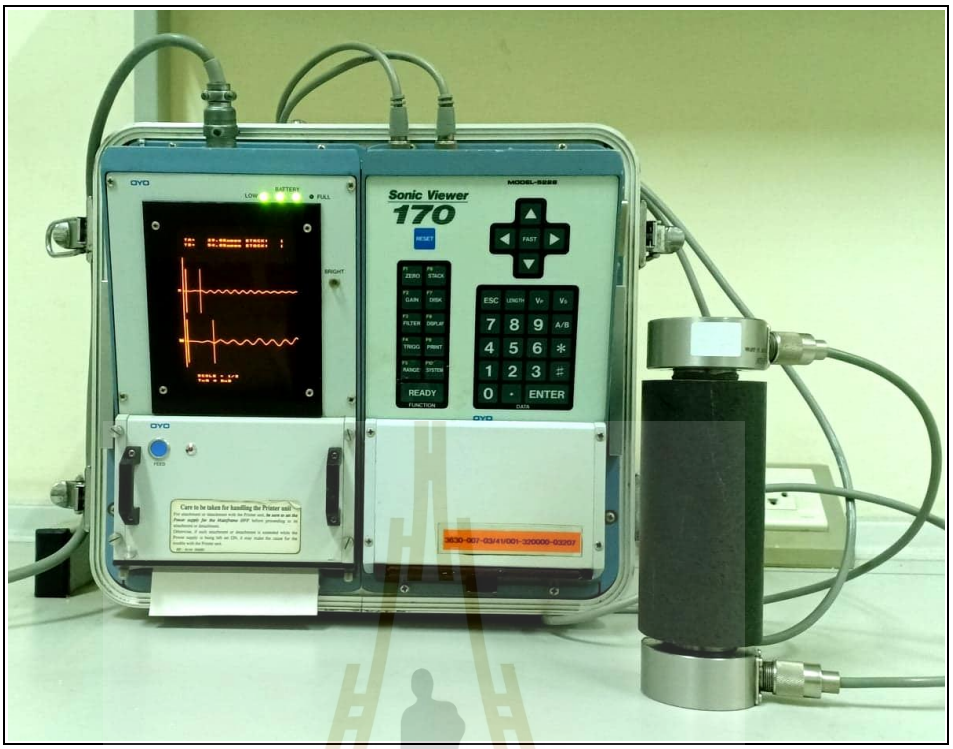

Figure 4.4 Wave velocity measurement device.

The wave velocities test results are shown in Figure 4.5 (details in Appendix A, Tables A.1 through A.6). The P-wave velocity of all rock groups ranges from 3.16 to 4.17 km/s, S-wave velocity ranges from 1.78 to 2.68 km/s. The largest fluctuations of both wave velocities seem to be the volcanic group. The andesite (PTrv) have highest wave velocity and gypsum (Tkb) have lowest wave velocity.

The dynamic Young's modulus (Figure 4.6) and dynamic Poisson's ratio (Figure 4.7) of all rock groups range from 16.20 to 45.52 GPa and 0.15 to 0.27, respectively. The fluctuations of the dynamic Young's moduli and Poisson's ratio depend on the P-wave and S-wave velocities results. The details are summarized in Appendix A, Tables A.1 through A.6).

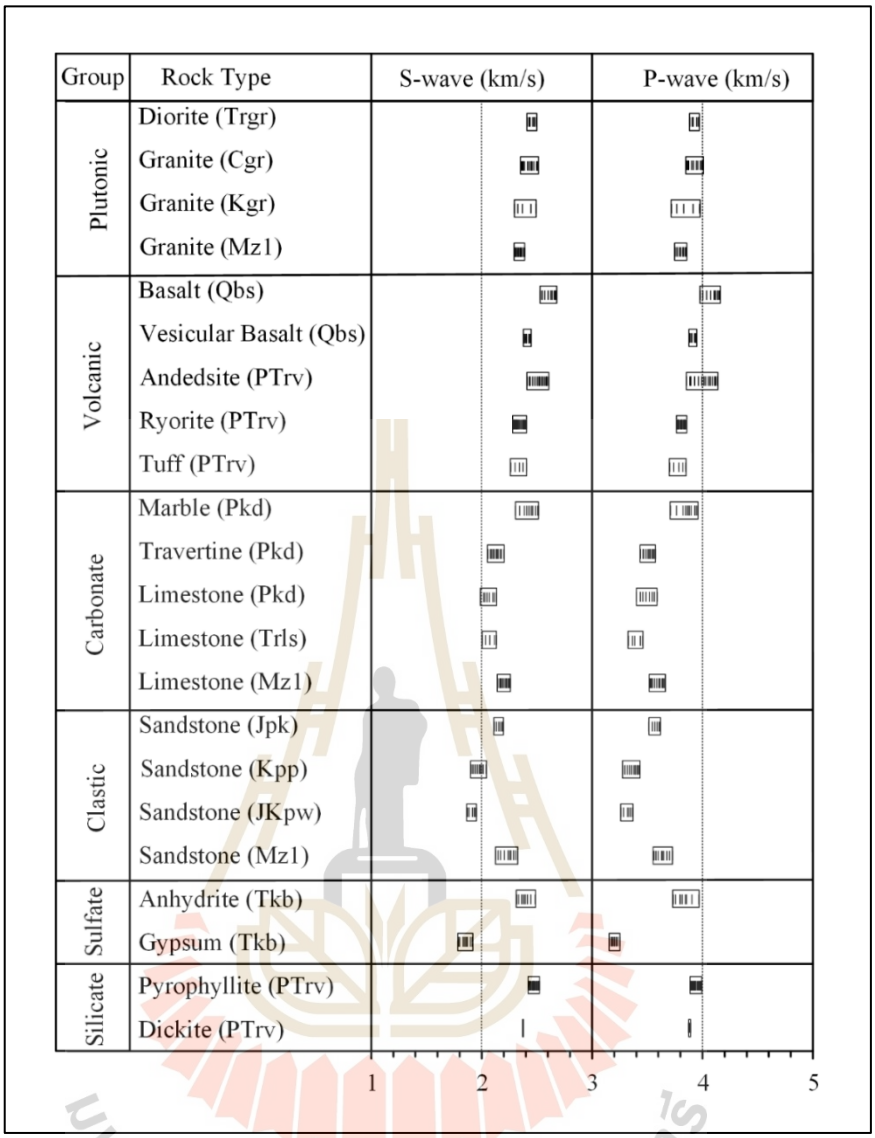

Figure 4.5 Ranges of P-wave and S-wave velocities for this study.

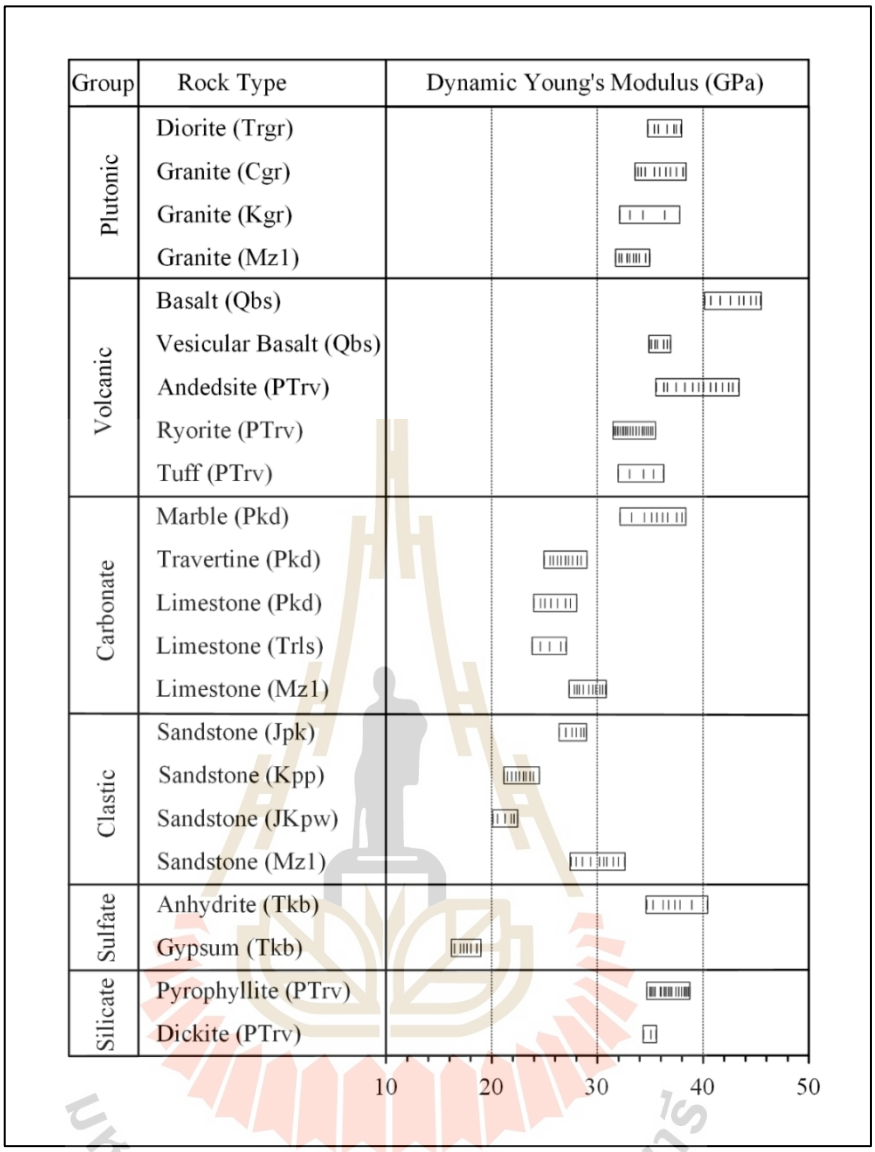

Figure 4.6 Ranges of dynamic Young's modulus for this study.

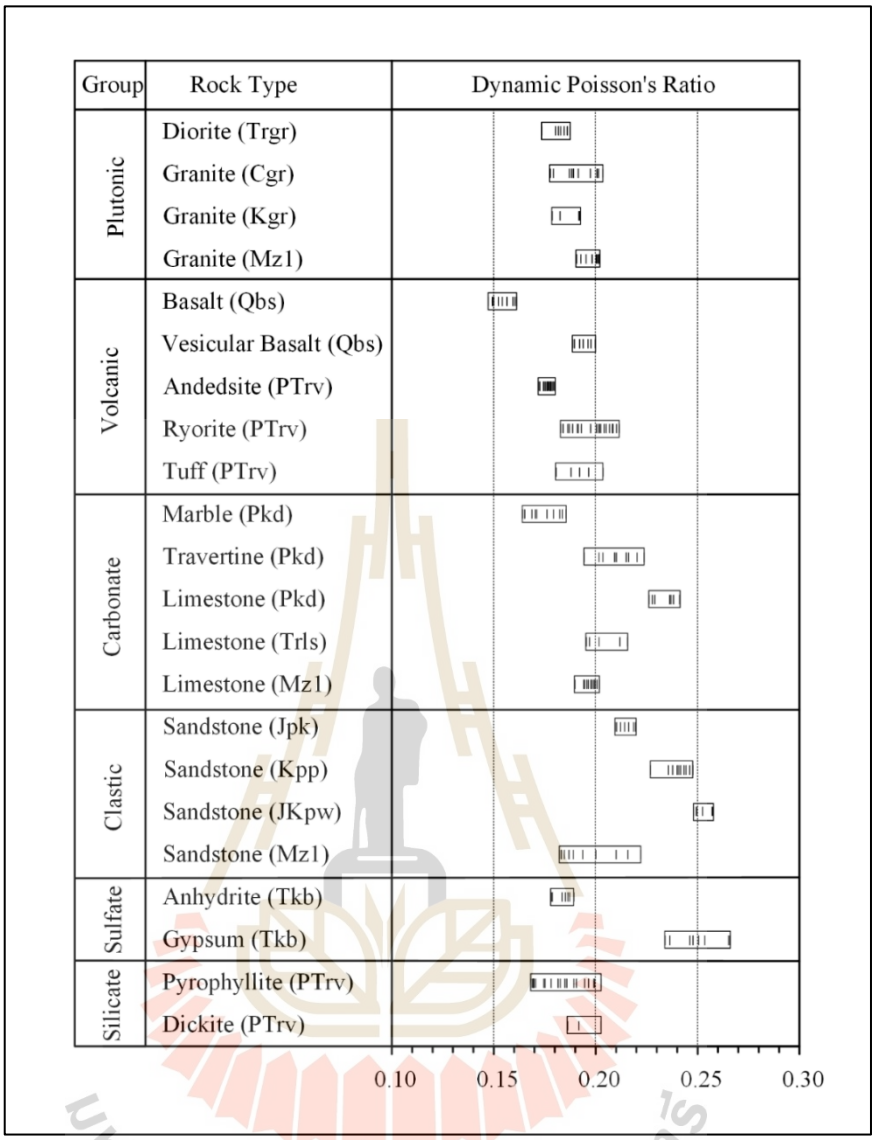

Figure 4.7 Ranges of dynamic Poisson's ratio for this study.

4.4 Uniaxial compressive strength test

The uniaxial compressive strength (UCS) test procedure and calculation follow the ASTM D7012 (2014) standard practice (Figure 4.8). In this study, the cylindrical specimens with a nominal diameter of 54 mm and length-to-diameter ratio of 2.0 - 2.5 are axially loaded until failure. Figure 4.9 shows an example of specimens before and after subjecting to UCS testing. The static Young's modulus (E_s) and

Poisson's ratio (ν_s) are calculated from the stress-strain curves at about 50% of the maximum stress level. The results obtained from the testing with standard deviations and stress-strain curves are given in Appendix A, Figures A.1 through A.6.

The uniaxial compressive strengths of all rock groups range from 5.91 to 132.40 MPa, as shown in Figure 4.10. The most fluctuations of the strength and the highest strength are found in igneous rocks (plutonic and volcanic groups). The static Young's moduli (Figure 4.11) of all rock groups range from 5.18 to 24.61 GPa. The static Poisson's ratio (Figure 4.12.) ranges from 0.15 to 0.23. The sandstone (JKpw) has the highest and andesite (PTrv) has the lowest static Poisson's ratio. The detailed of static mechanical properties results are given in Appendix A, Tables A.1 through A.6.

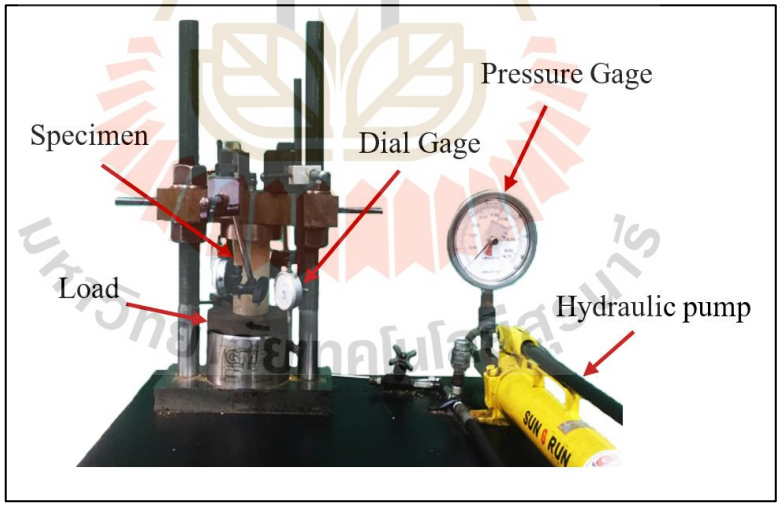

Figure 4.8 Uniaxial compression test device.

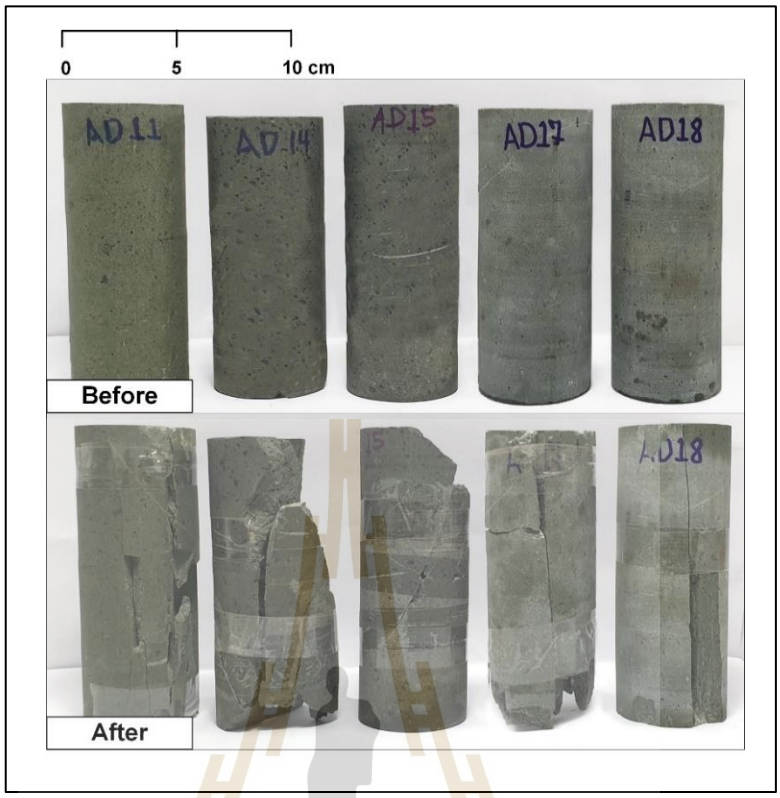

Figure 4.9 Example of andesite specimens before and after subjecting to uniaxial compression testing.

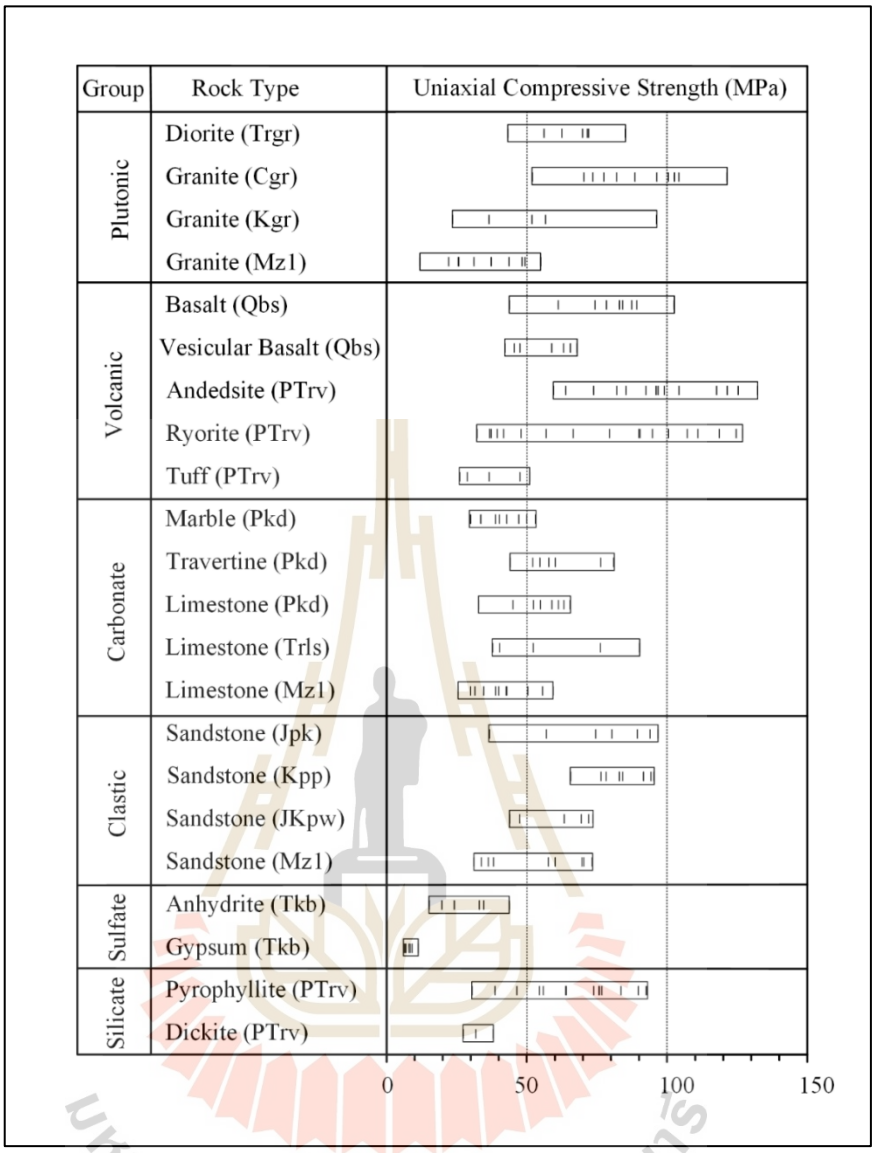

Figure 4.10 Ranges of uniaxial compressive strength (σ_c) for this study.

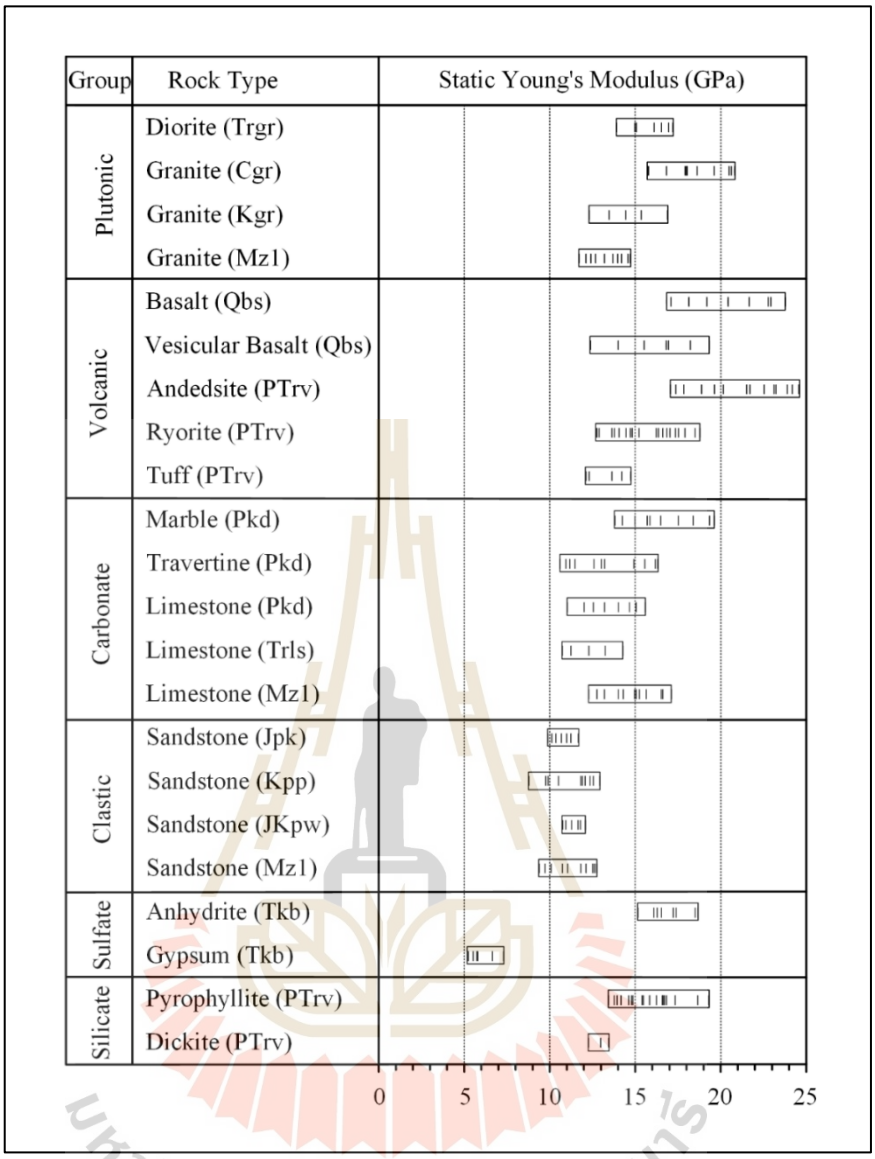

Figure 4.11 Ranges of static Young's modulus (E_s) for this study.

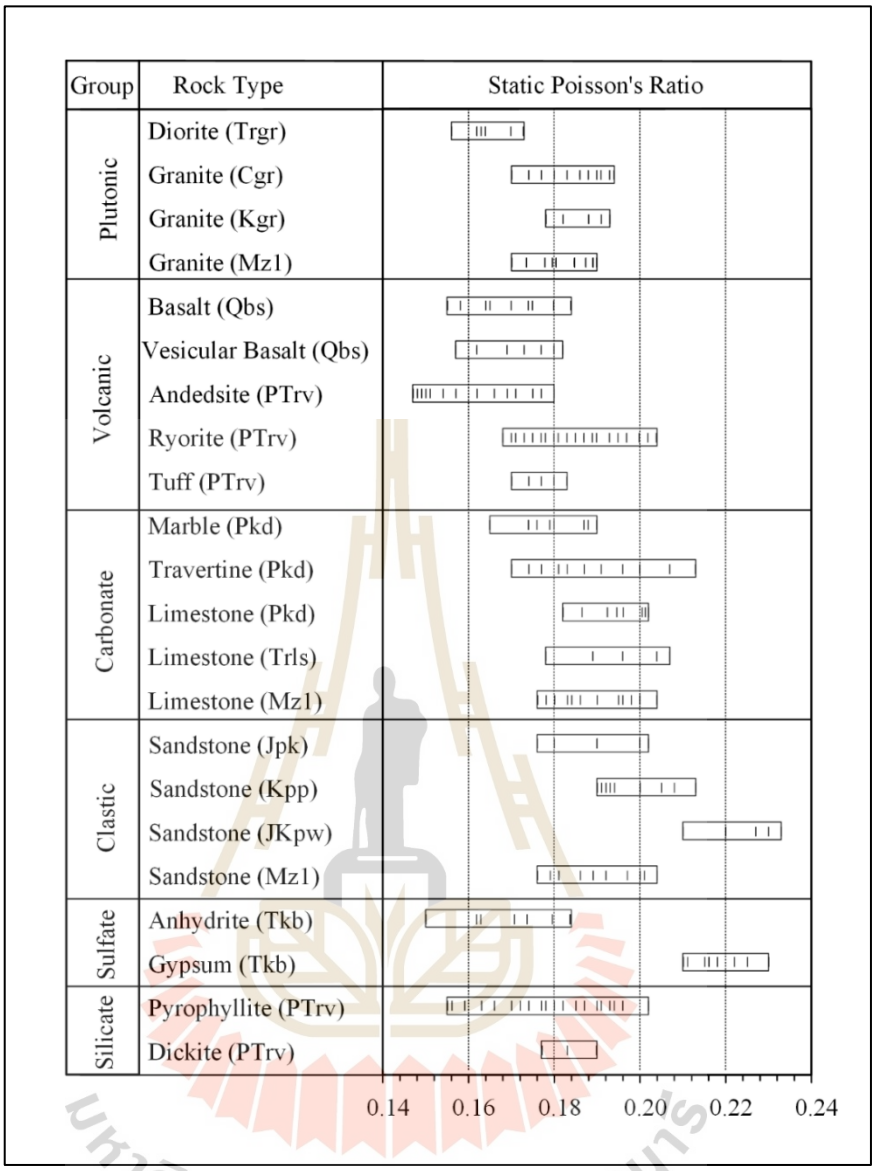

Figure 4.12 Ranges of static Poisson's ratio (ν_s) for this study.

4.5 X-ray diffraction analysis

The specimens after subjecting to the UCS test, is ground to obtain power with particle sizes of less than 0.25 mm (ASTM E1426-14e1 (2019)) (pass mesh #60). The specimen is used to determine collected mineral compositions by using X-ray diffraction method (XRD) (Figure 4.13). Individual mineral values cannot be evaluated from natural rock samples, but the overall performance of the technique can

be judged by the departure of sum from 100%. The results are shown in Tables 4.1 through 4.6.

Figure 4.13 X-ray diffractrometer-D2 phaser.

Table 4.1 Mineral compositions of rock specimens in plutonic group.

Rock Type	Density (g/cc)	Mineral Compositions (%)							
		Quartz	Muscovite	Chlorite	Albite	Orthoclase	Anorthite	Diopsite	Microcline
Diorite (Trgr)	2.52	44.83	6.28	3.65	22.60	15.30	3.69	3.65	0.00
	2.55	44.81	6.31	3.66	22.58	15.29	3.63	3.72	0.00
	2.59	41.45	4.38	4.16	15.12	12.21	14.83	7.85	0.00
Granite (Kgr)	2.55	15.21	17.96	0.73	39.44	11.53	11.03	4.10	0.00
	2.58	38.87	11.04	0.99	17.79	15.97	9.42	5.92	0.00
Granite (Cgr)	2.52	36.22	5.53	1.71	17.17	27.28	10.28	1.81	0.00
	2.54	29.99	5.96	1.04	16.80	29.13	13.86	3.22	0.00
	2.57	29.75	8.83	0.88	20.72	25.24	11.18	3.40	0.00
	2.58	19.19	10.40	1.13	20.34	35.98	7.69	5.27	0.00
Granite (Mz1)	2.51	40.07	0.33	1.36	21.64	0.00	2.27	2.76	31.57
	2.57	58.82	0.59	1.18	28.52	0.00	0.00	8.74	2.15

Table 4.2 Mineral compositions of rock specimens in carbonate group.

Rock Type	Density (g/cc)	Mineral Compositions (%)						
		Calcite	Quartz	Dolomite	Chalcopyrite	Fluorite	Microcline	Actinolite
Marble (Pkb)	2.55	95.12	0.21	3.24	1.43	0.00	0.00	0.00
	2.57	94.68	0.30	3.70	1.32	0.00	0.00	0.00
	2.59	93.19	0.33	3.59	2.89	0.00	0.00	0.00
	2.61	91.88	0.70	5.46	1.96	0.00	0.00	0.00
Travertine (Pkd)	2.42	97.18	0.10	1.92	0.80	0.00	0.00	0.00
	2.50	89.77	0.00	10.12	0.11	0.00	0.00	0.00
Limestone (Trls)	2.44	80.07	18.18	1.75	0.00	0.00	0.00	0.00
	2.49	76.19	21.65	2.16	0.00	0.00	0.00	0.00
Limestone (Pkd)	2.44	95.12	0.00	2.22	0.00	0.29	1.69	0.68
	2.50	89.35	0.00	7.88	0.00	0.15	1.89	0.73
Limestone (Mz1)	2.48	64.71	0.00	1.91	0.00	4.20	19.27	9.91
	2.54	70.60	0.00	2.03	0.00	2.56	15.22	9.59

Table 4.3 Mineral compositions of rock specimens in volcanic group.

Rock Type	Density (g/cc)	Mineral Compositions (%)										
		Quartz	Muscovite	Chlorite	Albite	Orthoclase	Anorthite	Diopsite	Microcline	Kaolinite	Hematite	Calcite
Andesite (PTrv)	2.59	36.77	17.93	11.38	15.03	0.00	1.05	5.87	11.97	0.00	0.00	0.00
	2.72	4.95	16.20	13.83	19.75	0.00	14.52	26.71	4.04	0.00	0.00	0.00
Basalt (PTrv)	2.70	1.37	9.99	3.66	18.01	0.00	22.80	27.40	16.77	0.00	0.00	0.00
	2.72	0.00	6.33	8.82	17.82	0.00	16.30	32.23	18.50	0.00	0.00	0.00
	2.76	0.00	8.93	4.12	20.89	0.00	14.56	36.00	15.50	0.00	0.00	0.00
Rhyorite (PTrv)	2.50	44.17	4.95	4.24	2.51	0.62	0.24	0.00	0.00	43.27	0.00	0.00
	2.53	53.17	3.57	3.30	3.13	0.45	0.32	0.00	0.00	36.06	0.00	0.00
	2.56	16.55	7.73	8.70	3.50	1.18	0.57	0.00	0.00	61.77	0.00	0.00
	2.59	43.01	4.00	4.31	3.31	0.98	0.67	0.00	0.00	43.72	0.00	0.00
Tuff (PTrv)	2.60	12.56	21.74	35.80	21.15	1.74	2.37	0.00	0.00	0.00	4.64	0.00
	2.65	2.58	23.24	33.04	12.30	2.20	2.83	0.00	0.00	0.00	6.49	17.32
Vesicular basalt (Qbs)	2.57	0.25	18.75	1.41	43.47	6.56	28.39	0.00	0.00	1.17	0.00	0.00
	2.59	0.00	17.52	0.96	43.59	5.73	31.40	0.00	0.00	0.80	0.00	0.00

Table 4.4 Mineral compositions of rock specimens in clastic group.

Rock Type	Density (g/cc)	Mineral Compositions (%)								
		Quartz	Kaolinite	Muscovite	Albite	Anorthite	Microcline	Calcite	Oligoclase	Chlorite
Sandstone (Mz1)	2.48	83.35	2.80	7.16	3.66	0.31	1.59	0.00	1.07	0.06
	2.50	75.60	9.09	9.90	2.36	0.26	1.67	0.00	1.05	0.07
	2.52	81.19	3.09	11.68	1.03	0.22	1.68	0.00	1.04	0.07
	2.53	72.34	7.20	13.03	4.40	0.21	1.70	0.00	1.04	0.08
	2.55	60.42	7.78	20.37	8.46	0.14	1.73	0.00	1.01	0.09
Sandstone (Jkp)	2.43	36.69	2.91	11.49	23.03	2.80	4.26	0.22	10.01	8.59
	2.48	40.01	2.97	12.24	21.07	1.97	4.59	0.25	9.04	7.86
Sandstone (Kpp)	2.35	85.55	7.01	0.90	3.80	0.00	0.50	0.00	0.00	2.24
	2.39	86.70	5.53	2.39	3.12	0.00	0.70	0.00	0.00	1.56
Sandstone (JKpw)	2.30	83.49	3.87	0.52	4.12	1.01	3.14	0.33	0.00	3.52
	2.36	83.50	4.00	0.80	3.70	1.04	3.32	0.21	0.00	3.43

Table 4.5 Mineral compositions of rock specimens in sulfate group.

Rock Type	Density (g/cc)	Mineral Compositions (%)		
		Anhydrite	Fluorite	Gypsum
Gypsum (Tkb)	2.01	0.00	0.70	99.30
	2.03	0.00	1.53	98.47
	2.07	0.00	1.53	98.47
	2.09	0.00	2.36	97.64
Anhydrite (Tkb)	2.72	99.54	0.46	0.00
	2.74	99.37	0.63	0.00
	2.75	99.34	0.66	0.00
	2.77	98.61	1.39	0.00

Table 4.6 Mineral compositions of rock specimens in silicate group.

Rock Type	Density (g/cc)	Mineral Compositions (%)		
		Dickite	Kaolinite	Quartz
Dickite (PTrv)	2.54	83.43	16.12	0.45
	2.55	80.88	18.54	0.58
	2.56	84.92	14.39	0.69
Pyrophyllite (PTrv)	2.55	41.11	37.37	21.52
	2.57	24.97	22.13	52.90
	2.58	25.55	15.59	58.86
	2.59	21.84	18.70	59.46
	2.60	19.59	14.95	65.46

4.6 Calculated porosity

A new technique is proposed here to obtain a more accurate volume of pore spaces of the specimen. This is a indirect method. The result is called here as "Calculated porosity". To determine the calculated porosity of the specimen, the mineral compositions identified by X-ray diffraction (XRD) analyses are used to calculated as:

$$n = [1-\rho.\sum_{i=1}^{n} W_i/S.G._i] \quad (4.7)$$

where W_i is wight of each mineral in specimen obtained from XRD and $S.G._i$ is specific gravity of each mineral.

The test results are shown in Table 4.7. The igneous rock group, silicate group, almost rock type from carbonate group and anhydrite from sulfate group have quite low calculated porosity (less than 10 %). The highest calculated porosity seems to be the clastic group and gypsum (Tkb) from sulfate group.

The calculated porosity determined from the mineral compositions of rocks gives more accurate results, when compare with the effective porosity of rocks by the standard practice of ASTM C97-02 (2002). This is due to the fact that most pore spaces (pores, microcracks, fissures, intercrystallite boundaries) are not connective, and hence water cannot penetrate into all pore spaces. However, this test takes a piece of the sample for XRD analysis. To obtain more accurate results, the rock fragments should be chosen from multiple points of rock specimen.

Table 4.7 Comparison between effective porosity and calculated porosity.

Group	Rock type	Density (g/cm^3)	Effective porosity (%)	Calculated porosity (%)
Plutonic	Diorite (Trgr)	2.52	1.17	3.61
		2.55	0.90	3.24
		2.50	0.41	2.60
	Granite (Kgr)	2.55	1.29	3.83
		2.58	0.56	2.68
	Granite (Cgr)	2.52	1.32	3.00
		2.54	0.88	2.86
		2.57	0.58	2.60
		2.58	0.26	2.00
	Granite (Mz1)	2.51	1.52	3.31
		2.57	0.52	2.94
Volcanic	Basalt (Qbs)	2.70	0.92	4.21
		2.72	0.86	4.01
		2.76	0.66	2.77
	Andesite (PTrv)	2.59	1.15	4.65
		2.72	0.30	2.26
	Rhyorite (PTrv)	2.50	1.33	6.22
		2.53	0.65	5.69
		2.56	0.52	5.45
		2.59	0.32	4.21
	Vesicular Basalt (Qbs)	2.57	2.97	6.23
		2.59	1.40	5.44
	Tuff (PTrv)	2.60	1.51	5.49
		2.65	0.50	4.26

Table 4.7 Comparison between effective porosity and calculated porosity (%) (cont.).

Group	Rock type	Density (g/cm^3)	Effective porosity (%)	Calculated porosity (%)
Clastic	Sandstone (Jpk)	2.43	6.83	9.16
		2.48	3.70	8.42
	Sandstone (Kpp)	2.35	9.69	11.83
		2.39	7.08	10.44
	Sandstone (JKpw)	2.30	12.15	14.11
		2.39	6.67	12.09
	Sandstone (Mz1)	2.48	5.89	6.70
		2.50	4.81	6.32
		2.52	4.25	5.71
		2.53	2.76	5.61
		2.55	1.62	4.79
Sulfate	Anhydrite (Tkb)	2.72	5.02	3.10
		2.74	4.41	2.82
		2.75	3.42	2.20
		2.77	2.72	1.94
	Gypsum (Tkb)	2.01	10.30	16.70
		2.03	9.60	15.52
		2.07	8.44	14.57
		2.09	7.36	13.88
Silicate	Pyrophyllite (PTrv)	2.55	0.83	7.17
		2.57	0.61	6.81
		2.58	0.47	6.70
		2.59	0.28	6.60
		2.60	0.21	5.60
	Dickite (PTrv)	2.54	0.07	6.29
		2.55	0.06	5.93
		2.56	0.05	5.90

Table 4.7 Comparison between effective porosity and calculated porosity (Cont.).

Group	Rock type	Density (g/cm^3)	Effective porosity (%)	Calculated porosity (%)
Carbonate	Marble Pkd	2.55	0.30	6.50
		2.57	0.26	5.90
		2.59	0.15	5.41
		2.61	0.03	4.77
	Travertine Pkd	2.42	2.70	13.51
		2.50	1.66	8.58
	Limestone (Mz1)	2.48	2.10	9.27
		2.54	0.60	8.38
	Limestone (Trls)	2.44	0.51	9.52
		2.49	0.23	8.14
	Limestone (Pkd)	2.44	0.80	11.77
		2.50	0.48	9.33

CHAPTER V

TEST ANALYSIS

5.1 Introduction

The purpose of this chapter is to determine the relationship between wave velocities (P- and S-waves), physical and mechanical properties of the studied rock specimens. The physical properties include porosity and density. The mechanical properties are uniaxial compressive strength, Young's modulus and Poisson's ratio.

5.2 Correlation between wave velocities and rock density

Linear relationships are proposed to correlate the P- and S- wave velocities with the density of twenty-two rock types. The results indicate that increasing of density will increase P- and S- wave velocities, as shown in Figures 5.1 and 5.2. Good correlations are obtained from both wave velocities ($R^2 > 0.85$). The following equations define their relationships:

$$V_p = A\,\rho + B \tag{5.1}$$

$$V_s = C\,\rho + D \tag{5.2}$$

where V_p is P-wave velocity (km/s), V_s is S-wave velocity (km/s), ρ is density (g/cc), A, B, C, D are constants depending upon the rock type (as shown in Tables 5.1 and 5.2).

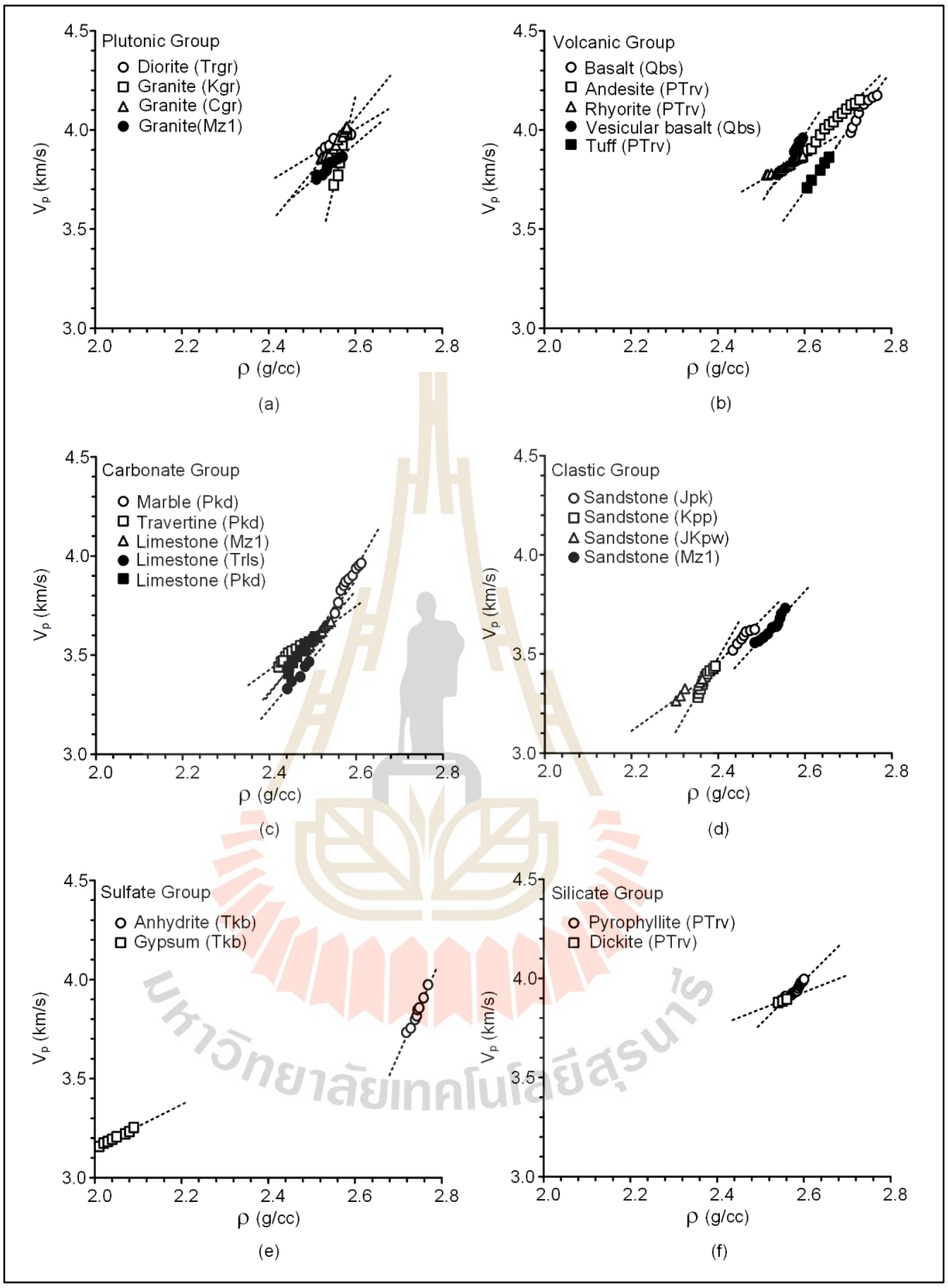

Figure 5.1 P-wave velocities (V_p) as a function of rock density (ρ).

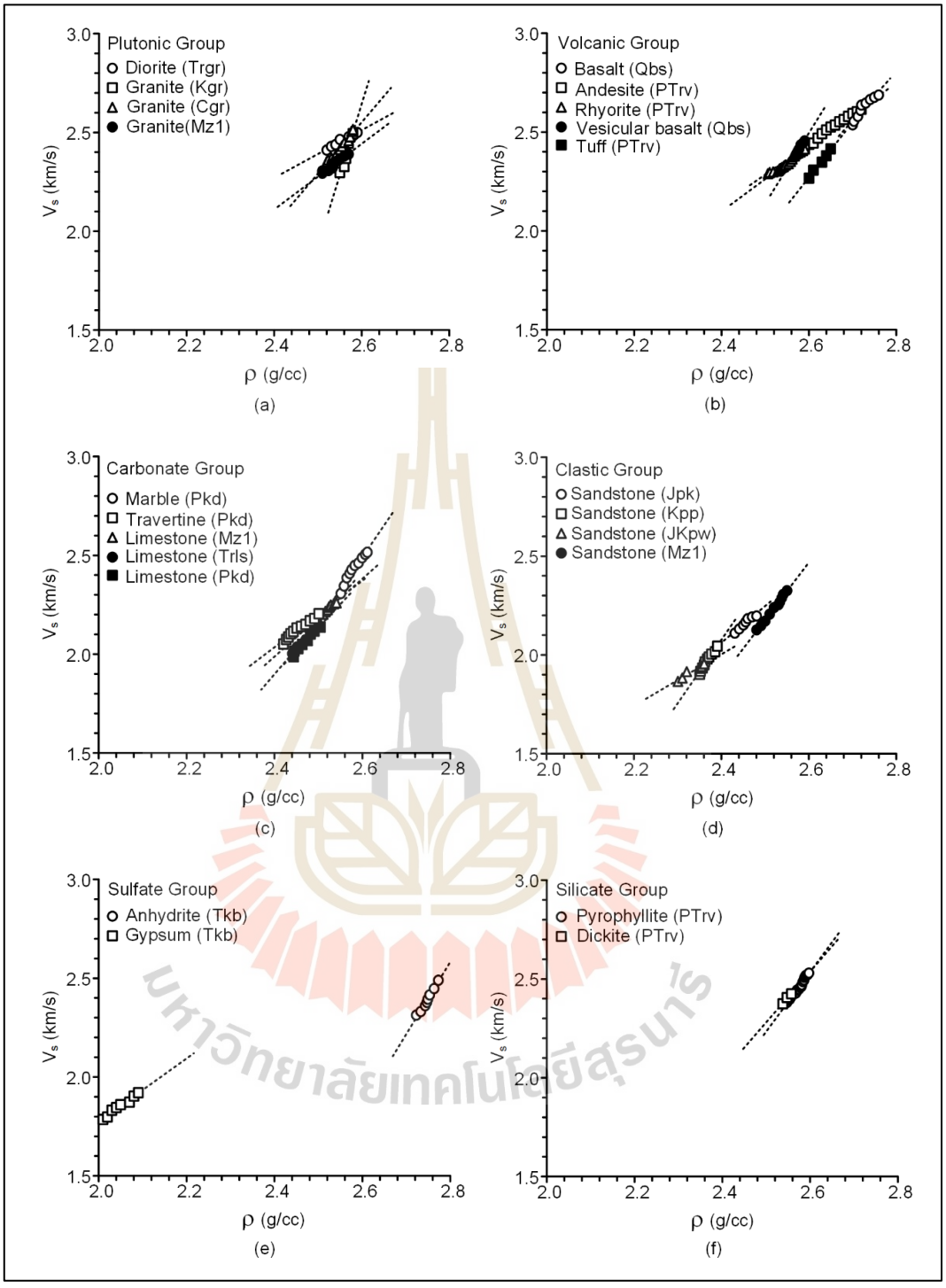

Figure 5.2 S-wave velocities (V_s) as a function of rock density (ρ).

Table 5.1 Empirical contents for P-wave velocities as a function of densities for each rock type.

Group	Rock Type	Code	$V_p = A\ \rho + B$ (km/s)		
			A	B	R^2
Plutonic	Diorite	Trgr	1.319	0.574	0.908
	Granite	Kgr	9.430	-20.34	0.955
	Granite	Cgr	2.681	-2.913	0.962
	Granite	Mz1	1.882	-0.961	0.908
Volcanic	Basalt	Qbs	3.071	-4.281	0.884
	Andesite	PTrv	2.242	-1.935	0.985
	Rhyorite	PTrv	1.271	0.572	0.963
	Vesicular basalt	Qbs	3.598	-5.363	0.968
	Tuff	PTrv	3.003	-4.101	0.996
Carbonate	Marble	Pkd	3.818	-5.982	0.928
	Travertine	Pkd	1.627	-0.478	0.948
	Limestone	Mz1	2.585	-2.891	0.989
	Limestone	Trls	2.602	-3.016	0.956
	Limestone	Pkd	2.882	-3.611	0.969
Classic	Sandstone	Jpk	2.187	-1.782	0.921
	Sandstone	Kpp	3.857	-5.761	0.929
	Sandstone	JKpw	1.591	-0.386	0.923
	Sandstone	Mz1	2.436	-2.501	0.940
Sulfate	Anhydrite	Tkb	4.937	-9.712	0.973
	Gypsum	Tkb	1.100	0.953	0.986
Silicate	Pyrophyllite	PTrv	2.007	-1.230	0.928
	Dickite	PTrv	0.842	1.742	0.999

Table 5.2 Empirical contents for S-wave velocities as a function of densities for each rock type.

Group	Rock Type	Code	$V_s = C\ \rho + D$ (km/s)		
			C	D	R^2
Plutonic	Diorite	Trgr	1.208	-0.628	0.965
	Granite	Kgr	7.094	-15.81	0.942
	Granite	Cgr	2.596	-4.198	0.967
	Granite	Mz1	1.654	-1.857	0.942
Volcanic	Basalt	Qbs	2.506	-4.215	0.906
	Andesite	PTrv	1.544	-1.580	0.991
	Rhyorite	PTrv	1.628	-1.811	0.963
	Vesicular basalt	Qbs	3.594	-6.854	0.977
	Tuff	PTrv	2.824	-5.080	0.989
Carbonate	Marble	Pkd	3.250	-5.955	0.958
	Travertine	Pkd	1.706	-2.059	0.970
	Limestone	Mz1	1.945	-2.675	0.983
	Limestone	Trls	2.546	-4.206	0.967
	Limestone	Pkd	2.328	-3.682	0.970
Classic	Sandstone	Jpk	1.887	-2.470	0.944
	Sandstone	Kpp	3.296	-5.833	0.967
	Sandstone	JKpw	1.332	-1.194	0.938
	Sandstone	Mz1	2.921	-5.124	0.991
Sulfate	Anhydrite	Tkb	3.673	-7.692	0.977
	Gypsum	Tkb	1.609	-1.446	0.968
Silicate	Pyrophyllite	PTrv	2.957	-5.166	0.969
	Dickite	PTrv	2.545	-4.092	0.980

5.3 Correlation between mechanical properties and rock density

Linear relationship can represent the uniaxial compressive strength as a function of specimen density. The results indicate that rock density increases with rock strength. The relationships are shown in Figure 5.3:

$$\sigma_c = E\,\rho + F \tag{5.3}$$

where σ_c is uniaxial compressive strength (MPa), E, F are constants depending upon the rock type (as shown in Table 5.3). For rock types, good correlation is obtained ($R^2 > 0.75$).

The static Young's modulus can also be described by the specimen density using a linear equation. The increasing of density will increase the specimen stiffness, as shown in Figure 5.4. The relationship can be represented by:

$$E_s = G\,\rho + H \tag{5.4}$$

where E_s is static Young's modulus (GPa), G and H are empirical constants (as shown in Table 5.4). Again, all rock types show good correlation ($R^2 > 0.85$).

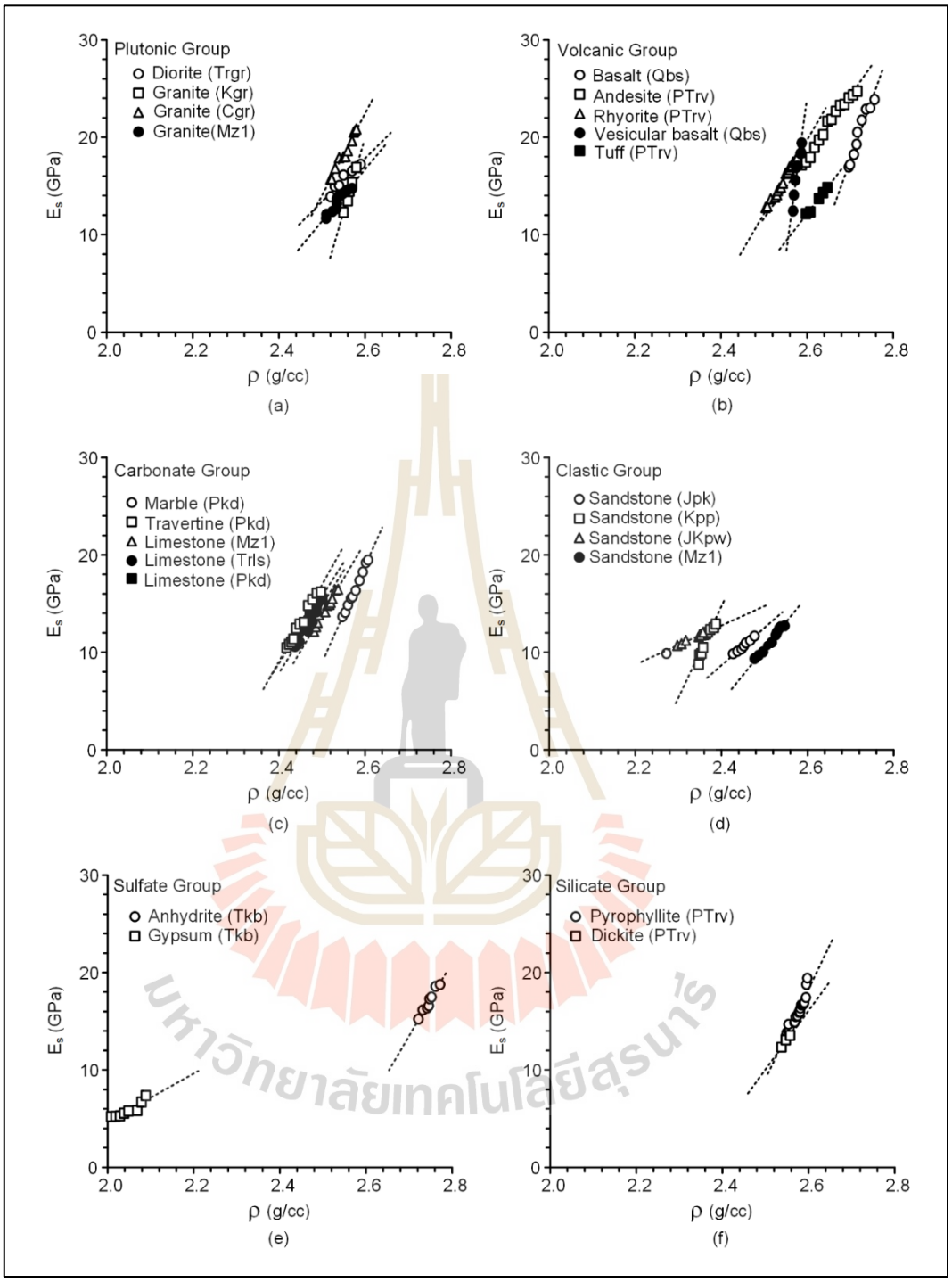

Figure 5.3 Uniaxial compressive strength (σ_c) as a function of rock density (ρ).

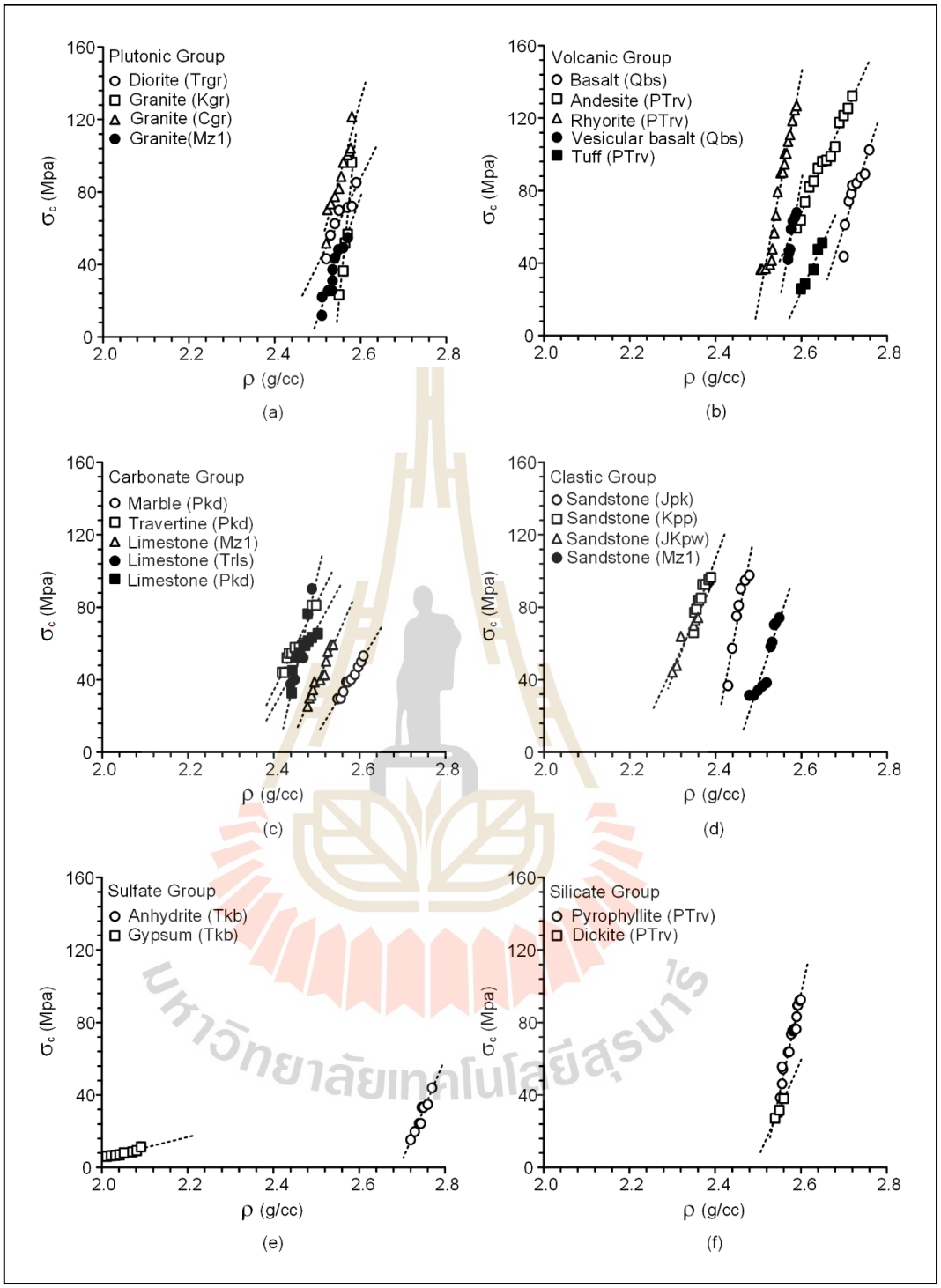

Figure 5.4 Static Young's modulus (E_s) as a function of rock density (ρ).

Table 5.3 Empirical contents for uniaxial compressive strength as a function of densities for each rock type.

Group	Rock Type	Code	$\sigma_c = E\,\rho + F$ (MPa)		
			E	**F**	**R^2**
Plutonic	Diorite	Trgr	475.5	-1149	0.873
	Granite	Kgr	2389	-6075	0.939
	Granite	Cgr	860.3	-2108	0.920
	Granite	Mz1	679.8	-1689	0.887
Volcanic	Basalt	Qbs	743.4	-1948	0.808
	Andesite	PTrv	532.2	-1317	0.979
	Rhyorite	PTrv	1270	-3159	0.952
	Vesicular basalt	Qbs	1327	-3365	0.889
	Tuff	PTrv	526.5	-1345	0.957
Carbonate	Marble	Pkd	390.6	-967.2	0.978
	Travertine	Pkd	475.8	-1108	0.922
	Limestone	Mz1	545.6	-1326	0.939
	Limestone	Trls	1053	-2538	0.907
	Limestone	Pkd	440.2	-1032	0.798
Classic	Sandstone	Jpk	1223	-2928	0.908
	Sandstone	Kpp	634.8	-1418	0.849
	Sandstone	JKpw	483.6	-1066	0.907
	Sandstone	Mz1	707.1	-1731	0.871
Sulfate	Anhydrite	Tkb	567.7	-1530	0.929
	Gypsum	Tkb	57.74	-110.5	0.901
Silicate	Pyrophyllite	PTrv	1104	-2775	0.950
	Dickite	PTrv	542.5	-1351	0.991

Table 5.4 Empirical contents for static Young's modulus as a function of densities for each rock type.

Group	Rock Type	Code	$E_s = G\rho + H$ (GPa)		
			G	H	R^2
Plutonic	Diorite	Trgr	44.94	-98.97	0.944
	Granite	Kgr	156.8	-387.6	0.992
	Granite	Cgr	83.91	-195.8	0.967
	Granite	Mz1	53.00	-121.1	0.901
Volcanic	Basalt	Qbs	122.7	-314.1	0.944
	Andesite	PTrv	62.48	-144.7	0.980
	Rhyorite	PTrv	74.84	-175.1	0.989
	Vesicular basalt	Qbs	305.6	-772.0	0.908
	Tuff	PTrv	56.41	-134.7	0.987
Carbonate	Marble	Pkd	100.1	-241.7	0.995
	Travertine	Pkd	78.89	-180.4	0.977
	Limestone	Mz1	74.26	-171.9	0.970
	Limestone	Trls	68.67	-157.0	0.973
	Limestone	Pkd	70.34	-160.1	0.955
Classic	Sandstone	Jpk	37.77	-82.02	0.978
	Sandstone	Kpp	94.81	-213.2	0.832
	Sandstone	JKpw	20.69	-36.86	0.968
	Sandstone	Mz1	53.74	-124.1	0.980
Sulfate	Anhydrite	Tkb	74.77	-188.3	0.949
	Gypsum	Tkb	24.41	-44.18	0.839
Silicate	Pyrophyllite	PTrv	91.33	-219.6	0.894
	Dickite	PTrv	60.50	-141.4	0.986

5.4 Correlation between dynamic and static properties

An attempt is made have to correlate the mechanical properties of twenty-two rock types with the dynamic properties. Linear relationships are used to describe the static young's modulus as a function of dynamic young's modulus. The results indicate that the dynamic young's moduli increase with increasing the static young's moduli. The following equations define the relations:

$$E_s = 0.461\ E_d - 0.200 \tag{5.5}$$

where E_d is dynamic young's modulus (GPa). Good correlation is obtained ($R^2 = 0.730$), as shown in Figure 5.5.

Similarly, the static Poisson's ration can be defined as a function of the dynamic Poisson's ratio using a linear equation. The relationship is shown in Figure 5.5, with a fair correlation ($R^2 = 0.667$). The Poisson's rations obtained from both methods tend to be comparable.

$$\nu_s = 0.407\ \nu_d + 0.103 \tag{5.6}$$

where ν_s is static Poisson's ratio, ν_d is dynamic Poisson's ratio.

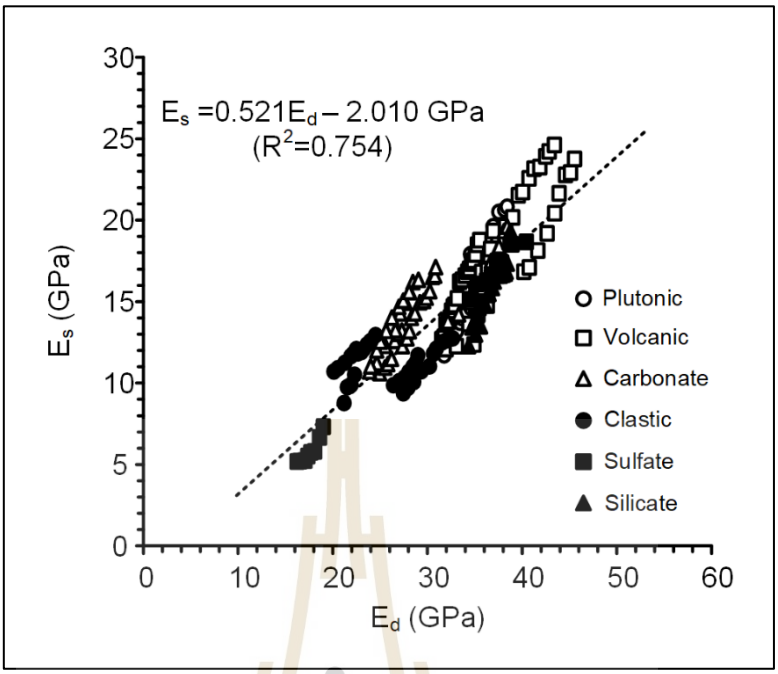

Figure 5.5 Static Young's modulus (E_s) as a function of dynamic Young's modulus (E_d).

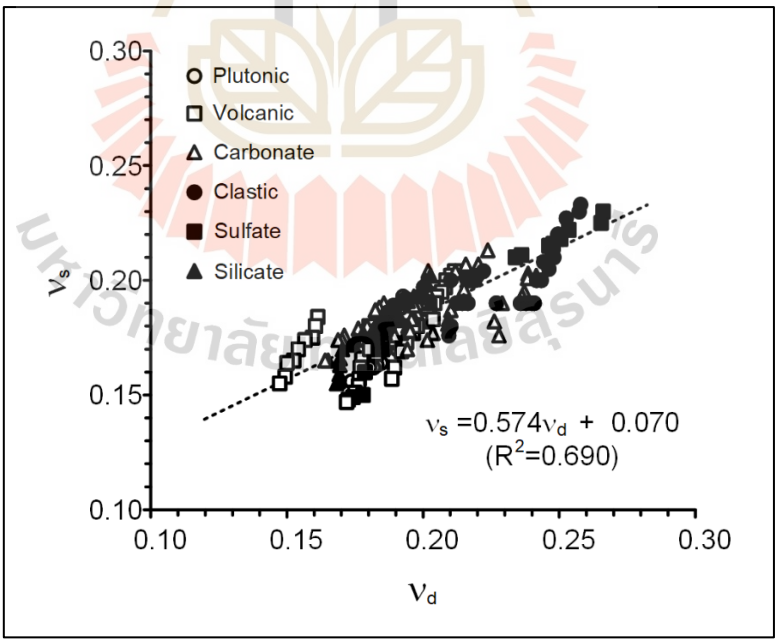

Figure 5.6 Static Poisson's ratio (ν_s) as a function of dynamic Poisson's ratio (ν_d).

5.5 Effect of rock porosity

As determined from chapter IV, the porosities of rocks define by the ASTM standard practice and by the XRD analysis are correlated with the wave velocities and the dynamic properties. Figure 5.7 compares the variation of the primary wave velocity as a function of the effective porosity (n_e) and of the calculated porosity (n). Similar comparison is made from the secondary wave velocity in Figure 5.8. Both wave velocities correlate better with the calculated porosities ($R^2 > 0.7$) than with the effective porosity ($R^2 > 0.5$).

The calculated porosity that has been calculated from the XRD results also correlates better with the dynamic properties (E_d and ν_d) than does the effective porosity, as shown in Figure 5.9 and 5.10. This is primary due to the fact that the calculated porosities of most rock are higher than the effective porosities. The effective porosities are determined from the saturation of the pore space during submerging in the water under negative pressure (of – 1 atm). The water cannot however penetrate through all pore spaces as most pore spaces in rocks are not connective. The results, therefore, give the porosity values lower than the actual. The calculated porosity values are determined from the weight density of all minerals comprising the rocks. As a result, the determined porosity is closer to the actual value. The correlations of the wave velocities and the dynamic properties with the calculated porosity reveal also test the rock porosity is the main factor-controlled wave properties.

The increase of the rock porosity shows down the P- and S- wave velocities linearly. This result is a linear decrease of the dynamic Young's modulus as the porosity increase (Figure 5.9). high porosity also results in a linear increase of the dynamic Poisson's rations of the rocks.

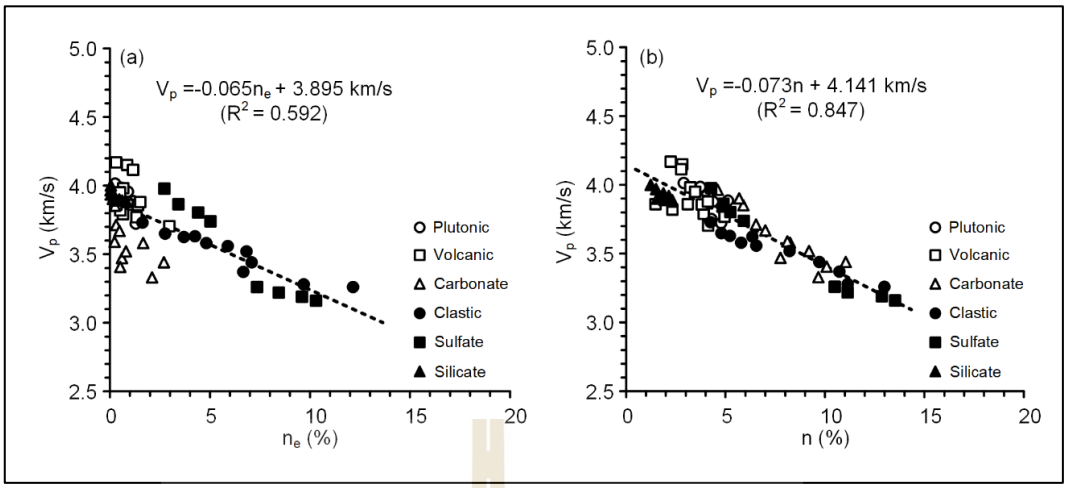

Figure 5.7 P-wave velocity (V_p) as a function of effective porosity (n_e)(a) and calculated porosity (n)(b).

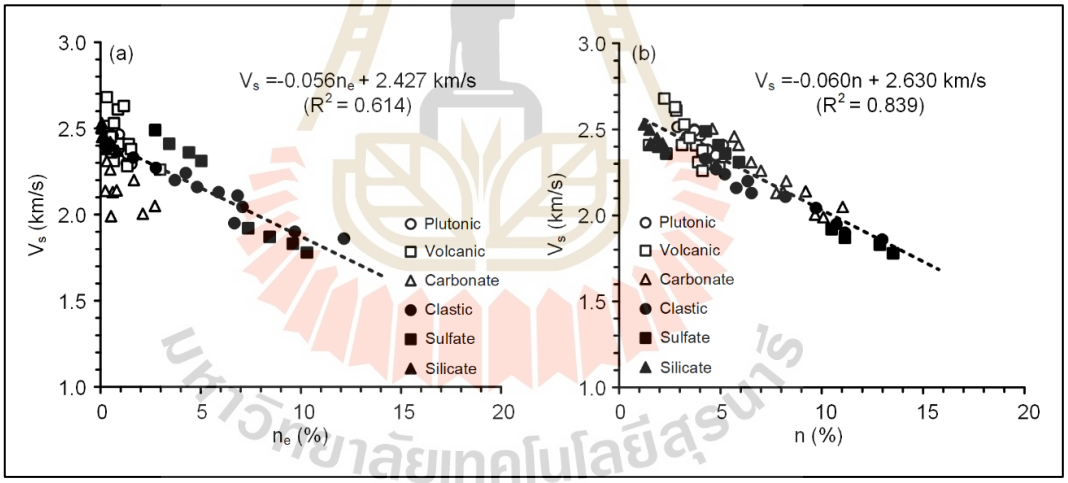

Figure 5.8 S-wave velocity (V_s) as a function of effective porosity (n_e)(a) and calculated porosity (n)(b).

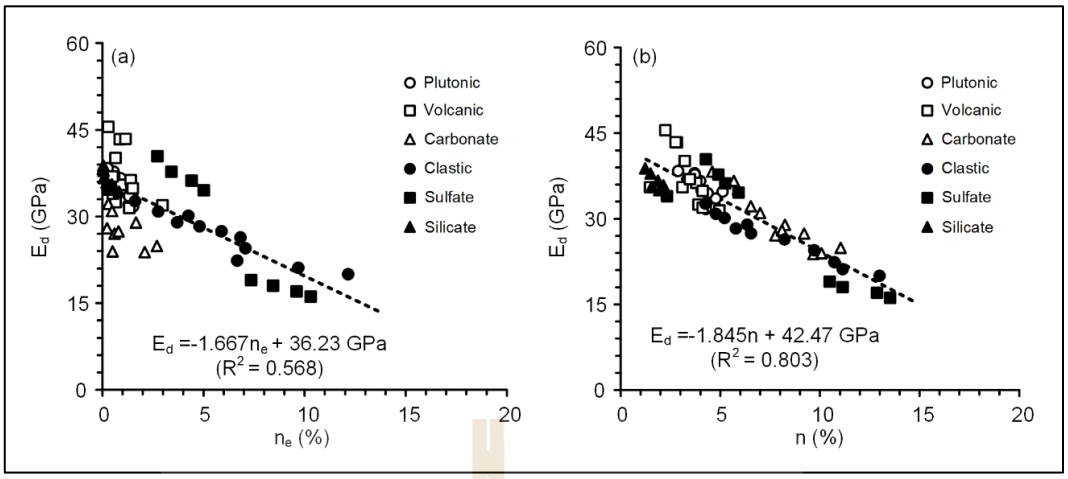

Figure 5.9 Dynamic Young's modulus (E_d) as a function of effective porosity (n_e)(a) and calculated porosity (n)(b).

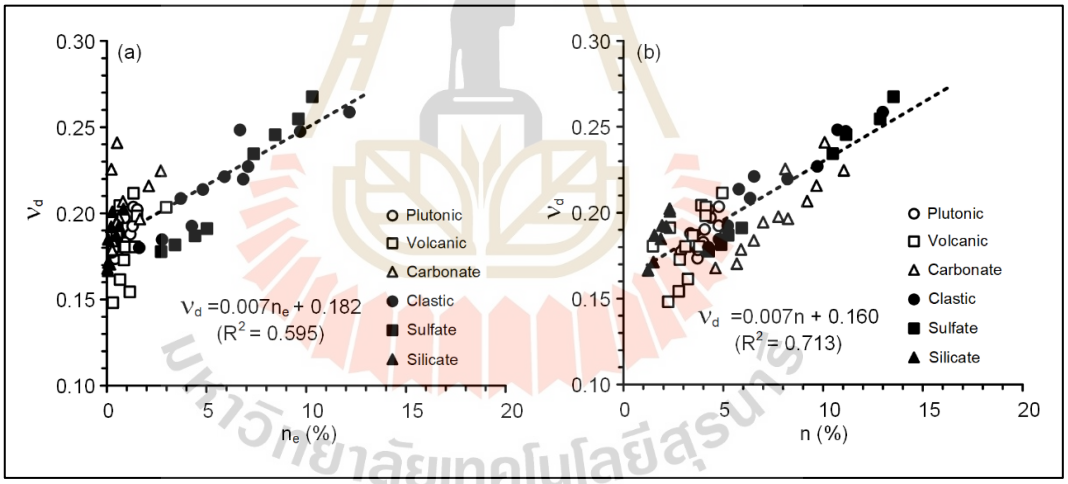

Figure 5.10 Dynamic Poisson's ratio (ν_d) as a function of effective porosity (n_e)(a) and calculated porosity (n)(b).

Figure 5.11(a) shows the P-wave velocity as a function of quartz contents, which selects only the rock with the highest quartz content comparing with other minerals. The results show that quartz contents tend to decrease with increasing P-wave velocities, and similarly, the calcite contents show an inconclusive trend with increasing

P-wave velocities as shown in Figure. 5.11(b). Note that the number of tested samples may not be sufficient for analysis. Other minerals are considered in Figure. 5.12, which show the P-wave velocity as a function of the highest specific gravity mineral content of rock type followed in Figure 5.11. The results show that the P-wave velocity increases with increasing mineral contents. It is possible that the highest specific gravity mineral content has a greater influence on wave velocity than the highest mineral content in rock. This conclusion agrees with Rao et al. (2006) and Tandon and Gupta (2013) who observed that the wave velocity increases with increasing feldspar/quartz constituents, which the feldspar has a higher specific gravity than quartz.

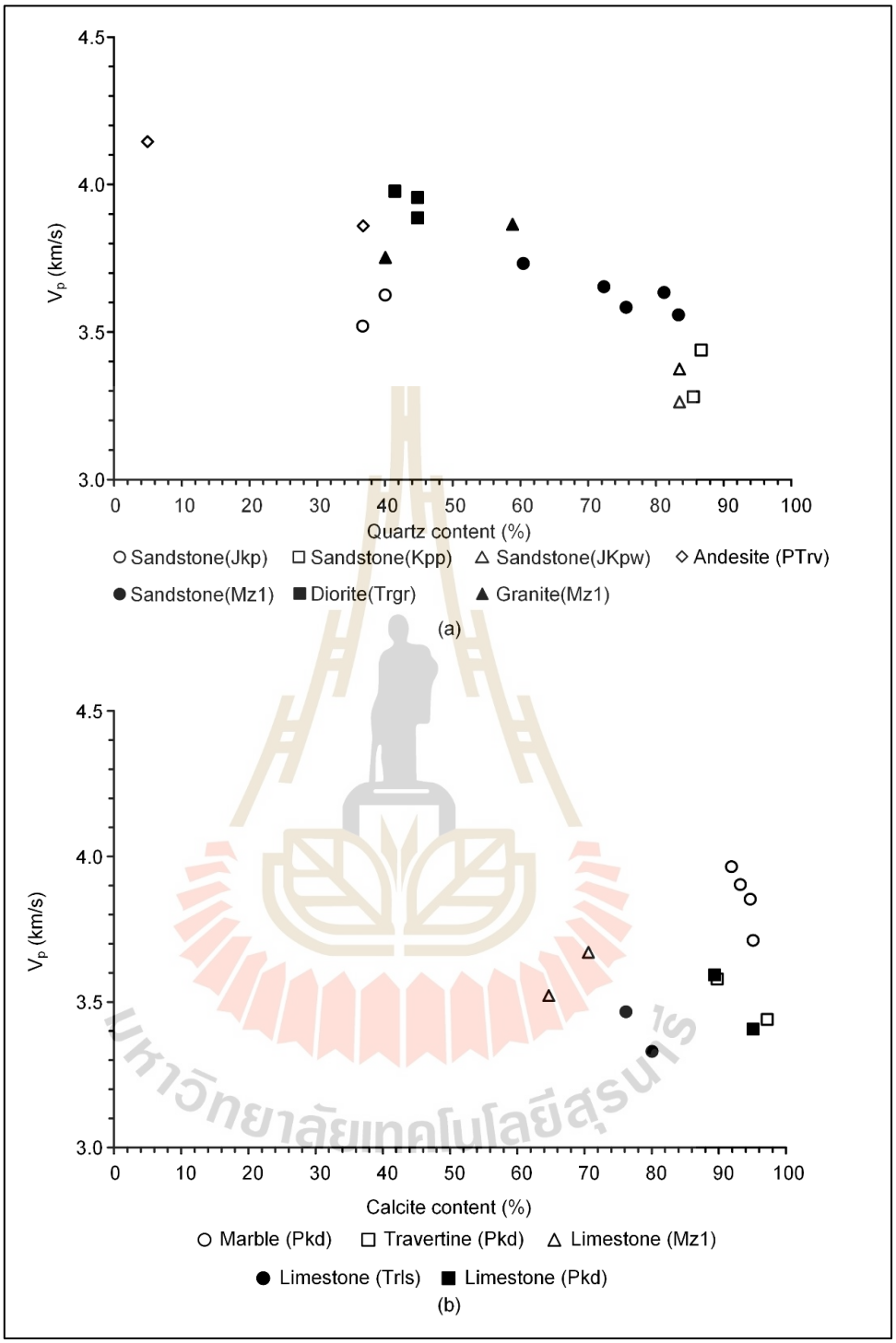

Figure 5.11 P-wave velocity (V_p) as a function of quartz (a) and calcite contents (b).

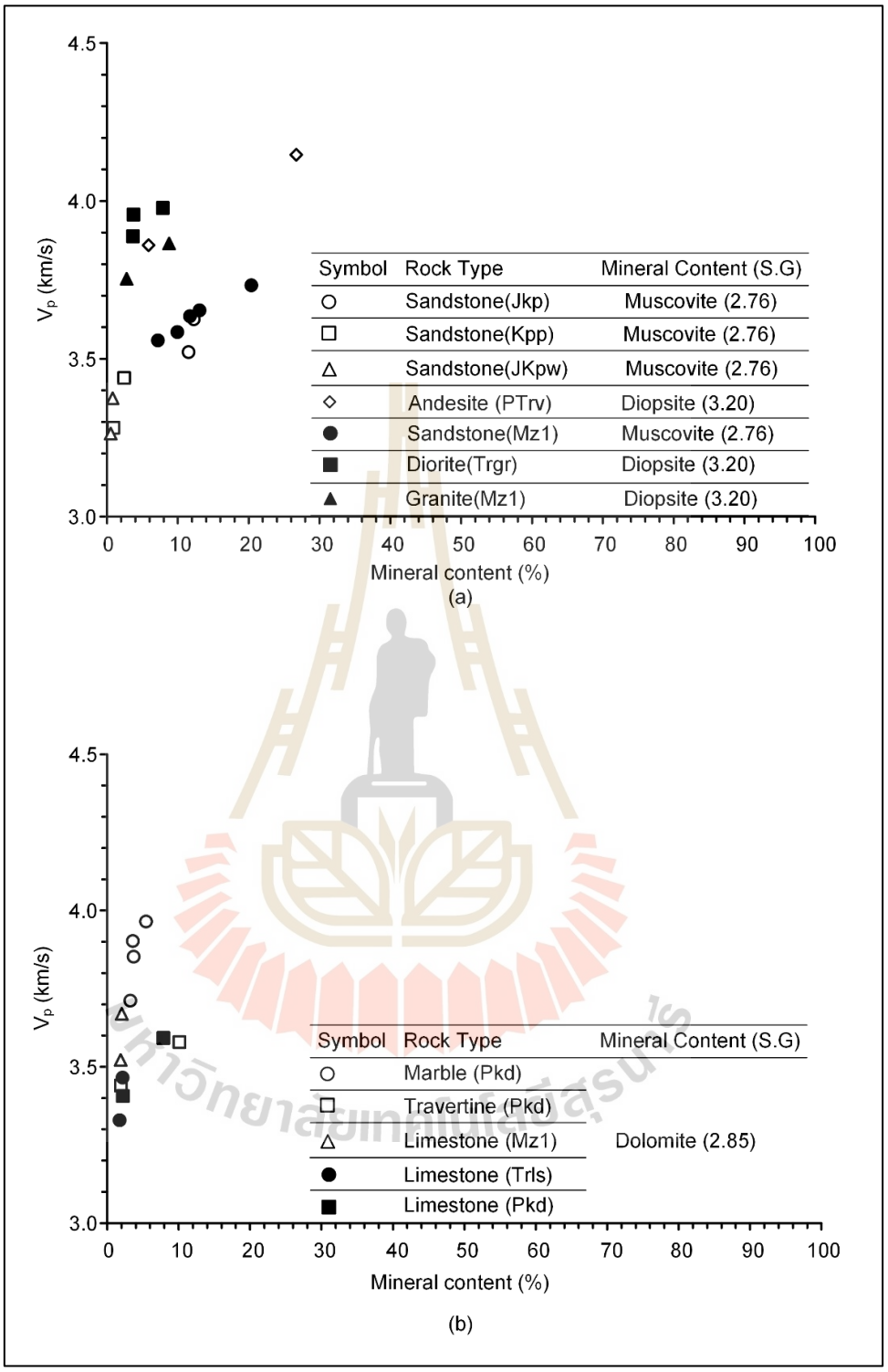

Figure 5.12 P-wave velocity (V_p) as a function of mineral contents.

CHAPTER VI

DISCUSSIONS AND CONCLUSIONS

6.1 Discussions

The presented study has focused on effects of the physical and mineral properties on wave velocities and mechanical properties of twenty-two rock types in Thailand.

The results show linear relationship between wave velocities and density (Figures 5.1 and 5.2) for each rock type ($R^2 > 0.85$). The P- and S- wave velocities increase with increasing density and decreasing porosity, and hence the wave velocities obtained from dense igneous rocks are higher than those obtained from lighter gypsum rock.

Figure 6.1 shows the relationship between the P-wave velocity and density obtained here comparing with other studies. The linear correlation found here agrees reasonably well with those of other researchers (Assefa et al. 2003; Khandelwal and Singh, 2009; Kurtulus et al. 2010; Kassab and Wellar, 2015; Kurtulus et al., 2016b and Selcuk and Nar, 2016). However, non-linear correlation has been presented by Wang et al. (2019) who suggested the positive power relationship for sandstone and mudstone, and by Rezaei et al. (2019) who proposed polynomial relationship for schist, phyllite and sandstone. The wave velocity depends on mineral compositions and porosity of the rocks (Garia, et al. 2019).

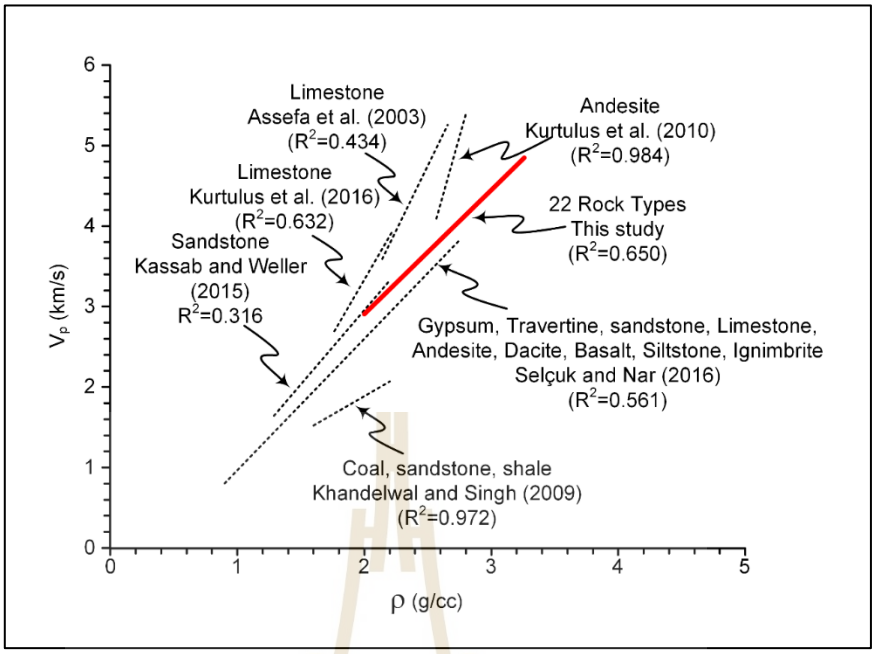

Figure 6.1 P-wave velocity (V_p) as a function of density (ρ).

Good correlations are also obtained between the density and mechanical properties. The uniaxial compressive strengths and elastic moduli linearly increases with increasing density, which agree with the results obtained by Vasanelli et al. (2015) and Yin et al. (2016). Rabat et al. (2020), however, use exponential equation to described the increase of uniaxial compressive strengths with increasing density of calcarenite rock. The effects of mineral composition and porosity on mechanical properties reveal that the rock strength and static young's modulus increases with increasing the highest specific gravity mineral content, and decreasing porosity.

The relationship between the static and dynamic young's moduli obtained here is compared with other studies in Figure 6.2. The positive correlation found here agrees reasonably well with those of other researchers (Starzec, 1999; Najibi et al., 2015; Yin et al., 2016; Chawre, 2018; Rabat et al., 2020). The static young's moduli increase linearly with the dynamic young's moduli. Good correlation is obtained ($R^2 > 0.7$). Such

positive relation is useful to estimate the static young's modulus from the dynamic young's modulus. The values of the static moduli are about an order of magnitude lower than those of the dynamic properties. This is due to the effect of loading rate. The pulse waves are much faster than those of the static loading. The Poisson's ratios obtained from the two methods are comparable.

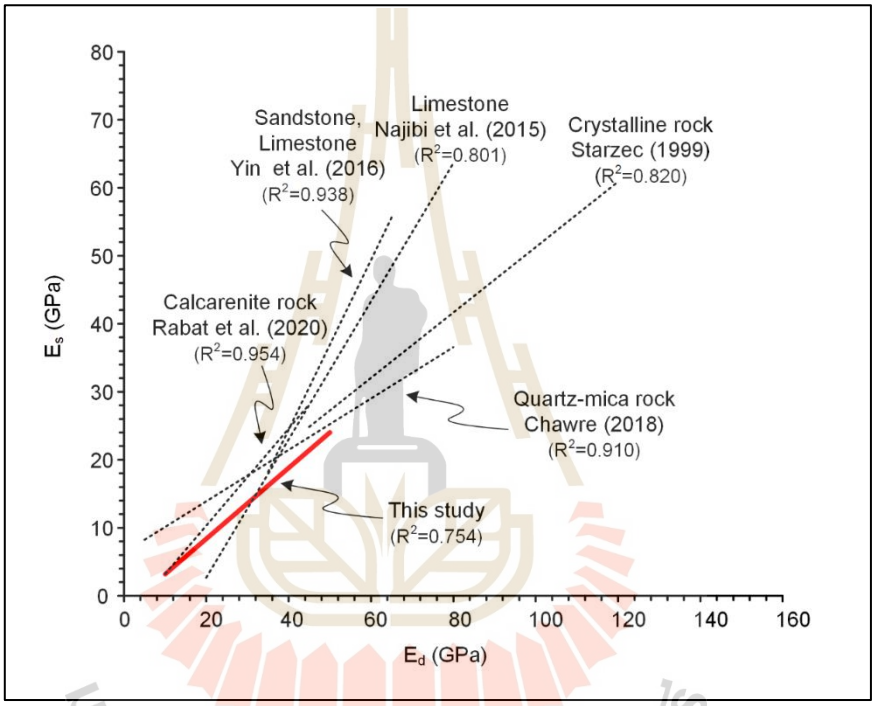

Figure 6.2 Static Young's modulus (E_s) as a function of dynamic young's modulus (E_d).

The correlation from dynamic-static young's modulus and Poisson ratio can be used for the preliminary stage of design where detailed data is not easily accessible. The main advantage of this ultrasonic technique is that it is non-destructive test and determination of the dynamic young's modulus is relatively simple, inexpensive and suitable for in-situ application. However, it is commonly known that the prediction equations derived by different researches are dependent of rock types, quality and test

conditions. Noted that, the proposed equations are valid only for rocks test here. Different forms of correlation equation are likely for other rocks.

The general method (ASTM C97-02) to determine the porosity of rock by immersing the rock in water to saturate may not give accurate results. This is due to the fact that most pore spaces (pores, microcracks, fissures, intercrystallite boundaries) are not connective. As a results water cannot penetrate into all pore spaces. Therefore, the new technique proposed here can give a more accurate volume of pore spaces. The calculated porosity has been estimated from the XRD results which can be correlated with the wave velocities and dynamic properties better than those obtained from the effective porosity.

Nevertheless, in order to further confirm the results obtained from this study, more testing should be performed with the higher number of specimens. Due to excessive cost and time, only the samples with maximum and minimum density for each rock types are analyzed under XRD analysis.

6.2 Conclusions

Results and analysis of the physical, mechanical, and mineral properties on UPV measurements can be calculated as follows:

1. P- and S- wave velocities correlate fairly well with the changes of the rock density using linear equations. The highest wave velocity is found in rock with high density of mineral compositions.

2. The porosity attenuates wave velocity in rock. It is evident in sedimentary rocks of similar mineral content. When the porosity increases, the wave velocity is significantly reduced.

3. Uniaxial compressive strengths and elastic moduli show positive linear relations with the rock densities.

4. Static Young's moduli can be estimated by the dynamic young's moduli with a rather high precision.

5. The calculated porosity from XRD analysis correlates better with the dynamic parameters (V_p, V_s, E_d and ν_d) than does effective porosity.

6. The highest specific gravity mineral content has a greater influence on wave velocity control than the highest mineral content in rock due to wave velocity travels well in high specific gravity mineral.

6.3 Recommendations for future studies

The uncertainties of the investigation and results discussed above lead to the recommendations for further studies as follows.

1. More X-ray diffraction analyses from several rock types would statistically enhance the reliability of the test results in this study.

2. The effect of mineralogical compositions, structure and geometry of the pores (their distribution, packaging and orientation), grain size and cementing material should be investigated.

REFERENCES

Aldeeky, H. and Al Hattamleh, O. (2018). Prediction of engineering properties of basalt rock in Jordan using ultrasonic pulse velocity test. **Geotechnical and Geological Engineering.** 36(6): 3511-3525.

Aşcı, M., Kaplanvural, I., Karakaş, A., Şahin, Ö. K., and Kurtuluş, C. (2017). Correlation of physical and mechanical properties with ultrasonic pulse velocities of sandstones in Çenedağ, Kocaeli-Turkey. **International Journal of Advanced Geosciences.** 5(2): 109-115.

Assefa, S., McCann, C., and Sothcott, J. (2003). Velocities of compressional and shear waves in limestones. **Geophysical Prospecting.** 51(1): 1-13.

ASTM C97-02 (2002). **Standard Test Methods for Absorption and Bulk Specific Gravity of Dimension Stone.** Annual Book of ASTM Standards, American Society for Testing and Materials, West Conshohocken, PA.

ASTM D2845-08 (2008). **Standard Test Method for Laboratory Determination of Pulse Velocities and Ultrasonic Elastic Constants of Rock.** Annual Book of ASTM Standards, American Society for Testing and Materials, West Conshohocken, PA.

ASTM D4543-07 (2007). **Standard Practices for Preparing Rock Core as Cylindrical Test Specimens and Verifying Conformance to Dimensional and Shape Tolerances.** Annual Book of ASTM Standards, American Society for Testing and Materials, West Conshohocken, PA.

ASTM D6473-15 (2015). **Standard Test Method for Specific Gravity and Absorption of Rock for Erosion Control.** Annual Book of ASTM Standards, American Society for Testing and Materials, West Conshohocken, PA.

ASTM D7012-14 (2014). **Standard Test Methods for Compressive Strength and Elastic Moduli of Intact Rock Core Specimens under Varying States of Stress Temperatures.** Annual Book of ASTM Standards, American Society for Testing and Materials, West Conshohocken, PA.

ASTM E1426-14e1 (2019). **Standard Test Method for Determining the X-Ray Elastic Constants for Use in the Measurement of Residual Stress Using X-Ray Diffraction Techniques.** Annual Book of ASTM Standards, American Society for Testing and Materials, West Conshohocken, PA.

Azimian, A. and Ajalloeian, R. (2015). Empirical correlation of physical and mechanical properties of marly rocks with P-wave velocity. **Arabian Journal of Geosciences.** 8(4): 2069–2079.

Azimian, A., Ajalloeian, R., and Fatehi, L. (2014). An Empirical correlation of uniaxial compressive strength with P-wave velocity and point load strength index on marly rocks using statistical method. **Geotechnical and Geological Engineering.** 32(1): 205–214.

Baechle, G. T., Weger, R., Eberli, G. P., and Massaferro, J. L. (2004). The role of macroporosity and microporosity in constraining uncertainties and in relating velocity to permeability in carbonate rocks. In **Proceedings of the SEG Int'l Exposition and 74th Annual Meeting** (pp. 1662-1665). Society of Exploration Geophysicists.

Blake, O. O., Faulkner, D. R., and Tatham, D. J. (2019). The role of fractures, effective pressure and loading on the difference between the static and dynamic Poisson's ratio and Young's modulus of Westerly granite. **International Journal of Rock Mechanics and Mining Sciences.** 116: 87-98.

Boulanouar, A., Rahmouni, A., Boukalouch, M., Samaouali, A., Géraud, Y., Harnafi, M., and Sebbani, J. (2013). Determination of thermal conductivity and porosity of building stone from ultrasonic velocity measurements. **Geomaterials.** 3: 138-144.

Carlson, R. L. and Jay Miller, D. (2004). Influence of pressure and mineralogy on seismic velocities in oceanic gabbros: Implications for the composition and state of the lower oceanic crust. **Journal of Geophysical Research: Solid Earth.** 109(B9).

Chawre, B. (2018). Correlations between ultrasonic pulse wave velocities and rock properties of quartz-mica schist. **Journal of Rock Mechanics and Geotechnical Engineering.** 10(3): 594-602.

Cheng, W., Ba, J., Fu, L. Y., and Lebedev, M. (2019). Wave-velocity dispersion and rock microstructure. **Journal of Petroleum Science and Engineering.** 183: 106466.

Diamantis, K., Bellas, S., Migiros, G., and Gartzos, E. (2011). Correlating wave velocities with physical, mechanical properties and petrographic characteristics of peridotites from the central Greece. **Geotechnical and Geological Engineering.** 29(6): 1049-1062.

Esamaldeen, A. (2015). Assessments of elastic anisotropy of banded amphibolite as a function of cleavage orientation using S-and P-Wave Velocity. **Journal of Geoscience and Environment Protection.** 3(5): 62-71.

Esteban, L., Pimienta, L., Sarout, J., Delle Piane, C., Haffen, S., Geraud, Y., and Timms, N. E. (2015). Study cases of thermal conductivity prediction from P-wave velocity and porosity. **Geothermics.** 53: 255-269.

Fawad, M., Mondol, N. H., Jahren, J., and Bjørlykke, K. (2011). Mechanical compaction and ultrasonic velocity of sands with different texture and mineralogical composition. **Geophysical Prospecting**. 59(4): 697-720.

Fener, M. (2011). The effect of rock sample dimension on the P-wave velocity. **Journal of Nondestructive Evaluation.** 30(2): 99-105.

Garia, S., Pal, A. K., Ravi, K., and Nair, A. M. (2019). A comprehensive analysis on the relationships between elastic wave velocities and petrophysical properties of sedimentary rocks based on laboratory measurements. **Journal of Petroleum Exploration and Production Technology**. 9(3): 1869-1881.

Gupta, V. and Sharma, R. (2012). Relationship between textural, petrophysical and mechanical properties of quartzites: a case study from northwestern Himalaya. **Engineering Geology**. 135: 1-9.

Jamshidi, A., Nikudel, M. R., Khamehchiyan, M., Sahamieh, R. Z., and Abdi, Y. (2016). A correlation between P-wave velocity and Schmidt hardness with mechanical properties of travertine building stones. **Arabian Journal of Geosciences.** 9(10): 1-12.

Jones, I. F. and Davison, I. (2014). Seismic imaging in and around salt bodies. **Interpretation.** 2(4): SL1-SL20.

Juneja, A. and Endait, M. (2017). Laboratory measurement of elastic waves in Basalt rock. **Measurement.** 103: 217-226.

Kahraman, S. (2001). Evaluation of simple methods for assessing the uniaxial compressive strength of rock. **International Journal of Rock Mechanics and Mining Sciences.** 38(7): 981-994.

Karaman, K., Kaya, A., and Kesimal, A. (2015). Effect of the specimen length on ultrasonic P-wave velocity in some volcanic rocks and limestones. **Journal of African Earth Sciences.** 112: 142-149.

Kassab, M. A. and Weller, A. (2015). Study on P-wave and S-wave velocity in dry and wet sandstones of Tushka region, Egypt. **Egyptian Journal of Petroleum.** 24(1): 1-11.

Kern, H., Mengel, K., Strauss, K. W., Ivankina, T. I., Nikitin, A. N., and Kukkonen, I. T. (2009). Elastic wave velocities, chemistry and modal mineralogy of crustal rocks sampled by the Outokumpu scientific drill hole: Evidence from lab measurements and modeling. **Physics of the Earth and Planetary Interiors**. 175(3-4): 151-166.

Khandelwal, M. (2013). Correlating P-wave velocity with the physico-mechanical properties of different rocks. **Pure and Applied Geophysics.** 170(4): 507-514.

Khandelwal, M. and Singh, T. N. (2009). Correlating static properties of coal measures rocks with P-wave velocity. **International Journal of Coal Geology.** 79(1-2): 55-60.

Kurtulus, C., Bozkurt, A., and Endes, H. (2012). Physical and mechanical properties of serpentinized ultrabasic rocks in NW Turkey. **Pure and Applied Geophysics.** 169(7): 1205-1215.

Kurtulus, C., CakIr, S., and Yoğurtcuoğlu, A. C. (2016a). Ultrasound study of limestone rock physical and mechanical properties. **Soil Mechanics and Foundation Engineering**. 52(6): 348-354.

Kurtulus, C., Sertcelik, F., and Sertcelik, I. (2016b). Correlating physico-mechanical properties of intact rocks with P-wave velocity. **Acta Geodaetica et Geophysica.** 51(3): 571-582.

Kurtulus. C., Irmak, T. S., and Sertcelik, I. (2010). Physical and mechanical properties of Gokceada: Imbros (NE Aegean Sea) Island andesites. **Bulletin of Engineering Geology and the Environment.** 69(2): 321-324.

Majstorović, J., Gligorić, M., Lutovac, S., Negovanović, M., and Crnogorac, L. (2019). Correlation of uniaxial compressive strength with the dynamic elastic modulus, P- wave velocity and S- wave velocity of different rock types**. Underground mining engineering.** (34): 11-25.

Mockovčiaková, A. and Pandula, B. (2003). Study of the relation between the static and dynamic moduli of rocks. **Metalurgija**. 42(1): 37-39.

Moradian, Z.A. and Behnia, M. (2009). Predicting the uniaxial compressive strength and static Young's modulus of intact sedimentary rocks using the ultrasonic test. **International Journal of Geomechanics.** 9(1): 14-19.

Najibi, A.R., Ghafoori, M., Lashkaripour, G. R., and Asef, M. R. (2015). Empirical relations between strength and static and dynamic elastic properties of Asmari and Sarvak limestones, two main oil reservoirs in Iran. **Journal of Petroleum Science and Engineering.** 126: 78-82.

Onaloa, D., Oloruntobi, O., Adedigba, S., Khan, F., James, L., and Butt, S. (2018). Static Young's modulus model prediction for formation evaluation. **Journal of Petroleum Science and Engineering.** 171: 394-402.

Palmstrøm, A. (1995). **A rock mass characterization system for rock engineering purposes.** Ph.D. Dissertation, Oslo University, Norway.

Pappalardo, G. (2015). Correlation between P-wave velocity and physical–mechanical properties of intensely jointed dolostones, Peloritani mounts, NE Sicily. **Rock mechanics and rock engineering**. 48(4): 1711-1721.

Rabat, A., Cano, M., and Tomás, R. (2020). Effect of water saturation on strength and deformability of building calcarenite stones: Correlations with their physical properties. **Construction and Building Materials.** 232:117259.

Rahmouni, A., Boulanouar, A., Boukalouch, M., Géraud, Y., Samaouali, A., Harnafi, M., and Sebbani, J. (2013). Prediction of porosity and density of calcarenite rocks from P-wave velocity measurements. **International Journal of Geosciences.** 4(9): 1292-1299.

Rao, M. V. M. S., Prasanna Lakshmi, K. J., Sarma, L. P., and Chary, K. B. (2006). Elastic properties of granulite facies rocks of Mahabalipuram, Tamil Nadu, India. **Journal of Earth System Science.** 115(6): 673-683.

Rezaei, M., Davoodi, P. K., and Najmoddini, I. (2019). Studying the correlation of rock properties with P-wave velocity index in dry and saturated conditions. **Journal of Applied Geophysics.** 169: 49-57.

Sarkar, K., Vishal, V., and Singh, T. N. (2012). An empirical correlation of index geomechanical parameters with the compressional wave velocity. **Geotechnical and Geological Engineering**. 30(2): 469-479.

Saxena, N., Mavko, G., Hofmann, R., Dolan, S., and Bryndzia, L. T. (2016). Mineral substitution: Separating the effects of fluids, minerals, and microstructure on P- and S-wave velocities. **Geophysics.** 81(2): D197-D210.

Selçuk, L. and Nar, A. (2016). Prediction of uniaxial compressive strength of intact rocks using ultrasonic pulse velocity and rebound-hammer number. **Quarterly Journal of Engineering Geology and Hydrogeology.** 49(1): 67-75.

Song, I., Suh, M., Woo, Y. K., and Hao, T. (2004). Determination of the elastic modulus set of foliated rocks from ultrasonic velocity measurements. **Engineering Geology.** 72(3-4): 293-308.

Soroush, H. and Qutob, H. (2011). Evaluation of rock properties using ultrasonic pulse technique and correlating static to dynamic elastic constants**.** In **Proceedings of the 2nd South Asain Geoscience Conference and Exhibition, GEOIndia2011.** Greater Noida, New Delhi, India.

Starzec, P. (1999). Dynamic elastic properties of crystalline rocks from south-west Sweden. **International journal of rock mechanics and mining sciences.** 36(2): 265-272.

Tandon, R. S. and Gupta, V. (2013). The control of mineral constituents and textural characteristics on the petrophysical and mechanical (PM) properties of different rocks of the Himalaya. **Engineering Geology.** 153: 125-143.

Tugrul, A. and Zarif, I. H. (1999). Correlation of mineralogical and textural characteristics with engineering properties of selected granitic rocks from Turkey. **Engineering Geology.** 51(4): 303-317.

Vasanelli, E., Colangiuli, D., Calia, A., Sileo, M., and Aiello, M. A. (2015). Ultrasonic pulse velocity for the evaluation of physical and mechanical properties of a highly porous building limestone. **Ultrasonics**. 60: 33-40.

Vasconcelos, G., Lourenco, P. B., Alves, C. A. S., and Pamplona, J. (2008). Ultrasonic evaluation of the physical and mechanical properties of granites. **Ultrasonics.** 48(5): 453-466.

Wang, Z., Li, W., Wang, Q., Liu, S., Hu, Y., and Fan, K. (2019). Relationships between the petrographic, physical and mechanical characteristics of sedimentary rocks in Jurassic weakly cemented strata. **Environmental Earth Sciences**. 78(5): 1-13.

Yasar, E. and Erdogan, Y. (2004). Correlating sound velocity with the density, compressive strength and Young's modulus of carbonate rocks. **International Journal of Rock Mechanics and Mining Sciences.** 41(5): 871-875.

Yılmaz, N. G., Goktan, R. M., and Kibici, Y. (2011). Relations between some quantitative petrographic characteristics and mechanical strength properties of granitic building stones. **International Journal of Rock Mechanics and Mining Sciences.** 48(3): 506-513.

Yin, S., Ding, W., Shan, Y., Zhou, W., Wang, R., Zhou, X., Li, A., and He, J. (2016). A new method for assessing Young's modulus and Poisson's ratio in tight interbedded clastic reservoirs without a shear wave time difference. **Journal of Natural Gas Science and Engineering.** 36: 267-279.

Yusof, N. Q. A. M. and Zabidi, H. (2016). Correlation of mineralogical and textural characteristics with engineering properties of granitic rock from Hulu Langat, Selangor. **Procedia Chemistry.** 19: 975-980.

APENDIX A

Laboratory test results

Table A.1 Physical, dynamic and mechanical properties of plutonic group specimens.

Rock Type	Physical Properties			Dynamic Properties				Static Mechanical Properties		
	ρ (g/cm^3)	n_e (%)	n (%)	V_p (km/s)	V_s (km/s)	E_d (GPa)	ν_d	E_s (GPa)	ν_s	σ_c (MPa)
Diorite (Trgr)	2.52	1.17	3.61	3.89	2.41	34.78	0.19	13.89	0.17	43.22
	2.53	1.04	-	3.91	2.43	35.40	0.19	14.97	0.17	56.14
	2.54	0.96	-	3.92	2.44	35.78	0.18	15.06	0.16	62.51
	2.55	0.90	3.24	3.96	2.46	36.64	0.18	16.11	0.16	69.90
	2.57	0.61	-	3.97	2.48	37.31	0.18	16.55	0.16	71.56
	2.58	0.57	-	3.98	2.48	37.53	0.18	16.97	0.16	72.10
	2.59	0.41	2.60	3.98	2.50	37.99	0.17	17.22	0.16	85.20
Granite (Kgr)	2.55	1.29	3.83	3.72	2.30	32.10	0.19	12.30	0.19	23.40
	2.56	1.11	-	3.77	2.33	33.07	0.19	13.47	0.19	36.50
	2.56	1.07	-	3.84	2.37	34.30	0.19	14.44	0.19	51.79
	2.57	0.62	-	3.93	2.45	36.38	0.18	15.36	0.18	56.71
	2.58	0.56	2.68	3.99	2.49	37.80	0.18	16.90	0.18	96.36
Granite (Cgr)	2.52	1.32	3.00	3.86	2.35	33.55	0.20	15.69	0.19	51.82
	2.52	1.00	-	3.86	2.36	33.82	0.20	15.73	0.19	70.30
	2.53	0.96	-	3.87	2.37	34.13	0.20	16.80	0.19	73.47
	2.54	0.88	2.86	3.88	2.38	34.51	0.20	17.90	0.19	77.47
	2.55	0.81	-	3.91	2.41	35.40	0.19	17.98	0.19	81.98
	2.56	0.66	-	3.93	2.43	35.90	0.19	18.02	0.19	88.50
	2.56	0.62	-	3.95	2.45	36.49	0.19	18.61	0.18	96.36
	2.57	0.58	2.60	3.97	2.46	36.91	0.19	19.62	0.18	100.51
	2.57	0.53	-	3.99	2.48	37.50	0.19	20.51	0.18	102.70
	2.58	0.48	-	4.01	2.50	38.12	0.18	20.64	0.17	104.30
	2.58	0.26	2.00	4.02	2.51	38.41	0.18	20.83	0.17	121.50

Table A.1 Physical, dynamic and mechanical properties of plutonic group specimens (cont.).

Rock Type	Physical Properties			Dynamic Properties				Static Mechanical Properties		
	ρ (g/cm^3)	n_e (%)	n (%)	V_p (km/s)	V_s (km/s)	E_d (GPa)	ν_d	E_s (GPa)	ν_s	σ_c (MPa)
Granite (Mz1)	2.51	1.52	3.31	3.75	2.29	31.73	0.20	11.70	0.19	11.90
	2.51	1.48	-	3.77	2.30	32.05	0.20	12.10	0.19	22.11
	2.52	1.31	-	3.77	2.31	32.30	0.20	12.40	0.19	25.51
	2.53	1.01	-	3.80	2.32	32.81	0.20	12.67	0.19	25.70
	2.53	0.96	-	3.81	2.33	33.06	0.20	13.20	0.19	31.11
	2.53	0.82	-	3.83	2.34	33.43	0.20	13.70	0.18	37.25
	2.54	0.79	-	3.83	2.35	33.67	0.20	13.98	0.18	43.61
	2.55	0.63	-	3.84	2.36	33.98	0.20	14.22	0.18	48.20
	2.56	0.62	-	3.86	2.38	34.58	0.19	14.60	0.17	49.30
	2.57	0.52	2.94	3.87	2.39	34.96	0.19	14.74	0.17	54.87

Table A.2 Physical, dynamic and mechanical properties of volcanic group specimens.

Rock Type	Physical Properties			Dynamic Properties				Static Mechanical Properties		
	ρ (g/cm^3)	n_e (%)	n (%)	V_p (km/s)	V_s (km/s)	E_d (GPa)	ν_d	E_s (GPa)	ν_s	σ_c (MPa)
Basalt (Qbs)	2.70	0.92	4.21	3.98	2.53	40.15	0.16	16.84	0.18	43.69
	2.70	0.90	-	4.01	2.55	40.74	0.16	17.09	0.18	61.20
	2.71	0.88	-	4.04	2.57	41.64	0.16	18.13	0.18	74.27
	2.72	0.87	-	4.08	2.60	42.61	0.16	19.19	0.17	78.34
	2.72	0.86	4.01	4.11	2.63	43.44	0.15	20.42	0.17	83.00
	2.73	0.80	-	4.12	2.64	43.90	0.15	21.65	0.17	84.20
	2.74	0.74	-	4.14	2.66	44.58	0.15	22.77	0.16	87.40
	2.75	0.71	-	4.16	2.67	45.09	0.15	22.91	0.16	89.23
	2.76	0.66	2.77	4.17	2.68	45.52	0.15	23.76	0.16	102.61
Andesite (PTrv)	2.59	1.15	4.65	3.86	2.41	35.52	0.18	17.05	0.18	59.47
	2.60	1.11	-	3.89	2.43	36.26	0.18	17.36	0.18	63.80
	2.61	1.07	-	3.90	2.44	36.59	0.18	17.83	0.18	73.79
	2.62	1.02	-	3.93	2.46	37.43	0.18	18.87	0.17	82.10
	2.63	0.93	-	3.97	2.48	38.26	0.18	19.63	0.17	85.30
	2.64	0.89	-	4.00	2.50	39.00	0.18	20.16	0.17	92.40
	2.65	0.85	-	4.02	2.52	39.58	0.18	21.53	0.16	96.10
	2.66	0.74	-	4.04	2.53	40.04	0.18	21.72	0.16	96.80
	2.67	0.73	-	4.06	2.55	40.73	0.18	22.56	0.15	99.00
	2.68	0.69	-	4.08	2.56	41.23	0.18	23.15	0.15	104.31
	2.69	0.50	-	4.10	2.57	41.85	0.17	23.26	0.15	117.71
	2.70	0.40	-	4.12	2.59	42.46	0.17	23.92	0.15	121.58
	2.71	0.37	-	4.13	2.60	42.85	0.17	24.22	0.15	125.47
	2.72	0.30	2.26	4.15	2.61	43.41	0.17	24.61	0.15	132.40

Table A.2 Physical, dynamic and mechanical properties of volcanic group specimens (cont.).

Rock Type	Physical Properties			Dynamic Properties				Static Mechanical Properties		
	ρ (g/cm^3)	n_e (%)	n (%)	V_p (km/s)	V_s (km/s)	E_d (GPa)	ν_d	E_s (GPa)	ν_s	σ_c (MPa)
Rhyorite (PTrv)	2.50	1.33	6.22	3.77	2.28	31.49	0.21	12.68	0.20	32.10
	2.51	1.30	-	3.77	2.28	31.59	0.21	12.72	0.20	36.59
	2.51	1.21	-	3.77	2.29	31.76	0.21	12.85	0.20	36.59
	2.52	1.11	-	3.77	2.29	31.94	0.21	13.60	0.20	37.11
	2.53	0.78	-	3.78	2.30	32.16	0.21	13.76	0.20	39.30
	2.53	0.69	-	3.78	2.30	32.38	0.21	14.02	0.19	41.60
	2.53	0.65	5.69	3.79	2.31	32.52	0.20	14.43	0.19	47.84
	2.54	0.64	-	3.79	2.31	32.69	0.20	14.69	0.19	56.76
	2.54	0.62	-	3.79	2.32	32.85	0.20	14.79	0.19	66.47
	2.55	0.57	-	3.81	2.33	33.12	0.20	15.20	0.19	79.50
	2.55	0.55	-	3.81	2.33	33.37	0.20	16.21	0.18	89.90
	2.56	0.54	-	3.82	2.34	33.66	0.20	16.33	0.18	90.30
	2.56	0.52	5.45	3.82	2.36	33.97	0.19	16.59	0.18	94.78
	2.56	0.49	-	3.83	2.37	34.25	0.19	16.84	0.18	100.57
	2.57	0.48	-	3.84	2.37	34.43	0.19	17.01	0.18	100.57
	2.57	0.42	-	3.84	2.38	34.65	0.19	17.34	0.18	107.25
	2.58	0.39	-	3.85	2.39	34.84	0.19	17.52	0.17	111.05
	2.58	0.37	-	3.85	2.39	35.05	0.19	17.89	0.17	118.67
	2.59	0.34	-	3.86	2.40	35.25	0.18	18.49	0.17	124.70
	2.59	0.32	4.21	3.86	2.41	35.52	0.18	18.77	0.17	127.00

Table A.2 Physical, dynamic and mechanical properties of volcanic group specimens (cont.).

Rock Type	Physical Properties			Dynamic Properties				Static Mechanical Properties		
	ρ (g/cm^3)	n_e (%)	n (%)	V_p (km/s)	V_s (km/s)	E_d (GPa)	ν_d	E_s (GPa)	ν_s	σ_c (MPa)
Vesicular Basalt (Qbs)	2.57	2.97	6.23	3.88	2.38	34.89	0.20	12.36	0.18	42.09
	2.57	2.81	-	3.89	2.39	35.09	0.20	13.98	0.18	45.48
	2.58	2.45	-	3.90	2.40	35.46	0.20	15.51	0.18	47.51
	2.58	2.23	-	3.91	2.41	35.68	0.19	16.81	0.17	58.90
	2.58	1.89	-	3.93	2.43	36.31	0.19	16.94	0.17	63.16
	2.59	1.66		3.94	2.44	36.65	0.19	18.22	0.16	65.60
	2.59	1.40	5.44	3.95	2.45	36.94	0.19	19.32	0.16	67.96
Tuff (PTrv)	2.60	1.51	5.49	3.70	2.26	31.96	0.20	12.08	0.18	25.90
	2.61	1.37	-	3.74	2.30	33.04	0.20	12.27	0.18	28.61
	2.63	1.11	-	3.79	2.34	34.38	0.19	13.62	0.18	36.50
	2.64	0.86	-	3.83	2.37	35.33	0.19	14.21	0.17	47.58
	2.65	0.50	4.26	3.86	2.41	36.30	0.18	14.75	0.17	51.03

Table A.3 Physical, dynamic and mechanical properties of carbonate group specimens.

Rock Type	Physical Properties			Dynamic Properties				Static Mechanical Properties		
	ρ (g/cm^3)	n_e (%)	n (%)	V_p (km/s)	V_s (km/s)	E_d (GPa)	ν_d	E_s (GPa)	ν_s	σ_c (MPa)
Marble Pkd	2.55	0.30	6.50	3.71	2.31	32.16	0.19	13.78	0.19	29.50
	2.56	0.29	-	3.77	2.34	33.27	0.18	14.21	0.19	29.79
	2.56	0.27	-	3.83	2.39	34.49	0.18	14.96	0.19	33.41
	2.57	0.26	5.90	3.85	2.41	35.16	0.18	15.67	0.18	38.75
	2.57	0.20	-	3.87	2.43	35.66	0.18	15.83	0.18	38.75
	2.58	0.17	-	3.89	2.45	36.22	0.17	16.47	0.18	40.15
	2.59	0.15	5.41	3.90	2.46	36.69	0.17	17.50	0.17	42.77
	2.60	0.11	-	3.94	2.49	37.55	0.17	18.38	0.17	47.16
	2.61	0.08	-	3.95	2.50	38.05	0.17	19.33	0.17	50.02
	2.61	0.03	4.77	3.97	2.51	38.39	0.16	19.61	0.17	53.19
Travertine Pkd	2.42	2.70	13.51	3.44	2.05	24.94	0.22	10.60	0.21	43.99
	2.43	2.64	-	3.46	2.08	25.50	0.22	10.94	0.21	44.05
	2.43	2.34	-	3.47	2.09	25.79	0.22	11.17	0.20	52.09
	2.44	2.28	-	3.49	2.10	26.20	0.22	11.48	0.20	54.72
	2.44	2.12	-	3.51	2.12	26.54	0.21	12.58	0.19	54.72
	2.45	2.04	-	3.52	2.13	26.97	0.21	13.02	0.19	57.87
	2.46	1.94	-	3.53	2.14	27.26	0.21	13.21	0.18	57.87
	2.47	1.83	-	3.55	2.15	27.64	0.21	14.93	0.18	60.19
	2.48	1.77	-	3.56	2.17	28.10	0.20	15.57	0.18	76.40
	2.49	1.71	-	3.57	2.18	28.46	0.20	16.19	0.17	81.10
	2.50	1.66	8.58	3.58	2.20	29.02	0.19	16.33	0.17	81.13

Table A.3 Physical, dynamic and mechanical properties of carbonate group specimens (cont.).

Rock Type	Physical Properties			Dynamic Properties				Static Mechanical Properties		
	ρ (g/cm^3)	n_e (%)	n (%)	V_p (km/s)	V_s (km/s)	E_d (GPa)	ν_d	E_s (GPa)	ν_s	σ_c (MPa)
Limestone (Mz1)	2.48	2.10	9.27	3.52	2.14	27.33	0.20	12.27	0.20	25.40
	2.48	2.04	-	3.53	2.16	27.83	0.20	12.74	0.20	29.88
	2.49	1.99	-	3.54	2.17	28.08	0.20	13.18	0.20	31.41
	2.49	1.83	-	3.55	2.18	28.28	0.20	13.99	0.20	34.53
	2.50	1.75	-	3.57	2.19	28.67	0.20	14.28	0.20	38.79
	2.51	1.60	-	3.59	2.20	29.19	0.20	14.95	0.19	39.89
	2.52	1.47	-	3.61	2.22	29.58	0.20	15.04	0.19	42.51
	2.52	1.22	-	3.62	2.23	29.85	0.20	15.23	0.18	42.79
	2.52	1.15	-	3.64	2.24	30.25	0.20	15.63	0.18	50.27
	2.53	0.90	-	3.65	2.25	30.51	0.19	16.51	0.18	55.50
	2.53	0.74	-	3.66	2.26	30.77	0.19	16.60	0.18	59.33
	2.54	0.60	8.38	3.67	2.26	30.87	0.19	17.11	0.18	59.33
Limestone (Trls)	2.44	0.51	9.52	3.33	2.00	23.84	0.22	10.71	0.21	37.60
	2.45	0.47	-	3.37	2.04	24.62	0.21	11.22	0.20	40.10
	2.47	0.36	-	3.39	2.07	25.50	0.20	12.28	0.20	52.20
	2.48	0.31	-	3.44	2.12	26.59	0.20	13.24	0.19	76.20
	2.49	0.23	8.14	3.47	2.13	27.08	0.20	14.27	0.18	90.25
Limestone (Pkd)	2.44	0.80	11.77	3.41	1.99	23.99	0.24	11.02	0.20	32.76
	2.44	0.77	-	3.44	2.02	24.62	0.24	12.01	0.20	45.05
	2.45	0.75	-	3.46	2.03	25.03	0.24	12.55	0.20	52.42
	2.46	0.61	-	3.49	2.05	25.60	0.24	13.20	0.20	54.90
	2.47	0.59	-	3.52	2.07	26.21	0.24	14.01	0.19	59.00
	2.48	0.54	-	3.55	2.10	26.98	0.23	14.67	0.19	61.37
	2.49	0.50	-	3.57	2.12	27.43	0.23	15.05	0.18	63.34

Table A.4 Physical, dynamic and mechanic properties of clastic group specimens.

Rock Type	Physical Properties			Dynamic Properties				Static Mechanical Properties		
	ρ (g/cm^3)	n_e (%)	n (%)	V_p (km/s)	V_s (km/s)	E_d (GPa)	ν_d	E_s (GPa)	ν_s	σ_c (MPa)
	2.50	0.48	9.33	3.59	2.14	28.04	0.23	15.59	0.18	65.53
Sandstone (Jpk)	2.43	6.83	9.16	3.52	2.11	26.39	0.22	9.87	0.20	36.42
	2.44	6.54	-	3.55	2.13	27.01	0.22	10.11	0.20	56.79
	2.45	6.17	-	3.58	2.15	27.59	0.22	10.35	0.19	74.42
	2.46	5.61	-	3.59	2.17	28.01	0.21	10.68	0.19	80.24
	2.46	4.42	-	3.61	2.18	28.46	0.21	11.00	0.19	89.39
	2.47	4.14	-	3.62	2.19	28.75	0.21	11.25	0.18	93.93
	2.48	3.70	8.42	3.63	2.20	28.98	0.21	11.70	0.18	96.78
Sandstone (Kpp)	2.35	9.69	11.83	3.28	1.90	21.17	0.25	8.76	0.21	65.46
	2.35	8.82	-	3.30	1.92	21.51	0.25	9.75	0.21	76.36
	2.36	8.70	-	3.32	1.93	21.90	0.24	9.89	0.21	78.18
	2.36	8.65	-	3.35	1.95	22.28	0.24	10.51	0.20	83.00
	2.36	8.62	-	3.36	1.96	22.62	0.24	11.82	0.20	83.00
	2.37	8.27	-	3.39	1.98	23.00	0.24	11.91	0.19	84.22
	2.37	8.20	-	3.40	1.99	23.25	0.24	12.08	0.19	91.74
	2.38	8.17	-	3.42	2.00	23.62	0.24	12.37	0.19	91.74
	2.39	7.85	-	3.43	2.02	23.94	0.24	12.56	0.19	94.36
	2.39	7.08	10.44	3.44	2.04	24.51	0.23	12.94	0.19	95.50
Sandstone (JKpw)	2.30	12.15	14.11	3.26	1.86	20.10	0.26	10.71	0.23	43.78
	2.31	11.70	-	3.29	1.88	20.54	0.26	10.90	0.23	47.41
	2.32	11.62	-	3.32	1.91	21.27	0.25	11.25	0.23	63.34
	2.35	8.89	-	3.34	1.93	21.87	0.25	11.64	0.22	69.40
	2.35	8.36	-	3.36	1.94	22.14	0.25	11.79	0.22	72.08
	2.36	6.67	12.09	3.37	1.95	22.48	0.25	12.09	0.21	73.60

Table A.4 Physical, dynamic and mechanic properties of clastic group specimens (cont.).

Rock Type	Physical Properties			Dynamic Properties				Static Mechanical Properties		
	ρ (g/cm^3)	n_e (%)	n (%)	V_p (km/s)	V_s (km/s)	n_e (%)	n (%)	E_s (GPa)	ρ (g/cm^3)	n_e (%)
Sandstone (Mz1)	2.48	5.89	6.70	3.56	2.13	27.42	0.22	9.36	0.20	31.12
	2.49	5.85	-	3.57	2.15	27.92	0.22	9.70	0.20	31.12
	2.50	4.81	6.32	3.58	2.17	28.53	0.21	10.06	0.20	33.77
	2.51	4.30	-	3.60	2.21	29.33	0.20	10.72	0.20	36.28
	2.52	4.25	5.71	3.63	2.24	30.19	0.19	11.03	0.19	38.08
	2.53	3.66	-	3.64	2.26	30.60	0.19	11.81	0.19	57.76
	2.53	2.76	5.61	3.65	2.27	30.90	0.19	12.11	0.19	60.18
	2.54	2.12	-	3.68	2.29	31.53	0.18	12.51	0.18	69.78
	2.54	1.79	-	3.71	2.31	32.03	0.18	12.63	0.18	70.49
	2.55	1.62	4.79	3.73	2.33	32.64	0.18	12.75	0.18	73.44

Table A.5 Physical, dynamic and mechanical properties of sulfate group specimens.

Rock Type	Physical Properties			Dynamic Properties				Static Mechanical Properties		
	ρ (g/cm^3)	n_e (%)	n (%)	V_p (km/s)	V_s (km/s)	E_d (GPa)	ν_d	E_s (GPa)	ν_s	σ_c (MPa)
Anhydrite (Tkb)	2.72	5.02	3.10	3.74	2.31	34.61	0.19	15.14	0.18	15.04
	2.73	4.62	-	3.76	2.33	35.22	0.19	16.07	0.18	19.56
	2.74	4.41	2.82	3.80	2.36	36.20	0.19	16.27	0.18	24.03
	2.74	3.76	-	3.82	2.38	36.71	0.18	16.52	0.17	24.03
	2.75	3.57	-	3.85	2.39	37.30	0.19	17.22	0.17	32.96
	2.75	3.42	2.20	3.86	2.41	37.81	0.18	17.39	0.16	32.96
	2.76	2.94	-	3.91	2.45	38.94	0.18	18.50	0.16	34.55
	2.77	2.72	1.94	3.98	2.49	40.44	0.18	18.67	0.15	43.69
Gypsum (Tkb)	2.01	10.30	16.70	3.16	1.78	16.20	0.27	5.18	0.23	5.91
	2.02	9.94	-	3.18	1.80	16.48	0.27	5.20	0.23	6.37
	2.03	9.60	15.52	3.19	1.83	17.05	0.25	5.24	0.22	6.48
	2.04	9.36	-	3.20	1.84	17.35	0.25	5.52	0.22	6.83
	2.05	8.79	-	3.21	1.86	17.67	0.25	5.74	0.22	7.88
	2.07	8.44	14.57	3.22	1.87	18.05	0.25	5.80	0.22	8.41
	2.08	7.73	-	3.24	1.90	18.60	0.24	6.66	0.21	9.05
	2.09	7.36	13.88	3.26	1.92	19.00	0.23	7.32	0.21	11.20

Table A.6 Physical, dynamic properties of silicate group specimens.

Rock Type	Physical Properties			Dynamic Properties				Static Mechanical Properties		
	ρ (g/cm^3)	n_e (%)	n (%)	V_p (km/s)	V_s (km/s)	E_d (GPa)	ν_d	E_s (GPa)	ν_s	σ_c (MPa)
Pyrophyllite (PTrv)	2.55	0.83	7.17	3.89	2.38	34.67	0.20	13.42	0.20	30.33
	2.55	0.80	-	3.90	2.39	34.95	0.20	13.76	0.20	38.57
	2.56	0.74	-	3.90	2.39	35.08	0.20	13.92	0.19	46.32
	2.56	0.72	-	3.91	2.40	35.26	0.20	14.16	0.19	54.46
	2.56	0.62	-	3.91	2.41	35.45	0.19	14.61	0.19	55.80
	2.57	0.61	6.81	3.92	2.42	35.95	0.19	14.77	0.19	63.80
	2.57	0.57	-	3.92	2.43	36.04	0.19	14.85	0.19	64.00
	2.57	0.55	-	3.93	2.44	36.33	0.19	15.39	0.19	64.00
	2.58	0.51	-	3.93	2.44	36.49	0.18	15.47	0.18	73.88
	2.58	0.47	6.70	3.94	2.45	36.70	0.18	15.83	0.18	75.83
	2.58	0.41	-	3.94	2.46	36.86	0.18	15.84	0.18	75.83
	2.58	0.37	-	3.94	2.47	37.04	0.18	16.24	0.18	76.73
	2.59	0.31	-	3.95	2.48	37.43	0.18	16.59	0.17	76.73
	2.59	0.29	-	3.96	2.49	37.70	0.17	16.59	0.17	76.79
	2.59	0.28	6.60	3.97	2.50	37.97	0.17	16.66	0.17	83.62
	2.59	0.26	-	3.98	2.51	38.20	0.17	16.71	0.17	89.84
	2.59	0.23	-	3.98	2.51	38.30	0.17	16.84	0.16	89.89
	2.60	0.23	-	3.99	2.52	38.45	0.17	17.34	0.16	92.58
	2.60	0.21	-	3.99	2.52	38.60	0.17	18.67	0.16	93.03
	2.60	0.21	5.60	4.00	2.53	38.75	0.17	19.32	0.16	93.03
Dickite (PTrv)	2.54	0.07	6.29	3.88	2.37	34.32	0.20	12.26	0.19	27.21
	2.55	0.06	5.93	3.89	2.40	35.06	0.19	12.99	0.18	31.75
	2.56	0.05	5.90	3.90	2.42	35.59	0.19	13.47	0.18	38.06

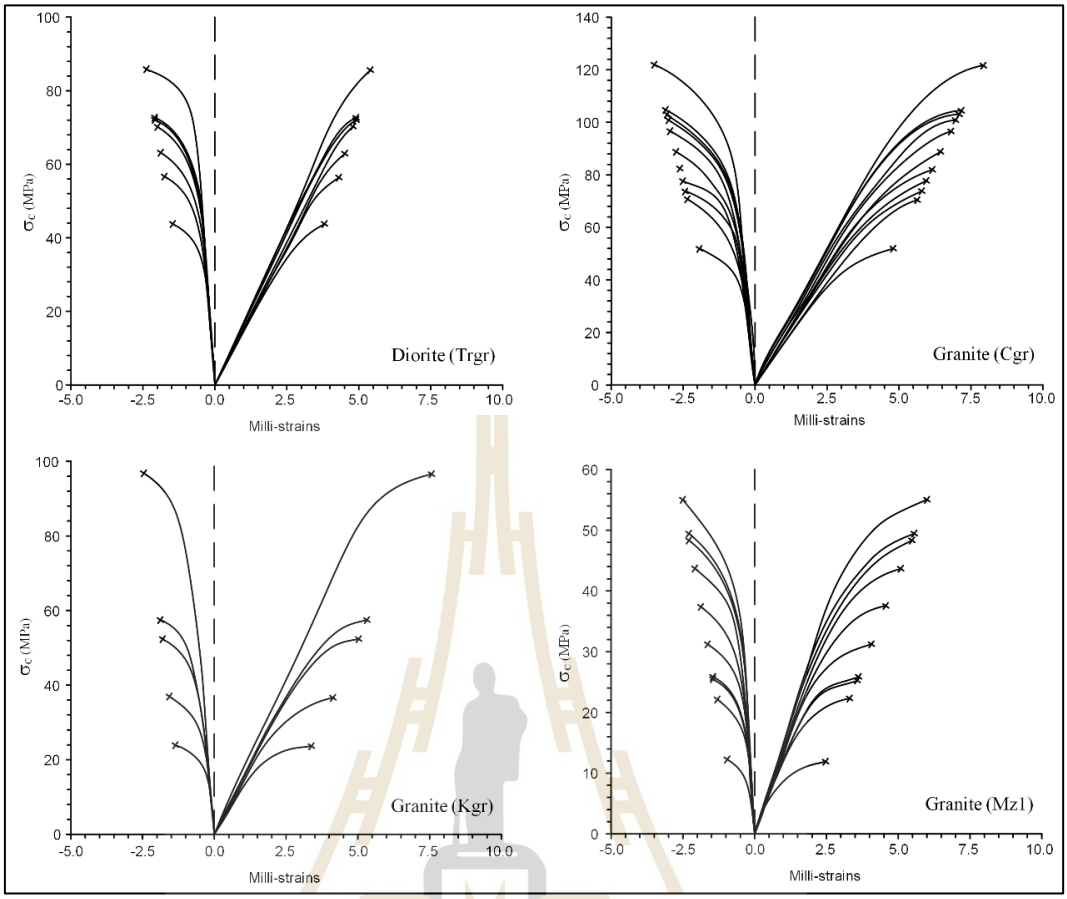

Figure A.1 Stress-strain curves obtained from plutonic group.

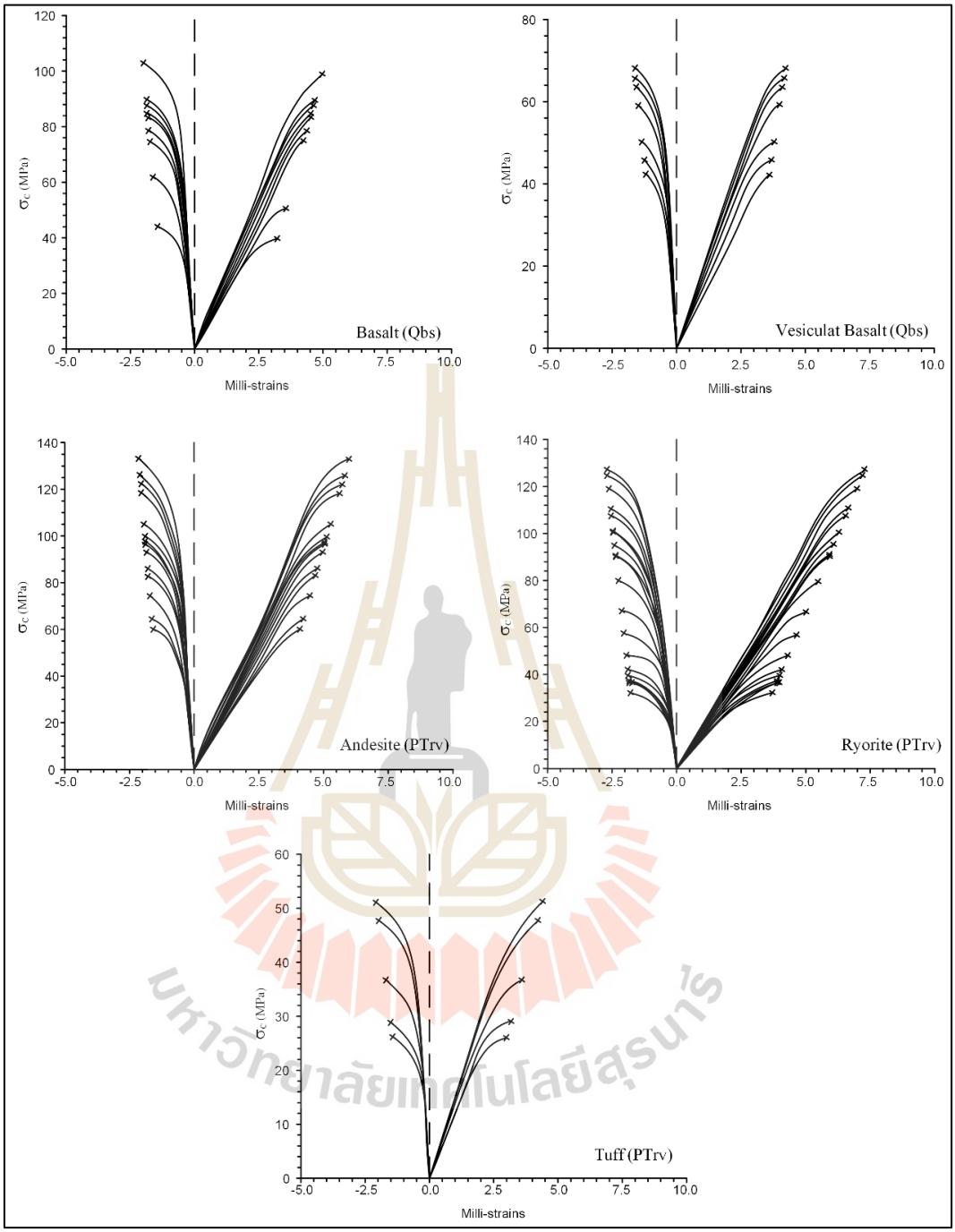

Figure A.2 Stress-strain curves obtained from volcanic group.

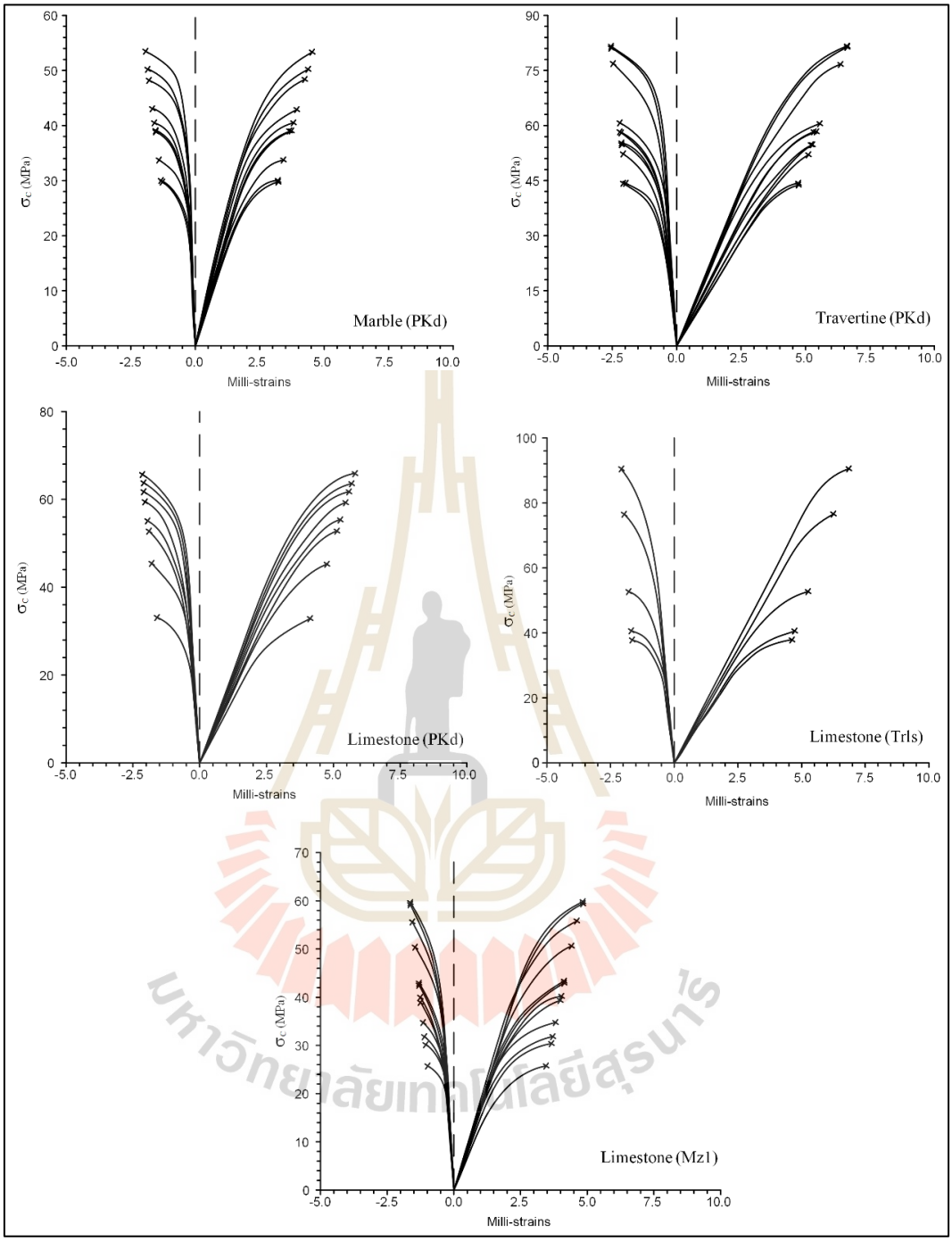

Figure A.3 Stress-strain curves obtained from carbonate group.

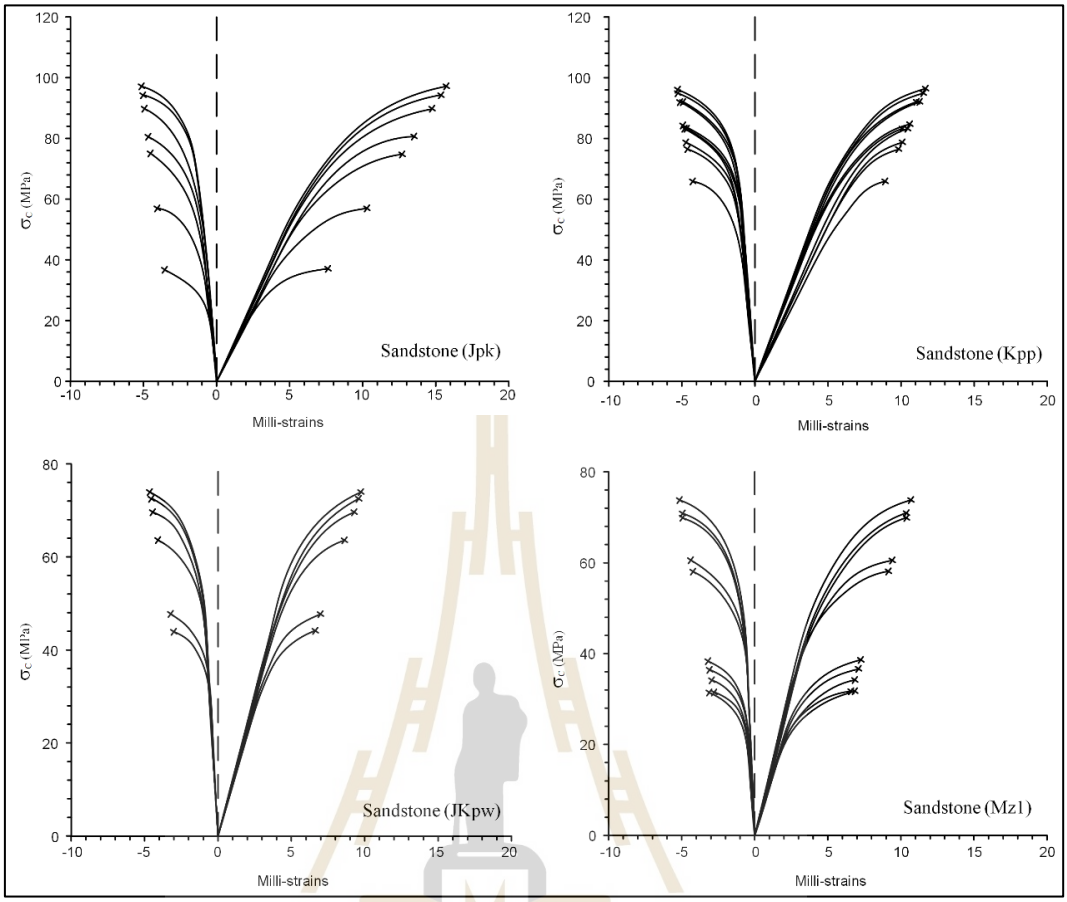

Figure A.4 Stress-strain curves obtained from clastic group.

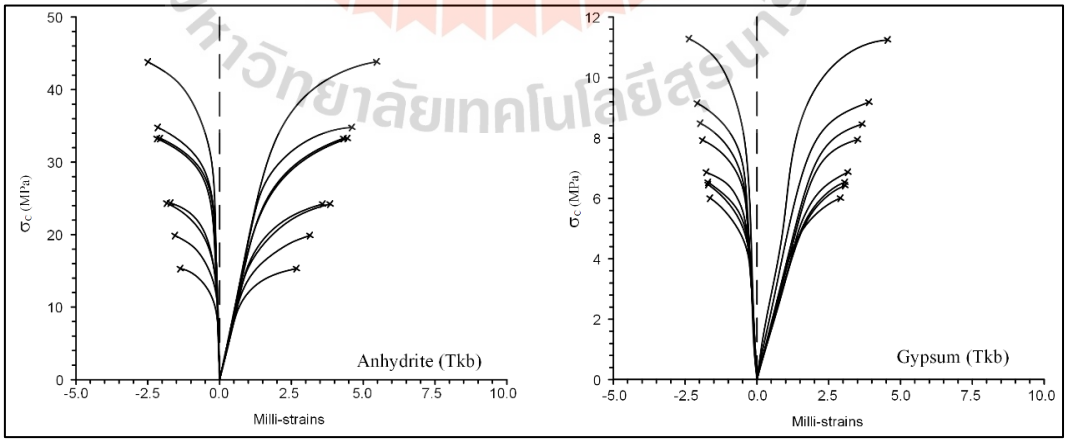

Figure A.5 Stress-strain curves obtained from sulfate group.

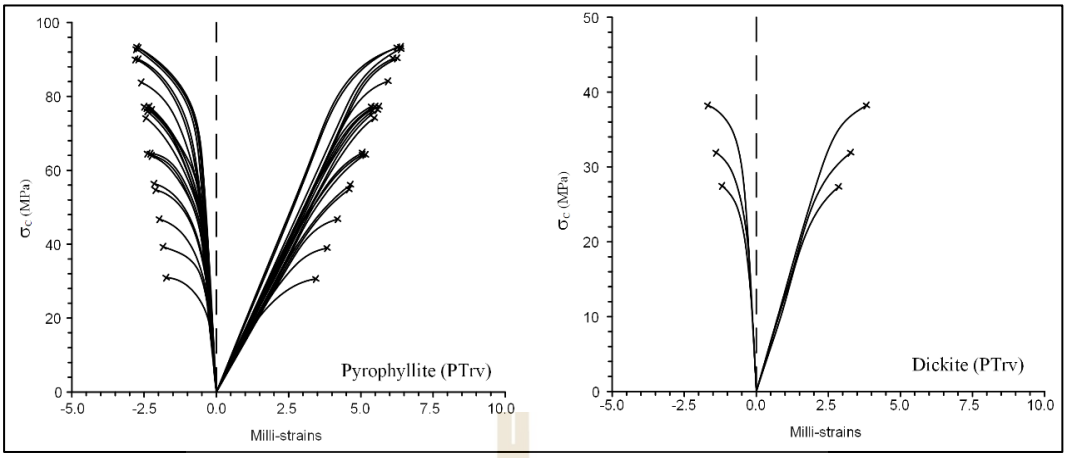

Figure A.6 Stress-strain curves obtained from silicate group.

BIOGRAPHY

Miss Suwaphit Chamwon was born on November 14, 1996 in Phatchabun Province, Thailand. She received her Bachelor's degree in Engineering (Geological Engineering) from Suranaree University of Technology in 2019. For her post-graduate, she continued to study with a Master's degree in the Geological Engineering Program, Institute of Engineering, Suranaree university of Technology. During graduation, 2019-2021, she was a part time worker in position of research assistant at the Geomechanics Research Unit, Institute of Engineering, Suranaree University of Technology.